Pilot-scale Microwave Treatment of Wastewater Slurries: Assessment of a 915 MHz Microwave Generator and Custom Applicator

by

Samuel Willson Bailey
BASc, University of British Columbia, 2012

A THESIS SUBMITTED IN PARTIAL FULFILLMENT OF THE REQUIREMENTS FOR THE DEGREE OF

MASTER OF APPLIED SCIENCE

in

The Faculty of Graduate and Postdoctoral Studies

(Civil Enginering)

THE UNIVERSITY OF BRITISH COLUMBIA
(Vancouver)

August 2015

Abstract

This study applied thermal-oxidative treatment to wastewater. It utilised a novel, pilot-scale microwave system with additions of hydrogen peroxide and acid. The system was instrumented to measure temperature, power and energy. This allowed aspects of process design, power draw and energy efficiency to be weighed against outcomes of treatment.

Preliminary tests with salt water established procedures and expectations for the system, highlighting system sensitivity to variations in the target fluid. Primary tests treated manure and waste activated sludge, evaluating improvements in solids reduction, biogas production, dewaterability and nutrient recovery, each described by a suite of parameters, and referenced to power and energy consumed.

Primary tests used various treatments, with some general trends observed. Acid solubilised inorganic constituents while fixing organics, improving settling and supernatant clarity. It had most acute effect on manure, achieving the majority of phosphorus released. Acid's impact on phosphorus in sludge was less dramatic, though it produced a clear supernatant and good settling. For sludge, early addition of H_2O_2 and heat, or heat alone released most phosphorus and produced highest peaks in phosphate. However, results suggested that acid could be necessary to reduce suspended solids to a level required for struvite recovery. For both wastes, though especially dramatic for sludge, no acid, high heat and late addition of H_2O_2 proved best to disrupt organics and improve bulk parameters: dissolving most suspended solids; solubilising most carbon, volatile fatty acids and ammonia; and improving overall settling. This treatment indicated the most benefit for biogas production.

This study shows some results similar to existing literature, though different processes may be used. This confirms a trend often noted in literature: that thermal treatments are largely reproducible, due to the dominant impact of heat. However, this study indicated that not all processes are equal in energy efficiency. Comparing continuous and semi-continuous operation, continuous runs showed slight detriment in treatment, but clear opportunity for improved energy efficiency. It increased stability in mechanical and chemical properties of target fluids, improving the stability and efficiency of microwave energy absorption.

Preface

The work in this dissertation represents the direction, contributions and assistance of the research group led by Dr. Victor Lo, professor in the department of UBC Civil Engineering. At the time of research the group consisted of post-doctoral fellow, Dr. Asha Srinivasan, and research assistants Dr. Ping Liao, Jeff McSween and Sam Bailey. The interpretations and writing in this manuscript are all original work by Sam Bailey. Questions and requests for supplementary information can be sent to the author.

Chapters 2 and 3 are original, unpublished work by Sam Bailey.

Chapter 4 is original, unpublished work designed in collaboration between Asha Srinivasan and Sam Bailey.

Chapter 5 is based on a research program designed by Asha Srinivasan and Ping Liao. Experiments were performed by Asha Srinivasan, Jeff MacSween and Sam Bailey. Analysis was performed by Jeff MacSween and Sam Bailey. A version of this research has been published. Srinivasan, A., Bailey, S., MacSween, J., Lo, K. V., Koch, F., and Liao, P. H. (2014). A continuous-flow 915-MHz microwave treatment of dairy manure. Journal of Environmental Engineering and Science, 9:155-157.

The Semi-continuous Run section of Chapter 6 is based on a research program designed by Asha Srinivasan, Ping Liao and Sam Bailey. All experiments and analysis were directed by Sam Bailey, with assistance from Jeff MacSween and Greg Archer. Select experiments from this research program have been published. Lo, K. V., Liao, P. H., Srinivasan, A., Bailey, S. and MacSween, J. (2014). H_2O_2 dosing strategy on microwave treatment of sewage sludge. Journal of Environmental Engineering and Science, 9:158-161.

The Continuous Run section of chapter 6 is original, unpublished work based on a research program designed by Sam Bailey, with direction and assistance from Asha Srinivasan and Ping Liao. All experiments and analysis were directed by Sam Bailey, with assistance from Jeff MacSween and Greg Archer.

Table of Contents

List of Tables

List of Figures

Acknowledgements

Many thanks to the following people:

For creating the research opportunity, their supervision and support throughout:

Dr. Victor Lo

Dr. Donald Mavinic

For direction and helping to define and evaluate research objectives:

Dr. Asha Srinivasan

Dr. Ping Liao

For their time, technical expertise and guidance:

Mr. Glenn Blaker

Dr. Terry Enegren

For their immense help with experimentation and analysis:

Mr. Jeff MacSween

Mr. Greg Archer

For their mastery in the lab, providing material, guidance and analytical assistance:

Mr. Timothy Ma

Ms. Paula Parkinson

For guidance, inspiration, stimulating conversation and imparting countless life lessons on everything from handiwork to music to ethics:

Mr. Fred Koch

Finally, endless appreciation to our cohort of MASc and PhD candidates, whose dedication and enthusiasm made our journey through the program so very rich.

Dedication

To my family for being a base of support, comfort and love in stages of life leading to now, and for their continued grounding and guidance in stages to come.

1 Introduction

The effective management of residuals from industrial, agricultural and municipal activity is a growing focus of regulation, research and the development of new solutions and products. In virtually every process, the reduction of residuals stands to reduce handling costs. This can also lend to improvements in safety, reducing any risks that residuals might pose to human health or the environment. From necessity, as well as creative insight, they may even gain recognition as valued resources.

The present study explores thermal-oxidative treatment as a technique for managing residual solids and sludge of agriculture and municipal wastewater processes. The specific targets of treatment are liquid manure from dairy production and Waste Activated Sludge (WAS) from municipal wastewater treatment. The thermal-oxidative treatment employed uses microwave (MW) energy for heating and hydrogen peroxide (H_2O_2) oxidation.

The application of both thermal and oxidative treatments to wastewater solids has been studied for decades, with commercialized products successfully installed at full scale. However, the use of MW energy specifically for thermal treatment of wastewater solids is a relatively new and burgeoning field, having first appeared in literature in the early 2000's. The present study introduces additional novelty by utilizing a pilot-scale MW system, which includes equipment specifications and configurations not previously reported in literature. Further, the choice and design of the equipment affords a level of modularity and scalability unavailable to bench-scale systems, typical to previous research. Paired with instruments that closely monitor temperature, energy and power draw, this equipment makes available a detailed investigation of the effects of process design on the efficacy, in terms of objectives explored in previous studies, as well as energy efficiency of treatments.

The body of this study is broken into five chapters. It begins with Chapter 2, which is a literature review providing: background information on significance, source and character of waste solids; objectives, methods and measurable outcomes in treating them; detail on thermal and oxidative treatments; and suggested areas for further research.

Chapter 3 provides a detailed description of the apparatus used, the operating procedures employed, and the analytical methods used in assessing treatment outcomes. Chapter 4 is an expanded investigation of the apparatus. It provides details of a preliminary experiment on the system, subjecting tap water with varying dose of salt (NaCl) and different flow rates to MW radiation. Physical data from this experiment was recorded and used to inform subsequent experiments.

Chapter 5 and 6 are the focal point of this study, wherein the MW system was deployed for the treatment of liquid dairy manure and WAS, respectively. In these sections, the efficacy of treatment was assessed in terms of improved: solids reduction; biogas production, taking solubilised carbon and fatty acids as proxy results; dewaterability; and nutrient recovery, with particular focus on phosphorus. Experiments on dairy manure were conducted with the overarching aim of confirming the comparability of this new system, relative to an earlier system (similar in configuration but with different specifications), deployed previously by our research group. Due to the challenging physical and chemical properties of liquid dairy manure, as well as the severe treatment employed, this experiment was also an extreme initial trial of the system, testing its ability to withstand heat, corrosion, abrasion and acid attack.

Waste activated sludge experiments were conducted in two sections to contrast the effect of different operating mode. The first section used semi-continuous processing, investigating the effect of different H_2O_2 addition timing and dose, recycle flow rate and acidification. In terms of MW energy efficiency, this experiment assessed the impact of variable temperature on energy absorption. The second section used a continuous process configuration, introducing a fresh feed and adjusted modes of H_2O_2 delivery. It investigated the effect of presence or absence of oxidants, and assessed energy absorption patterns, given relative stability in temperature and, where employed, oxidant additions.

Ultimately, this study enabled an exploration of the foreseeable opportunities and challenges in developing MW treatment systems for full-scale application.

2 Literature Review

Research presented in this document contributes to knowledge in stand-alone treatment, or strategic pre-treatment of residual sludge and solids, aiding in their management, reduction and disposal. The specific treatment process investigated here employed simultaneous thermal hydrolysis and chemical oxidation, with select tests employing acid, in application to solids originating from agricultural and municipal wastewater processes. It explored a novel pilot-scale process configuration, utilizing simultaneous microwave heating and oxidation by hydrogen peroxide.

The following review gathers studies that lend perspective on wastewater solids management, focusing on the processes and technologies employed in their treatment. It discusses the characteristics and challenges specific to organic sludge, and describes work highlighting the benefits of microwave and oxidant treatments.

2.1 Significance

Residuals of manufacturing, processing and treatment originate in many forms. Examples include: crude extraction from oil sands resulting in tailings containing toxic naphthenic acids (Mishra et al., 2010); the textile industry producing residual azo dyes (Bi et al., 2009); pharmaceutical production creating synthetic, recalcitrant residuals and byproducts (Y. Yang et al., 2009); and pesticides, both from residuals of production and runoff after application, resulting from food production (Zhang et al., 2007). Of interest to this project are residuals from agricultural and municipal origin. Of particular focus are solids originating from biological activated sludge treatments employed in municipal wastewater treatment.

Municipal wastewater collection and treatment underpins the quality of life and health of modern urban societies. There are evident, positive correlations between a nation's overall development and improvements in sanitation and public health (LeBlanc et al., 2008). Where collection and treatment is practiced, the production of waste solids, typically recovered in slurry with water and known as sludge, is a consequence of prevailing contemporary municipal wastewater treatment technologies.

Sludge management is a challenge of municipal wastewater treatment, and due to several complicating factors, the problem is anticipated to grow. Currently, where secondary treatment is achieved, sludge management is reported as constituting up to 50-60% of total wastewater processing costs (Dhar et al., 2011; Pino-Jelcic et al., 2006; Sui et al., 2011; Toreci et al., 2010; Zhang et al., 2009). In Canada, this represents substantial public investment, considering that an approximate 68% of the population is serviced by treatment plants with secondary treatment or higher (Environment Canada, 2013).

Further, in Canada, updated regulations have been proposed to improve effluent standards, necessitating a level of quality equal or greater to that achieved by secondary treatment (Canada Gazette, 2010). Similar trends exist internationally. In the US, the EPA intends to have more than 99% of future wastewater treatment needs met by secondary treatment or higher (Tchobanoglous et al., 2003). Naturally, increasing demand and requirement for more advanced treatment will result in the increased production of sludge (LeBlanc et al., 2008), and increased global expenditure on its management.

This is further complicated by a concurrent trend for more stringent standards for sludge disposal. Traditional sludge management includes disposal to sea, landfills or incinerators and reuse in land applications. Sea disposal is widely banned (Chu et al., 2009; Hospido et al., 2010; Ødegaard et al., 2000) and the remaining routes are increasingly constrained. The capacity and number of acceptable landfill sites are decreasing, while public acceptance and regulatory compliance limit potential sites for landfills and incinerators (Tchobanoglous et al., 2003).

Alternatively, sludge application to land is becoming safer as we update our knowledge and standards regarding allowable loads of metal, non-stabilized carbon and pathogens in receiving environments (Ødegaard et al., 2000). Regulation and technology have evolved to address these concerns, including measures such as the US EPA Biosolids Standards and Classification (Tchobanoglous et al., 2003; US EPA, 1993a). Given the regulatory climate, where sludge is managed in accordance to standards, it has gained recognition as a resource due to high nutrient and organic matter content (LeBlanc et al., 2008). In order

to reduce concerns and explore nutrient recovery from residual wastewater sludge, advanced solids management techniques and treatments become necessary.

2.2 Origin and Characteristics of Waste Solids

This section provides information on the origin and composition of waste solids studied in this project, namely dairy manure and municipal wastewater solids.

2.2.1 Dairy Manure

Dairy manure is relatively homogeneous in source, however, its composition can be heterogeneous due to variability in animal diet and in techniques of transport, storage and treatment (Sommer et al., 2013). In the present study, liquid dairy manure was collected from the outlet of a solids/liquids separation process. The liquid portion is comprised of a slurry of cow urine and faeces, wash water, sand (the bedding material of choice at the UBC Dairy Research Centre) and leftover feed material. This slurry is high in ionic strength, containing high concentrations of calcium, magnesium, sodium and potassium, mostly bound in particulates, such as: phosphate or carbonate compounds; calcite, apatite and struvite crystals – the latter being a dominant sink of phosphorus; and attached to negatively charged organic particles (Sommer et al., 2013). The organic content of dairy manure is comprised largely of carbohydrates, including cellulose fibres, followed in prevalence by proteins, lipids, lignins and short-chain organic acids (Sommer et al., 2013).

2.2.2 Municipal Wastewater Solids

Solids that find their way to municipal wastewater treatment typically originate from domestic drains in sinks, showers and toilets, and can also include stormwater drains and some industrial sources. As might be obvious, this lends to diverse inputs, limited only by what fits down the drain as well as local bylaw and regulation. As a result, the organic matter present in sewage is highly variable, though generally includes proteins, lipids, polysaccharides, humic substances and nucleic acids in variable proportion of soluble, colloidal and particulate phase (Guellil et al., 2001). All solids, organic and inorganic, are collected and carried, suspended in a slurry typically consisting of more than 99% water on a mass basis (Tchobanoglous et al., 2003).

Once sewage is collected and delivered to wastewater treatment facilities, successive stages of treatment remove varying fractions of influent contaminants. In the first stages of treatment, large, inert solids and some unprocessed organic solids are removed. Preliminary treatment removes coarse materials such as rocks, sand, sticks, rags, metal and other debris, following which primary treatment settles out a fraction of suspended solids and organic matter, and can involve floatation of scum (LeBlanc et al., 2008; Tchobanoglous et al., 2003). In secondary treatment biological and chemical processes remove dissolved and degradable solids, the most widely employed process involving biodegradation through controlled microbial metabolism and growth (LeBlanc et al., 2008; Tchobanoglous et al., 2003). In conventional practice, excess microbial growth is withdrawn as waste solids in order to maintain process stability. Finally, tertiary treatment encompasses a wide array of context specific, effluent polishing steps. Tertiary residuals can include filter separated or precipitated nutrients and chemical coagulants (LeBlanc et al., 2008; Tchobanoglous et al., 2003).

2.2.2.1 Character of Solids Removed in Preliminary and Primary Treatment

Preliminary solids consist of nuisance grit and debris, which is generally of little further use. However, settled solids from primary treatment contain substantial amounts of organic matter, of which more than 50% are carbohydrates, with proteins and lipids representing a respective 20 and 10% (Gavala et al., 2003). These solids are a preferred feed stock for digestion, as they are easily hydrolysed (Eskicioglu et al., 2007b), and in the case of anaerobic digestion, readily yield biogas (Skiadas et al., 2005). Factors that can limit their degradability in digesters, that may be remedied by pretreatment, include large particle size and degradation resistant structures of more complex molecules and substances (Zheng et al., 2009).

2.2.2.2 Character of Solids Removed in Secondary Treatment: Cells, EPS and Humics

In secondary treatment, a complex community of microorganisms become a prevalent part of the slurry, where they metabolize and incorporate suspended particulate and dissolved solids leftover from preliminary and primary treatment. Secondary solids comprise a consortium of live and dead microorganisms as well as organic and inorganic compounds bound together in polymer networks of extracellular polymeric substances

(EPS) (Dhar et al., 2012). These EPS networks determine the overall character of secondary sludge, not only due to their quantity but also their function. While they have not been entirely elucidated due to their heterogeneity, they are known to be pivotal for their role: in the formation of microbial aggregates by facilitating adhesion, forming structure; protecting cells from environment shifts including changes to pH, salt content and hydraulic pressure; and controlling the speciation and distribution of metals (Guibaud et al., 2008, 2005).

The inorganic content of EPS includes bound and adsorbed metals as well as mineral particles (Guibaud et al., 2005). The organic content consists of polysaccharides, proteins and lipids, as well as humic, uronic and deoxyribonucleic acids, with the latter, DNA, typically low in concentration, with higher concentration indicating a higher degree of cell death and lysis (Liu and Fang, 2002). The organic polymers of EPS contain ionisable carboxylic, phosphoric, amino and hydroxyl functional groups, the presence or absence of which contributes to their adsorptive and adhesive properties, giving potential binding sites for metal ions (Guibaud et al., 2008). The ability of EPS to bind metal is considered to be both a physical and chemical process, involving adsorption, ion exchange, complexation and precipitation; the extent of which is determined by such factors such as pH, temperature and bulk ionic and organic matter concentrations (Comte et al., 2008).

Humic acids are another interesting and dynamic component of sludge. As mentioned, they are present in influent sewage and secondary sludge and compose a fraction of EPS. Studies on humic acids invariably note their immense diversity, however, it is generally accepted that they consist of a collection of relatively low molecular weight subunits forming dynamic aggregates, stabilized by hydrophobic interactions and hydrogen bonds (Conte and Piccolo, 1999; Klučáková et al., 2012). In biological reactors their relative concentration has been estimated at 15-20% of volatile solids, which has been shown to positively correlate with microbial enzyme activity, suggesting that they immobilize extracellular enzymes in chemically stable but suppressed form (Frølund et al., 1995). Similar to EPS, they are also known to bind or trap metals and mineral particles as well as organic compounds such as pesticides and other contaminants (Wang et al., 2013).

Further, it is recognized that their propensity to coagulate has remarkable influence on their interactions with aqueous solutes and contaminants (Wang et al., 2013). Of particularly strong influence is pH. At neutral pH, relatively weak hydrophobic forces dominate aggregate bonding; at low pH, due to increased protonation, strong hydrogen bonds begin to dominate, and at a pH below 2 humic acids are virtually insoluble; and at high pH, the functional groups of humic acids begin to ionize, gaining in net charge and intermolecular repulsion (Conte and Piccolo, 1999; Tipping, 2002; Wang et al., 2013). Another influence to coagulation is the presence of cations, particularly divalent, which can neutralize ionized functional groups, induce coagulation and the formation of micelle structures and larger aggregates (Wang et al., 2013). Finally, even a change in the bulk concentration of humic acids can influence the extent of their coagulation, as increased proximity of aggregates increases hydrophobic interaction (Klučáková et al., 2012).

The immensely varied and dynamic composition of wastewater sludge is an invariable complication of sludge treatment. Different treatments have profoundly different effect; the same treatment on different sludge sources may achieve different results; and the character of a single sludge source may even change day to day. This dynamic nature is a necessary consideration when evaluating treatment outcomes.

2.3 Objectives of Sludge Treatment

The study by Camacho et al. (2002) accurately states that treatment processes are designed with the objective to destroy, stabilize or valorise residual sludge. Here, Camacho et al. (2002) use destruction to refer to the maximized mineralisation of sludge, achieved by incinerators or wet-air oxidation. However, less intensive, more targeted destruction may also be desired for specific hazardous and refractory pollutants including phenolic compounds, dyes and pharmaceutical wastes (Bi et al., 2009; Esplugas et al., 2002; Hong et al., 2004; Wei et al., 2003; S. Yang et al., 2009; Yang Yu et al., 2010). Sludge stabilisation includes pathogen reduction, odour removal or inhibition, and reduction or elimination of the potential for putrefaction (Tchobanoglous et al., 2003). Finally, valorisation includes treatments that add value and increase the potential to reuse sludge,

and may involve composting or other methods of recovering resources like carbon, nitrogen and phosphorus (Camacho et al., 2002; Kuroda et al., 2002; Lin et al., 2009; Novak et al., 2003).

These objectives can certainly overlap. An optimal treatment might strategically destroy, stabilize and valorise certain fractions of residual sludge. However, destruction may limit outcomes of valorisation, and vice versa. Destruction via mineralisation converts carbonaceous organic matter permanently to carbon dioxide and water (Klán and Vavrik, 2006) as well as, in the case of incineration, the benefit of recoverable heat (LeBlanc et al., 2008). However, it can also be advantageous to retain this organic matter for recycle. As previously mentioned, land application is a primary and in many cases increasing deposit point for residual sludge, where its organic content has value as a soil conditioner (LeBlanc et al., 2008; Ødegaard et al., 2000; Yoshida et al., 2013). Further, organic matter loading to biological digestion processes is a key control of its performance. Sludge pretreatments that increase the soluble fraction of organic matter increase the stability of digestion at shorter retention time (Coelho et al., 2011; Eskicioglu et al., 2007a; Mehdizadeh et al., 2013; Park et al., 2004; Toreci et al., 2010, 2009; Wang et al., 1997; Zheng et al., 2009), while maintaining or improving biogas production (Abe et al., 2013; Bougrier et al., 2008, 2007; Carrère et al., 2008; Dewil et al., 2007; C Eskicioglu et al., 2008a; Kim et al., 2003; Toreci et al., 2011). Pursuing improved biogas production is an objective of the research herein, so retaining carbonaceous materials is preferred.

2.3.1 Destruction

As mentioned, there are some components of sludge better destroyed. Although not explored in depth in this study, endocrine disrupting compounds (EDCs), personal care products and pharmaceuticals (PCPPs) are emergent concerns in sludge reuse (Brisolara and Qi, 2013; Eskicioglu et al., 2008b; Oller et al., 2011). However, in an exploration of current Life Cycle Assessment tools and standards, the study by Hospido et al. (2010) conclude that EDCs and PCPPs currently rank low in overall impact and toxicity compared to other sludge associated concerns, though it was observed that treatments employed in the study unanimously reduced their impact. As the impacts of these contaminants become

better understood, and perhaps more controlled, opting to destroy them may become a more important objective in the future.

2.3.2 Stabilisation

Stabilisation includes elements of destruction and valorisation. Its overall aim is to process sludge solids into a form that can be disposed or reused with minimal risk. Pathogens, such as bacteria, viruses, protozoa and helminths, are a primary concern of sludge disposal (Hong et al., 2004; Pino-Jelcic et al., 2006). All treatments achieve some level of pathogen reduction, although some, like thermal, offer significant benefit over others, such as mechanical (Eskicioglu et al., 2007b; Müller, 2001).

Stabilisation also includes minimizing components of sludge that have the potential to putrefy. The target is to reduce organic content, characterized by the volatile fraction of solids, which when left untreated may further degrade following disposal. The organic content found in waste activated sludge (WAS) is largely bound in microbial cells or enmeshed in EPS, which limits its immediate biodegradability (Coelho et al., 2011) and imposes challenges to stabilisation. Primary sludge contains a lot of organic material, though it is easily degraded. Therefore, the stabilisation of WAS typically determines treatment designs.

The oldest and most widely used treatment for sludge stabilisation is anaerobic digestion (Tchobanoglous et al., 2003). Several pretreatments have been proposed, some commercialized, that target biological sludge disintegration to improve subsequent digestion and overall stabilisation (Chauzy et al., 2008; Kepp et al., 1995). These treatments add an extra barrier, ensuring that processed sludge meets stabilisation standards set out by the US EPA (1993). This includes minimal pathogenicity as well as minimal potential for putrefaction, which serves to minimize the attraction and infection of vector pests: i.e. known pathogen and disease carriers.

2.3.3 Valorisation

Pretreatments that improve digestion and stabilisation also achieve valorisation. As stated previously, increasing the soluble fraction of organic carbonaceous material

improves the production of biogas, which has value as an offset to plant energy costs and as a potentially saleable product (Appels et al., 2013; Hospido et al., 2010; LeBlanc et al., 2008). This solubilisation is essentially accelerated hydrolysis, the rate limiting first step of digestion (Bougrier et al., 2007; Dewil et al., 2007; Kim et al., 2003; Skiadas et al., 2005). Pretreatment can also result in net production of volatile fatty acids (see Park et al., 2004), which pre-empts acidogenesis and, where acetates are formed, acetogenesis, the second and third stages of digestion, respectively. Ultimately, these improvements stand to enhance methanogenesis, the fourth and final stage of digestion, adding value by producing more methane in less time, as noted previously.

Nutrient recovery is of increasing value around the world. Phosphorus is of particular interest due to its': integral role in biological processes, including agriculture; dwindling availability as a mineral resource; and high concentration in wastewaters, which can cause problems in receiving waters, such as eutrophication (Kuroda et al., 2002), and treatment plants, due to a tendency to precipitate as scale in pipe systems (Britton et al., 2005).

In recent years, commercially available technologies for the recovery of phosphorus have gained traction in the wastewater treatment market, evidenced by several installed and proposed Ostara Inc. nutrient recovery systems in the United Kingdom and across North America (Ostara Nutrient Recovery Technologies Inc., 2014). These systems require not only phosphorus, in the form of reactive phosphate, but a soluble stream of ammonia and magnesium. Therefore, pretreatments that maximize and retain soluble magnesium, ammonia – as opposed to stripping it (see Lin et al., 2009) – and phosphate, stand to add value to this process.

Other valorised outcomes of pretreatment include improved sludge settling (Chu et al., 2009; Y. Yang et al., 2009) and dewaterability (Haug et al., 1978). This improves solids separation from water, lending to more concentrated sludge, and reductions in the overall mass or volume requiring disposal. In general, this is concurrent with savings in time and energy required for separation.

2.4 Methods for Sludge and Residuals Treatment

There are many different technologies available for residuals treatment. They are generally categorized as being mechanical, thermal, chemical and biological (Müller, 2001). Examples of mechanical processes include ball milling, high pressure homogenisation and freeze/thaw cycles (Baier and Schmidheiny, 1997; Climent et al., 2007; Müller, 2001; Zhang et al., 2013). Thermal processes include conventional (e.g. water or oil bath), autoclave and microwave heating (Bougrier et al., 2007; Carrère et al., 2008; Jones et al., 2002; Kappe, 2004). Chemical processes include acidification or basification, chemical catalysis or inhibition, and the addition of oxidants such as persulfate, ozone or hydrogen peroxide (Boehler and Siegrist, 2007; Mukherjee and Levine, 1992; Rivero et al., 2006; Wei et al., 2003; Wong et al., 2007; S. Yang et al., 2009). Finally, biological processes include microbial digestion, such as aerobic or anaerobic, mesophilic or thermophilic digestion, and enzymatic hydrolysis (Dohanyos et al., 1997; Gavala et al., 2003; Guellil et al., 2001).

Several studies have employed combined treatments to achieve additive, catalysed and synergistic results. Examples of combinations include enzyme-mechanical (Dohanyos et al., 1997), thermal-alkali (Chang et al., 2011), and thermal-oxidative treatments (Dhar et al., 2011). Sonication and cavitation could also be considered combination treatments, as they employ mechanical processes that induce chemical and thermal mechanisms (Climent et al., 2007). Further, many studies investigate the benefits of treatments in aim of strategically boosting the efficiency or recovery of downstream processes. Examples which strongly motivate the current study include enhanced thermal hydrolysis of wastewater sludge in advance of digestion (Gavala et al., 2003) and thermal-oxidative hydrolysis to enhance phosphate solubilisation for recovery as struvite (Wong et al., 2007, 2006b).

2.5 Measuring the Efficacy of Sludge Treatment

The efficacy of sludge treatment has received substantial focus for several decades, however general standards for characterizing and comparing impacts of treatment do not yet exist (Burger and Parker, 2013). Regardless, in addition to basic measurements to characterize sludge, certain common indicators of treatment efficacy have emerged.

Indicators that pertain to solids management are presented in Table 1, whereas those that identify potential improvements to downstream processing are given in Table 2.

Treatment energy efficiency is another measure of efficacy that has been explored in previous studies and deserves more attention (Boehler and Siegrist, 2007; Chang et al., 2011; Climent et al., 2007; Zhang et al., 2013). For example, in advanced oxidation, figures of merit have been established to allow comparison between different technology based on energy efficiency (Bolton et al., 2001). In sludge treatment, specific energy, or energy required to treat one kilogram of either total or suspended solids, has been proposed (Bougrier et al., 2006; Camacho et al., 2002; Chang et al., 2011; Climent et al., 2007), although, it is not widely reported. If energy is thoroughly and transparently estimated, and comprehensively reported, a figure-of-merit for energy can provide reference to compare different technologies, as well as to compare improvements of the same technology.

Table 1: Indicators of Treatment Improvement to Sludge Management

Indicator	Reported As:	Comments	Example References
Soluble (S) and Total (T) Carbonaceous Oxygen Demand (COD)	- Ratio: SCOD/TCOD - Percent solubilisation: $(SCOD_{final} - SCOD_{initial})/TCOD \times 100$	- The most ubiquitous indicator - Represents partitioning of carbonaceous material - Increase relates to cell lysis, release of soluble cytoplasmic material, and disintegration of cell walls and floc structure	(Bougrier et al., 2006; Chang et al., 2011; Eskicioglu et al., 2006; P. H. Liao et al., 2007; Park et al., 2004)
Soluble and Total biopolymers: proteins and carbohydrates	Ratio or reductions to each	- Helps to elucidate the treatment target; favoured degradation of a component may help to suggest treatment mechanism	(Eskicioglu et al., 2006; Guellil et al., 2001; Novak et al., 2003; Q. Yu et al., 2010; Zhang et al., 2013)
Volatile Suspended Solids (VSS) and Total Suspended Solids (TSS)	Ratio or reductions to each	- Similar to COD but not as ubiquitous - Represents partitioning of solids - VSS also indicates biomass activity	(Burger and Parker, 2013; Dhar et al., 2012; Procházka et al., 2012; Tyagi and Lo, 2012)
Particle Size Distribution (PSD)	Treatment compared to control	- Elucidates mean particle diameter and how it changes with treatment	(Bougrier et al., 2006; Kim et al., 2003; Q. Yu et al., 2010)
Capillary Suction Timer (CST)	- Treated compared to control - Ratio to total solids (TS) makes comparison more available	- Shows effect of treatment on solid dewaterability - Increased time result of more small, colloidal or hydrophilic solids, slowing capillary movement of water across absorbent paper	(Bougrier et al., 2006; Pino-Jelcic et al., 2006; Tyagi and Lo, 2012)
Settling Rate or Sludge Volume Index (SVI)	Treatment compared to control	- Shows effect of treatment on solid settleability - Faster settling desired for solid/liquid separation	(Bougrier et al., 2008; Y. Yang et al., 2009)

Table 2: Indicators of Treatment Improvements to Downstream Processes: Nutrient Recovery and Digestion

Indicator	Reported As:	Comments	References
Speciation of soluble and total phosphorus	- Ortho-phosphate (PO_4^{3-}) - Soluble fraction of Total Phosphorus (TP) - Total fraction TP	- Used where phosphorus recovery is desired - Ortho-phosphate is readily recovered, reactive phosphorus, whereas TP measures PO_4^{3-} and less bioavailable poly-phosphate and organic phosphate	(Kuroda et al., 2002; Sui et al., 2011; Wong et al., 2007, 2006a, 2006b; Yin et al., 2007)
Speciation of soluble and total nitrogen	- Most often ammonia (NH_3) and total Kjeldahl Nitrogen (TKN): organic nitrogen, ammonia and ammonium - Sometimes NO_x: nitrate/nitrite	- Ammonia is important for struvite recovery, - Can also be toxic or inhibitive in high concentration - Reductions in organic nitrogen can indicate the degradation of compounds such as protein	(Dhar et al., 2011; Dytczak et al., 2007; Eskicioglu et al., 2007c; Haug et al., 1978; Lin et al., 2009; Procházka et al., 2012; Zheng et al., 2009)
Speciation of Volatile Fatty Acids (VFAs)	Changes to total VFA concentration and speciation	- Degradation of long chain and intermediate VFAs to acetic acid can help accelerate anaerobic digestion - Accumulation of VFAs may also cause acidification	(Climent et al., 2007; Eskicioglu et al., 2007c; Park et al., 2005; Procházka et al., 2012; Skiadas et al., 2005; Yang Yu et al., 2010)
Metals	Treatment compared to control	- Due to their function in cells and floc structure, solubilisation of metals can indicate disintegration - Magnesium is important for struvite recovery - Beneficial to identify metals that may be toxic - Can confirm total phosphorus results	(Danesh et al., 2008; Menéndez et al., 2005, 2004; Sui et al., 2011; Wong et al., 2006a; Yang Yu et al., 2010)

2.6 Microwave Thermal and Oxidative Treatments

In this study, organic slurries were heated with microwave (MW) energy, and oxidized by hydrogen peroxide (H_2O_2) of different dose, introduced with different methods and timing. In general, this achieves combined benefits of thermal and oxidative treatment. Research combining thermal and oxidative treatments, using MW energy and H_2O_2 has been a focus of our research group for roughly a decade (see Liao et al., 2005). This study builds on the established precedence and benefits of thermal-oxidative treatment, which are detailed in the following sections.

2.6.1 Thermal Treatment

Thermal processing has been of interest for wastewater sludge treatment for several decades (see Haug et al., 1978). Thermal treatment achieves many of the objectives discussed previously, with benefits unique to heat including: pasteurisation through predetermined combinations of temperature and holding time (Hong et al., 2004); enhanced thermal activation of reactions (Kubrakova, 2000; S. Yang et al., 2009); and thermal suppression of inhibitive enzymes in biological systems (Wang et al., 2009).

Treatment temperatures of interest for sludge are generally within the range of 40 - 180°C (Müller, 2001), but can be as high as 420°C (Camacho et al., 2002). Studies have shown that temperature is often more dominant than holding time on treatment outcomes (Bougrier et al., 2007), though ensuring the temporal similarity of heating profiles is important when comparing heat treatments (Eskicioglu et al., 2008b). It is widely held that thermal treatment degrades wastewater sludge through thermally activated hydrolysis (Chauzy et al., 2008; Kepp et al., 1995; Mehdizadeh et al., 2013). Generally speaking, hydrolysis is the addition of water to a compound, cleaving bonds and dissolving the compound into smaller constituent parts. It is a process that proceeds naturally, though it can be catalysed by enzymes (Frølund et al., 1995; Guellil et al., 2001; Park et al., 2005), oxidation (Müller, 2001), and thermal energy. When cells are subjected to rapid thermal hydrolysis, their membranes become increasingly fluid and unstable, resulting in permeation and eventual structural failure (Asay et al., 2008).

Another outcome of thermal treatment is the off-gassing of volatile components (Dhar et al., 2011; Lin et al., 2009). A formative effect of elevated temperature includes complexation of sugars

and amino acids, called Maillard-Browning, which occurs as low as 37°C, with more aggressive reaction as temperatures rise (Baisier and Labuza, 1992). These newly formed substances may be to blame for what many studies report as refractory and inhibitory substances when treatment temperatures exceed 180°C (Bougrier et al., 2008; Mehdizadeh et al., 2013; Toreci et al., 2011).

2.6.2 Microwave Energy for Thermal Treatment

The application of MW energy is relatively new for thermal treatment of waste sludge. The earliest study reviewed, specific to municipal wastewater, is Menéndez et al. (2002). However, industrial microwave applications date back to 1950 (Pino-Jelcic et al., 2006), with applications similar to sludge including pasteurisation of liquid foods (Anantheswaran and Liu, 1994; Koutchma and Ramaswamy, 2000) as well as soil and water remediation to treat chemical contaminants (Abramovitch, 1998; Jou and Tai, 1998; Tai and Jou, 1999).

Microwaves are a low energy (10^{-5} eV), non-ionizing radiation, occupying a band of the electromagnetic spectrum between radio and infrared frequencies (Jones et al., 2002; Mudhoo and Sharma, 2011). This band contains wavelengths from 1 mm - 1 m, corresponding to frequencies of 0.3 - 3 GHz. To avoid telecommunication interference, MWs operate at pre-set frequency (e.g. 915, 2450, 5180 and 22125 MHz), most commonly 2450 MHz (Kappe, 2004; Lidström et al., 2001; Tai and Jou, 1999). For higher power industrial applications, 915 MHz is often employed (Eskicioglu et al., 2007b).

2.6.2.1 Microwave Thermal Effects

Microwave heating involves the direct interaction of target molecules with an electromagnetic energy source through the mechanisms of dipole rotation, ionic conductance and interfacial polarisation (Remya and Lin, 2011; Taylor et al., 2005). Dipole rotation is the action of polar molecules, such as water or acetic acid, attempting to align with an alternating MW electric field while suspended in a matrix of other molecules that exert resistance (Kappe et al., 2012a; Lidström et al., 2001). Alternating field and repeated change in polar orientation agitates these molecules resulting in intermolecular friction and heat (Perreux and Loupy, 2001). Ionic conduction also works on the principle of friction: dissolved ionic molecules oscillate in the electric field, colliding with neighbouring molecules (Kappe et al., 2012a). In terms of heat generation, the conductive

mechanism is much stronger than dipole rotation (Lidström et al., 2001), becoming stronger still as temperatures rise (Kappe, 2013).

Interfacial polarisation involves the combined action of dipole rotation and ionic conductance on solid, conductive materials subjected to a MW field (Taylor et al., 2005). Throughout literature, different terms have been used for this mechanism: charge space polarisation (Perreux and Loupy, 2001), resistance (ohmic) heating (Kappe, 2004), Maxwell-Wagner polarisation (Menéndez et al., 2010), and interfacial polarisation (Taylor et al., 2005). However, they all seem to refer to an electric field inducing electron movement through solid conductors, with material resistance to this current resulting in heat.

Interfacial polarisation can result in dramatic heating. In illustration, microwaving carbon can cause it to reach temperatures of over 1000°C in under a minute (Perreux and Loupy, 2001; Quan et al., 2007). In some instances, it can also result in the jump of free electrons from solids to their surroundings in the form of plasma hot spots and arcing (Menéndez et al., 2010). In a mix of water and activated carbon subjected to MW, Quan et al. (2007) cited this as the cause of a measured dissociation of water to hydroxyl radicals, in effect similar to cavitation (von Sonntag, 2006a). Further, Menéndez et al., (2002) mixed dewatered sludge with carbon and observed accelerated heating and higher reaction temperatures. The study shows that, without added carbon, these effects are not apparent, suggesting that interfacial polarisation in unaltered sludge solids is minor.

2.6.2.2 Microwave 'Athermal' Effects

The thermal effects of MW are undisputed; however, there has been substantial debate over the existence of 'athermal' or 'non-thermal' MW effect, explained as the direct influence of the MW electrical field with specific molecules in a target medium (Kappe, 2004; Kappe et al., 2013). Studies proffering their existence give evidence of accelerated and improved results of MW compared to conventional forms of heating (Eskicioglu et al., 2007c; Hong et al., 2004; Pino-Jelcic et al., 2006). However, it has been suggested that these studies employ inadequate temperature measurement (Kappe, 2013) or do not closely reproduce MW heating profiles in attempts to compare conventional equipment (Moseley and Kappe, 2011). Studies that take care to reproduce identical heating rates and thermal history, using appropriate sensors such as fibre-optic probes, optimal sensor placement and stirring, report no difference between the two forms

of heating (Herrero et al., 2008; Kappe, 2013; Mehdizadeh et al., 2013; Nüchter et al., 2003; Shazman et al., 2007). These studies show that athermal effect is either functionally indistinguishable from thermal effect or is non-existent. For sludge, it may be that any difference in effect is buried in the inherent heterogeneity of the medium. In any case, the current study followed recent trends in literature and assumed MW treatment mechanisms are thermal.

2.6.2.3 Unique Advantages of Microwave Heating

The absence of athermal effect does not rule out advantages of MW heating. In fact, it is often the unique and unexpected advantages of MW heating that are unaccounted for and mistaken for extraordinary results. These advantages are a result of the unique mechanisms of MW heating discussed previously, and include: non-contact, inside-out heating; instantaneous and rapid volumetric heating; and selective heating (Mudhoo and Sharma, 2011).

Non-contact heating results in an inverted heating profile compared to conventional, conductive heating (de la Hoz et al., 2005). This can result in superheating. Nucleation sites for boiling typically occur on container surfaces or at liquid-gas interfaces – the inverted heating profile causes these to heat last, allowing liquid at a distance from any interface to reach temperatures higher than its boiling point (Kappe et al., 2012a). Volumetric heating occurs due to the ability of MW irradiation to raise the temperature of a liquid volume simultaneously (Kappe, 2013). This is widely reported to result in more rapid heating (Jones et al., 2002). Finally, selective heating occurs due to preferential absorbance, which can be used for targeted heating (Moseley and Kappe, 2011). This can also result in the formation of hot spots caused by concentrated pockets of highly MW absorbing dipoles, ions or solids resulting in heterogeneous heating profiles (Eskicioglu et al., 2007b). These hot spots may also form due to heterogeneity in MW field strength (de la Hoz et al., 2005)

It is important to note that these phenomenon often result in differential heating in non-homogeneous reaction mixtures (Kappe et al., 2012a). Localized temperatures can be as much as 15-40°C different from bulk temperature measurements (Herrero et al., 2008). These heating phenomena also offer advantages over conventional heating in terms of process design. Some processing advantages, as stated in literature, include: energy savings; quick start and stop; rapid and flexible processing; reduced equipment size; equipment availability and maintainability;

portability; simple automation; and added safety due to automation and enclosed reactors (Jones et al., 2002; Kappe, 2013; Lidström et al., 2001; Menéndez et al., 2010).

2.7 Oxidative Treatment

Oxidative processes have been employed for water treatment for over a century, with ozone first used to treat water in France as early as 1906 (Glaze, 1988) and for municipal sludge treatment, in full-scale operation, as early as 1996 in Japan (Sakai et al., 1997). The benefits of oxidation to treatment include enhanced degradation with improved potential for mineralisation of target pollutants as well as disruptive attack of microbial floc, cell walls and intracellular components, promoting disinfection (Crittenden et al., 2012; Dewil et al., 2007; Dytczak et al., 2007; Elovitz and von Gunten, 1999; Zhang et al., 2009; Zimmermann et al., 2011).

2.7.1 Common Oxidants

Of the studies reviewed, ozone (O_3) and hydrogen peroxide (H_2O_2) are the most commonly employed oxidants, due to their strong oxidation potential ($E°_{H2O2}$ = +1.78 V and $E°_{O3}$ = +2.07 V), and typically innocuous degradation products, including short lived radical species, oxygen and water (Hoigne and Staehelin, 1982; Koutchma and Ramaswamy, 2000; Schumb et al., 1955). Persulfate is another common oxidant, with a similarly high oxidation potential ($E°_{S2O8(2-)}$ = +2.01 V), however, its degradation produces sulphate (S. Yang et al., 2009) a precursor of hydrogen sulphide. These are often undesirable byproducts (Dhar et al., 2011).

Ozone is used around the world as a drinking water disinfectant and multi-purpose oxidant (von Gunten, 2003). At ambient conditions it exists as an unstable gas, so it is typically produced on site. Corona discharge is the most widely used method for ozone generation, employing electrolytic dissociation of oxygen (US EPA, 1999). A disadvantage of O_3 is the production of bromate, a potentially carcinogenic by-product of oxidation (Zimmermann et al., 2011).

Hydrogen peroxide has been used as a textile bleaching agent for over a century (Schumb et al., 1955), as a bleach and disinfectant in the food industry (Koutchma and Ramaswamy, 2000), and recently, seems to be gaining popularity in water treatment for use in advanced oxidation. It is produced at industrial scale through autoxidation involving anthraquinone, the result being a relatively stable liquid, often diluted in aqueous solution and dosed with buffers to increase

stability (Schumb et al., 1955). Due to this stability, it is typically made off-site and shipped in as needed (US Peroxide, 2009). Per kilogram, production of H_2O_2 is stated as being cheaper than O_3 (Han et al., 2004; Wang et al., 2009), though shipping costs can surpass production savings.

The use of H_2O_2 excludes the formation of bromate (Katsoyiannis et al., 2011). Although as a disadvantage, molecular H_2O_2 reacts slower and more selectively than other oxidants (Dhar et al., 2011; Eskicioglu et al., 2008b; Klán and Vavrik, 2006) and residual concentrations may be toxic (Gogate and Pandit, 2004). In most cases, it is a benign addition to receiving environments, given that it occurs naturally in aerobic biological systems as a byproduct of cellular respiration (Schumb et al., 1955). In evolved balance, aerobic cells also produce the enzyme catalase, which prevents the accumulation of H_2O_2 by decomposing any excess to water and oxygen (Wang et al., 2009). However, this can be inhibitive to targeted oxidation. Ultimately, it is possible to inactivate catalase with heat, as it gradually denatures at temperatures between about 40 – 70°C (Shazman et al., 2007; Wang et al., 2009). Heating waste activated sludge in a MW, Wang et al. (2009) observed that catalase was inactive in a sample raised to 45°C.

In the present study O_3 was investigated in a preliminary experiment, though H_2O_2 became the primary interest, due to established precedence in our research group and simple applicability.

2.7.2 Mechanisms of Oxidative Degradation

The general mechanism of oxidation is destructive electron exchange. Specific reactions are heterogeneous and highly variable. In an exploration of these mechanisms, advanced oxidation by hydroxyl radicals is first discussed, followed by a discussion of the more heterogeneous, selective and generally slower reaction of conventional oxidation (Crittenden et al., 2012; Gogate and Pandit, 2004), specifically highlighting H_2O_2, the oxidant of interest to this study.

2.7.2.1 Hydroxyl Radicals

In terms of mechanism, arguably the most homogeneous reactions occur in advanced oxidation, where hydroxyl radicals are the primary oxidant species (Haag and Yao, 1992). By definition, advanced oxidation is the production of hydroxyl radicals at ambient temperature (25°C) and pressure (1 atm) (Crittenden et al., 2012), involving the catalysed decomposition of oxidants, or in select instances, water itself. These radicals are highly electrophilic ($E°_{OH}$ = +2.33

V), reacting indiscriminately with most organic compounds, primarily through addition to double bonds, hydrogen abstraction and electron transfer (von Sonntag, 2006b). Further, their rate of reaction is often only limited by how fast they diffuse in water (Christensen et al., 1982). Catalysts that produce hydroxyl radicals from oxidants at standard temperature and pressure include: ultraviolet light (photocatalysis); titanium dioxide; Fenton (iron) reagents; sonolysis; electrolysis; ozone at elevated pH and; combined H_2O_2 and O_3 (Crittenden et al., 2012). Hydroxyl radicals can also be produced at high temperature and pressure (Troe, 2011), though by strict definition this is not advanced oxidation.

2.7.2.2 Hydrogen Peroxide

Information on the specific mechanisms of H_2O_2 attack on organics and cell constituents is dispersed. It lacks a modern, definitive textbook, as is available for ozone (see Langlais et al., 1991). However, the work by Schumb et al. (1955), although somewhat dated (e.g. H_2O_2 structure not yet confirmed in 1955, etc.), gathers over 1000 references from nearly 150 years of research, giving the most thorough account of H_2O_2 reviewed here, including detailed descriptions of physical, chemical and thermodynamic properties.

Schumb et al. (1955) give the disclaimer that unequivocally predicting H_2O_2 reactions is not possible. However, they provide some general mechanisms, beginning with reaction precursors:

- Molecular H_2O_2 is not strongly reactive with many organics, however;
- Hydrogen peroxide, chemically similar to water, can solvate organic molecules:
  - Result is substantially reduced stability of target molecule;
  - Causes a shift in charge, disrupting the target molecule, perhaps inducing reaction;
  - Note: catalase is expected to react with H_2O_2 in this way
- Separate from or in sequence to solvation, H_2O_2 may dissociate by five primary pathways:

	Reaction Pathway:	**Reactive Product:**
1)	$H_2O_2 \rightarrow 2OH$	hydroxyl radicals
2)	$H_2O_2 \rightarrow HO_2 + H$	hydroperoxyl radical
3)	$H_2O_2 \rightarrow OH^- + OH^+$	hydroxide ion
4)	$H_2O_2 \rightarrow HO_2^- + H^+$,	hydroperoxyl anion
5)	$H_2O_2 \rightarrow HO_2^+ + H^-$	hydroperoxyl cation

In regard to the above, the electron shells of H_2O_2 are complete so it must dissociate to react. Following dissociation, simultaneous electron sharing may occur with attached or nearby organics. While other mechanisms are imaginable, their activation energies are greater than those listed, making them less likely (Schumb et al., 1955).

According to Schumb et al. (1955), the dissociation of H_2O_2 to hydroxyl radicals by reaction 1) is predominant only in the presence of: ionizing radiation, such as that provided by high energy ultraviolet light; metal catalysts such as Fenton reagents; and when subjected to reaction temperatures in excess of 420°C. To illustrate the impact of temperature, Schumb et al. (1955) estimate that without catalysis, the dissociation rate by 1) at room temperature is one molecule of H_2O_2 in every 10^{27} dissociating to one hydroxyl radical per second, whereas at 300°C, this rises to one in a million per second, and so on, with theoretically homogeneous dissociation at 420°C.

To expand on thermal effect, Troe (2011) state that the only reliable data on heat dissociation exists between temperatures of 225 - 725°C. This high temperature positively correlates to the relatively high bond dissociation energy (BDE) of the H_2O_2 oxygen-oxygen bond, which must be satisfied for dissociation to occur. To illustrate: pernitrous acid has a BDE of 92±8.5 kJ/mol and radically dissociates at room temperature; persulfate, with a BDE of 120±11 kJ/mol, dissociates at 70°C; finally, H_2O_2 has a BDE of 210±2.5 kJ/mol, which by extrapolation, requires a substantially higher temperature for dissociation (von Sonntag, 2006a). Up until this point, dissociation and subsequent reaction will be highly heterogeneous (Baldwin et al., 1961); the reactions displayed above shift in dominance as temperature and pressure conditions change.

At temperatures of concern in the liquid phase, there is too little energy to activate radical dissociation (Schumb et al., 1955). Therefore, in liquid phase applications, dissociation by 3) and 4) is most likely. Other reports confirm that dissociation by 4) and subsequent reaction or destabilisation by hydroperoxyl (a.k.a. perhydroxyl) anion, is most favourable (De et al., 1999). Once solvation and/or dissociation has occurred, Schumb et al. (1955) describe some general reaction patterns, including:

- Reaction of dissociated radical or ionic forms with organics:
  - Radicals indiscriminately react, as mentioned previously
  - Ions typically react at functional groups, more readily:
    - With amino than with carboxyl or hydroxyl groups, and;
    - At highly electronegative atoms like nitrogen, oxygen and fluorine
  - Products can be organic peroxide and peroxy acids:
    - These can overtake H_2O_2 and its dissociation products as the most active oxidant in a system, due to their electronic asymmetry, instability and propensity for further reaction
- Molecular H_2O_2 slowly reacts with carbohydrates and fats:
  - Products include oxygen, hydrogen, carbon dioxide, aldehydes and formic and other acids
- Hydrogen peroxide and its dissociative products indicate strong reaction with amino acids
  - Cysteine, which bridges long chain proteins, is particularly susceptible, as indicated by studies on hair and wool
  - Products include aldehydes, nitrate, carbohydrates, fatty acids, ammonia and phosphate

The preceding mechanisms cannot be interpreted as complete. However, they provide insight into the mechanisms of oxidation, and can help to describe some of the observed outcomes of treatments. For example, both O_3 and H_2O_2 seem to have an affinity for oxidizing nitrogen rich compounds such as protein. This would explain increased solubilisation of protein, fatty acids, ammonia and phosphate following sludge oxidation.

Overall, although powerfully oxidative hydroxyl radicals are products of H_2O_2 decomposition and dissociation, in liquid-phase at neutral pH, only targeted catalysis makes them dominant oxidants. Further, although sludge contains trace metallic, Fenton-like catalysts, or carbon minerals that could absorb and discharge significant catalytic heat in MW-oxidative systems, their impact is likely very infrequent compared to the thermodynamically favourable ionic and molecular reactions described above.

2.8 Combined Thermal-Oxidative Treatment

Some benefits of combined thermal and oxidative treatment were mentioned in previous sections. Increased temperature can deactivate antioxidant enzymes such as catalase, which can

otherwise consume oxidants (Wang et al., 2009). Additionally, it can increase the reaction rate of oxidants with target materials. This follows the well-known Arrhenius law, which relates reaction rate, *k*, to the product of optimal orientation and position of potential reactants (A), and the fraction of reactants capable of overcoming barriers of reaction activation energy ($\exp(-E_a/RT)$) (Taylor et al., 2005). According to this relation, increased temperature improves the likelihood that reactants will overcome activation energy to react. Certain studies have claimed the impact of MW athermal effect on reaction rates, athough, as mentioned previously, this study assumes that thermal effects dominate (Kappe et al., 2012a; Lidström et al., 2001).

2.9 Knowledge Gap

Thermal sludge treatment is a proven technology, deployed at commercial scale in the Cambi, Exelys and BioTHELYS processes (Burger and Parker, 2013; Carrère et al., 2008). These all employ high pressure thermal hydrolysis (HPTH), which has confirmed benefit as a sludge pretreatment for anaerobic digestion (Burger and Parker, 2013). Microwave has gained attention as a potential alternative to conventional forms of heating typically used in the thermal hydrolysis of sludge. Previous studies, primarily at lab scale, have identified comparable benefits to digestion using either MW or conventional heat treatment (Mehdizadeh et al., 2013). However, MW may offer the additional benefit of reduced process times and energy savings (Mehdizadeh et al., 2013; Q. Yu et al., 2010). Numerous preliminary studies have confirmed the viability and reproducible benefits of MW thermal treatment. Further study is needed to address the potential for energy savings and the feasibility of scaling these technologies for commercial application.

The design of large scale MW systems introduces many complicating factors to readymade bench-scale household or laboratory generators and reactors. In scaling up, energy efficiency, processing consistency, and control become increasingly important design considerations, all of which depend to some degree on the dielectric and mechanical properties of the target material (Mehdizadeh, 1994). These properties are inherently variable in sludge, a factor that requires exploration. Furthermore, scale-up requires an appropriate choice of microwave frequency and applicator design, which can dictate the uniformity of delivered energy and its penetration depth, in turn determining the design volume of reactors (Mehdizadeh, 1994). Lower frequencies typically reduce issues associated with energy uniformity and penetration depth, and make larger

treatment volumes more realistic (Moseley and Kappe, 2011). For this reason, and the wider availability of larger-scale units, 915 MHz generators are of increasing interest. Further study on MW thermal sludge treatment at increased scale is needed, investigating energy, capital and operation costs and savings, in order to validate the feasibility of the technology (Saha et al., 2011).

Reducing the otherwise intensive energy requirement of MW treatment is an important area for study (Moseley and Kappe, 2011; Remya and Lin, 2011). Research has shown that even where biogas and energy recovery is improved by MW thermal treatment, given the current state of technology, recovered energy is insufficient to offset required inputs (Appels et al., 2013). Elements of process design may be able to overcome this discrepancy, such as choice of equipment or configurations that promote target material consistency and stable operation. Combining chemical additions such as oxidants may offer energy savings to thermal treatment, by affording improved outcomes compared to heating alone (Tyagi and Lo, 2012). These combined treatments might also eliminate the need to employ temperatures above 100°C, used in Cambi, Exelys and BioTHELYS processes. Implicit benefits would include reductions in input energy, as well as the elimination of pressure vessels, improving process safety and simplicity.

Combined thermal-oxidation, using H_2O_2, has been studied previously; however, further study is needed to compare different frequency and process configurations to existing research (see Wong et al., 2006b); to confirm an appropriate dose of H_2O_2 (Eskicioglu et al., 2008b); and to explore optimal ways to introduce chemical additions to maximize their effect (Gogate and Pandit, 2004; Wang et al., 2009)

3 Materials and Methods

This research was an assessment of microwave (MW) thermal-oxidative treatment with a pilot scale system, recently acquired by UBC Civil Engineering and used here for the first time. As such, substantial effort went into designing, constructing, troubleshooting and developing procedures for the equipment. This chapter provides an overview of the apparatus used, the operating procedure as well as the sampling and analytical methods employed. The aim is to provide a high level of detail so that procedures can be replicated.

3.1 Apparatus

Figure 1 is a photograph of the pilot-scale MW system employed in this study. Numbers indicate the three fundamental components of the system: the 1) generator, 2) applicator, and 3) reactor system. Details of these components are discussed in the following sections.

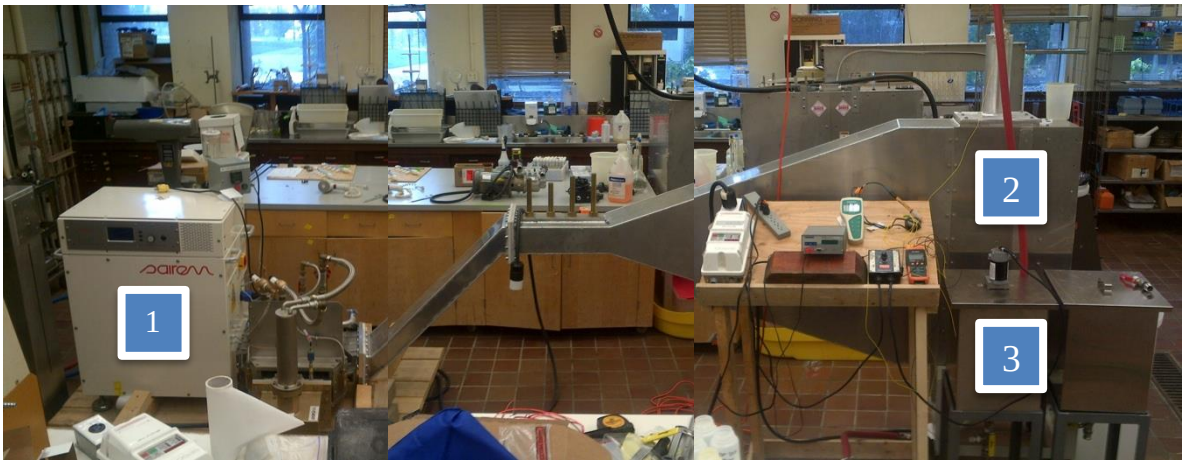

Figure 1: Pilot Scale Microwave System: 1) Generator, 2) Applicator and 3) Reactor System

3.1.1 The Microwave Generator

In reference to Figure 1, number 1 corresponds to the MW generator. The generator is a commercially available model manufactured by Sairem (2013), employing a frequency of 915 MHz, with power adjustable between 0.6 and 5 kW. It houses the magnetron, i.e. the component that generates MW energy, as well as supporting components for power supply, air and water cooling, control and containment. As shown in Figure 2, attached and immediately adjacent to the base of the (a) generator is the b) isolator, as well as a c) water cooling system that circulates water to the magnetron and to the isolator reservoir. The isolator is an imperative part of the system's

safe operation. It is essentially a conduit, containing a one-way ferrite lens that allows MW energy to travel away from the magnetron, diverting any returning energy to a circulating reservoir of water. It plays the imperative role of protecting the magnetron, isolating it from any field fluctuations in the applicator that can couple with the magnetron and interfere with the consistency of generated MWs (Meredith, 1998). Furthermore, because water absorbs errant, reflected power, it has less chance of leaking to surroundings.

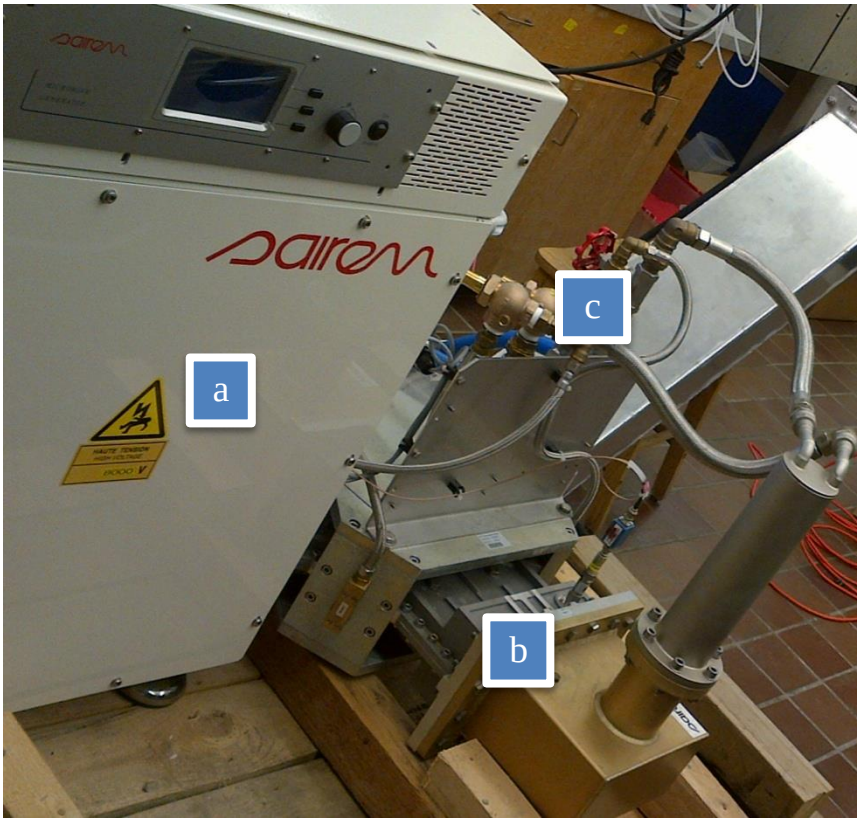

Figure 2: System a) Generator, b) Isolator and c) Water Cooling System

Direct, manual control of the generator is facilitated through the interface visible in Figure 2. This includes a display, three buttons that correspond to displayed prompts, a dial that allows on screen navigation as well as power adjustment, and an on/off switch. For the current study, manual control was assumed. In future iterations, the option of remote control is available, and can be connected through a selection of communication ports on the side of the generator.

In order to operate, the generator requires that three safety preconditions be satisfied. The first is positive indication of a load in the system. In this research, the load is liquid flowing in the

reactor. Without an adequate load, MW energy produced by the generator is unused and unabsorbed, reflecting back to the isolator. Load indication is currently satisfied with a positive digital signal bridged between pins of the generator's RS-232 port, leaving the onus on the operator to ensure that liquid is flowing. In the future, a flow switch could be installed for this function. In the current iteration, a switch capable of operating in a slurry heated above 90°C was not found.

The second and third preconditions are associated with adequate flow of water to the magnetron cooling system and to the isolator reservoir. Shown in Figure 3, these conditions are each satisfied by a d) paddle flow switch, manually calibrated to report a fault when flow falls below 7 L/min (minimum of 6.5 L/min indicated by the manufacturer). Water for this system is drawn from municipal supply, controlled by a e) diaphragm valve and adjusted to required pressure (<58 psi) and temperature (17-22°C) by a g) pressure regulator and f) thermostatic mixing (temperature control) valve. The generator does not send or receive information regarding pressure and temperature, so these parameters must be monitored manually with an installed gauge and

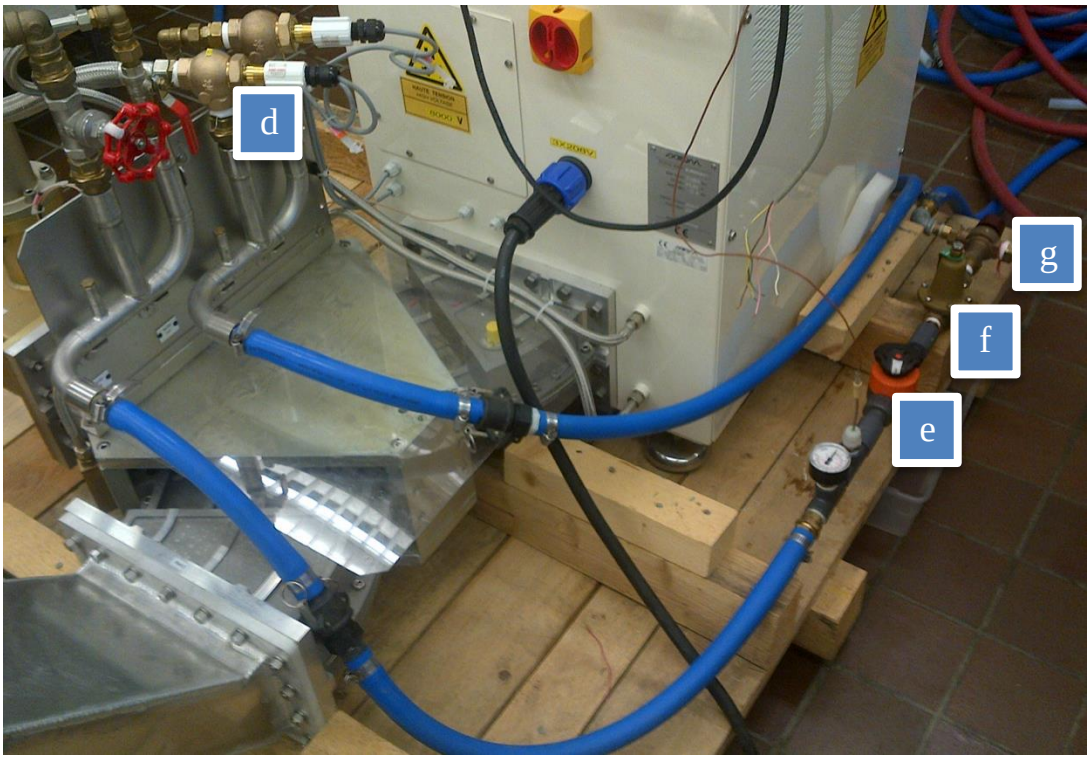

Figure 3: Water cooling system: d) Paddle Flow Switches; e) Diaphragm Valve;
f) Pressure Regulator; and g) Thermostatic Mixing Valve

thermometer. When the flow of water is inadequate to satisfy the flow switches, the generator is sent a fault signal, which simultaneously cuts power from the magnetron and indicates the signal source on the control display. Faults must be satisfied to commence or restore normal operation.

A final source of feedback between the generator and isolator is a radiation sensor that measures the magnitude of reflected power and reports it to the generator display. This sensor is not a switch. Should it fail, the only indication is a zero reported for reflected power, with no interruption to the generator. Reflected power gives vital information on system efficiency, so in the event of failure a replacement should be found before operating the generator. The difference of reflected power and the selected forward input power, both of which are reported on the display, gives the overall power delivered to the applicator. The reflected power can be minimized, and delivered power maximized, by making adjustments to tuning pegs installed on the applicator.

3.1.2 The Applicator

In reference to Figure 1, number 2 corresponds to the applicator. This custom designed component acts as conduit and radiation reaction chamber as electromagnetic waves travel from the generator to the load. It is made out of aluminium, which reflects and confines waves to the chamber interior. Exceptions to this include minimal amounts of energy that may be absorbed by the aluminium itself (Metaxas and Meredith, 1983) or leaked through joints and small holes in the chamber. Major leaks in the applicator entrance and exit are contained with custom aluminium conduits. Minor leaks are sealed with aluminium tape. Seals were confirmed by a radiation survey.

The applicator was designed to convey the electric field of electromagnetic waves with their peak amplitude oriented vertically. The design promotes the formation of a uniform wave, akin to a single-mode system. The alternative is a multimode system, typical in household MWs, where electromagnetic waves are deliberately stirred into a chaotic distribution (Kappe et al., 2012b).

The peak amplitude of a uniform wave correlates to maximum energy intensity (Kappe et al., 2012b). In theory, the applicator was designed to align this peak with a pipe running through the applicators wide end, promoting maximum energy transfer to the load. Any unabsorbed energy is reflected by an aluminium wall at the end of the applicator, the position of which was adjusted to correspond with a multiple of the 915 MHz wavelength (32.75 cm) (Kappe et al., 2012a) to reflect

waves in-phase. The applicator was designed with a wide, expanded end to provide a larger reaction space. With this expansion, liquid flowing through MW transparent pipes is irradiated over a longer distance. This is in contrast to conventional applicators, which are typically a rectangular shape with a constant width, directing energy to a batch reaction vessel.

The applicator was carefully designed to target electromagnetic energy at the load. However, in reality, the propagation of waves in the applicator is likely inhomogeneous, due in part to: a distribution of frequencies generated by the magnetron: 915±10 MHz (Sairem, 2013); unpredictable patterns of wave reflection and scattering in the applicator; and heterogeneity of the target medium, including changing composition and dielectric properties. This changes how energy is absorbed and effects the overall distribution of electromagnetic fields and power intensity in the applicator (Zhu et al., 2007).

The reflected power, sensed by the radiation probe in the isolator and reported to the generator display, provides feedback about these field fluctuations. Changes in the field generally correspond to an observable change in the reflected power. This illustrates the concept of load matching. A simple analogy would be a motor changing gears to provide the most efficient transfer of energy to a drive shaft. So too must a magnetron generator be adjusted to match a load. Specifically, to maximize power transfer and minimize reflection, a generator's internal impedance must match the load impedance (Metaxas and Meredith, 1983). Where the load fluctuates, due to changes in target composition and dielectric properties, the impedance requires adjustment for optimal energy transfer efficiency. In practical application, it is typically not feasible to tune a generator, so applicators are fit with tuning devices (Meredith, 1998). The applicator employed here uses a manual tuning system of 4 brass screws, set at ¼ intervals along the approximately 33 cm, 915 MHz wavelength.

As these screws wind into the applicator, they couple with the electric field and alter the load impedance. Trial and error is needed to minimize reflected power as much as possible, ideally less than one tenth of the forward input power, as is typical for most industrial MW applications (Metaxas and Meredith, 1983). For small mismatches, screws are said to adjust independently, whereas for large mismatches, they are interdependent and sequential adjustment is required

(Meredith, 1998). It is necessary to avoid winding the screws in more than half the waveguide height, as they can become resonant and dissipate MW energy as heat (Meredith, 1998).

The tuning configurations used are provided for reference in Table 3. Screw length refers to the length of screw protruding from the applicator, including the securing bolts. Limiting length is 21.5 cm, where the screw does not intrude into the applicator and is inactive in tuning. Attempts at adjusting the tuning as an experiment progressed proved ineffective, so a single tuning was set for each target medium. For semi-continuous experiments, this proved to be a limitation of the system, as a single setting often proved suboptimal over the range of experimental temperatures. This was not an issue for continuous operation.

Table 3: Applicator Tuning Configurations

Target Medium	**Screw Length (cm)**			
	1	2	3	4
Tap Water	21.5	16	14	21.5
Manure (4% TS)	21.5	16	21.5	21.5
Sludge (0.8% TS)	21.5	16.8	18.2	21.5

Ultimately, although suboptimal, a single setting meant that experiments were performed under equivalent conditions, allowing consistent comparison between runs. Details of tuning, in terms of reflected power, will be discussed in following chapters.

3.1.3 The Reactor System

In reference to Figure 1, number 3 indicates the reactor holding tank, which represents the central holding unit for a wider network of pipes and pumps making up the reactor system. This system serves to contain and convey a target liquid as it circulates through the applicator and is subjected to MW irradiation. This system was designed and constructed with the priority of easy modification, facilitating different scales and modes of operation. Two reactor configurations were deployed in this research: a semi-continuous system and a continuous system. These are discussed in detail in the following sections.

3.1.3.1 Semi-continuous Reactor System

A diagram of the semi-continuous reactor system is provided in Figure 4**.** This configuration was used in initial water tests as well as semi-continuous manure and sludge experiments.

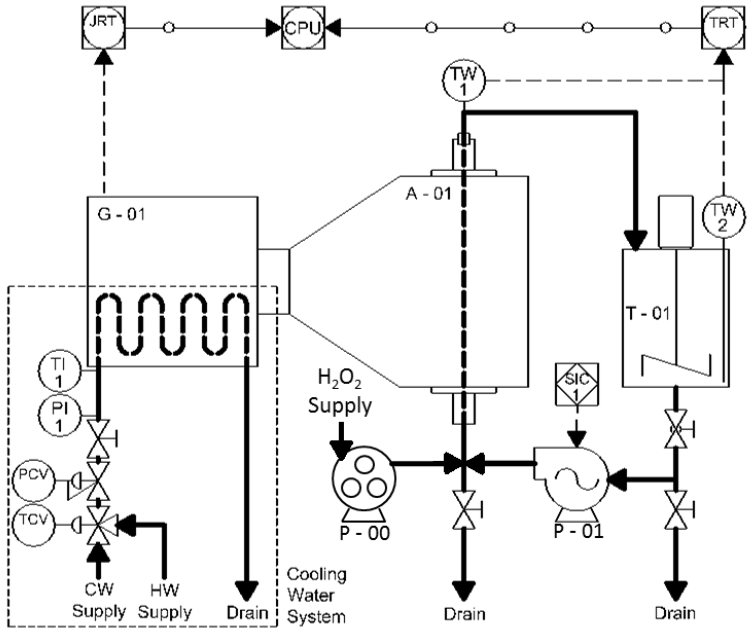

Legend

Key Equipment:

G-01	Generator
A-01	Applicator
T-01	Reactor holding tank
P-00	Peristaltic Pump
P-01	Progressive Cavity Pump

Instrumentation and Monitoring:

PI	Pressure indicator
TI	Temperature indicator
JRT	Power recorder/transmitter
TW	Fibre optic temperature probe
TRT	Temperature recorder/transmitter

Process Control:

TCV	Temperature control valve
PCV	Pressure control valve
SIC	Variable frequency drive

Figure 4: Semi-continuous Reactor System Diagram

A progressive cavity pump, P-01 (Moyno, 332 rotor/stator) circulates liquid through the applicator. Insulated synthetic rubber hose carries liquid to and from the applicator. Inside the applicator, liquid is irradiated as it flows through two MW transparent, silicon hoses. These hoses hold 0.6 L of liquid in the applicator at any time. The change in liquid temperature, from inlet to outlet, depends on the generator input power and liquid retention time in the applicator, which is dictated by an adjustable flow rate. Note that hydrogen peroxide (H_2O_2) was delivered by peristaltic pump (P-00) in sludge experiments, whereas manure runs had H_2O_2 dosed all at once.

3.1.3.2 Continuous Reactor System

A diagram of the continuous reactor system is provided in Figure 5. This configuration was used for continuous experiments with sludge as the target liquid. It retains all elements of the semi-continuous system listed above, adding: a continuous feed holding tank (T-03) and mixer for untreated liquid; a second progressive cavity pump (P-02) (Moyno, 331 rotor/stator) to drive fresh feed; and an overflow pipe from the reactor holding tank (T-01) to an identical second holding tank (T-02).

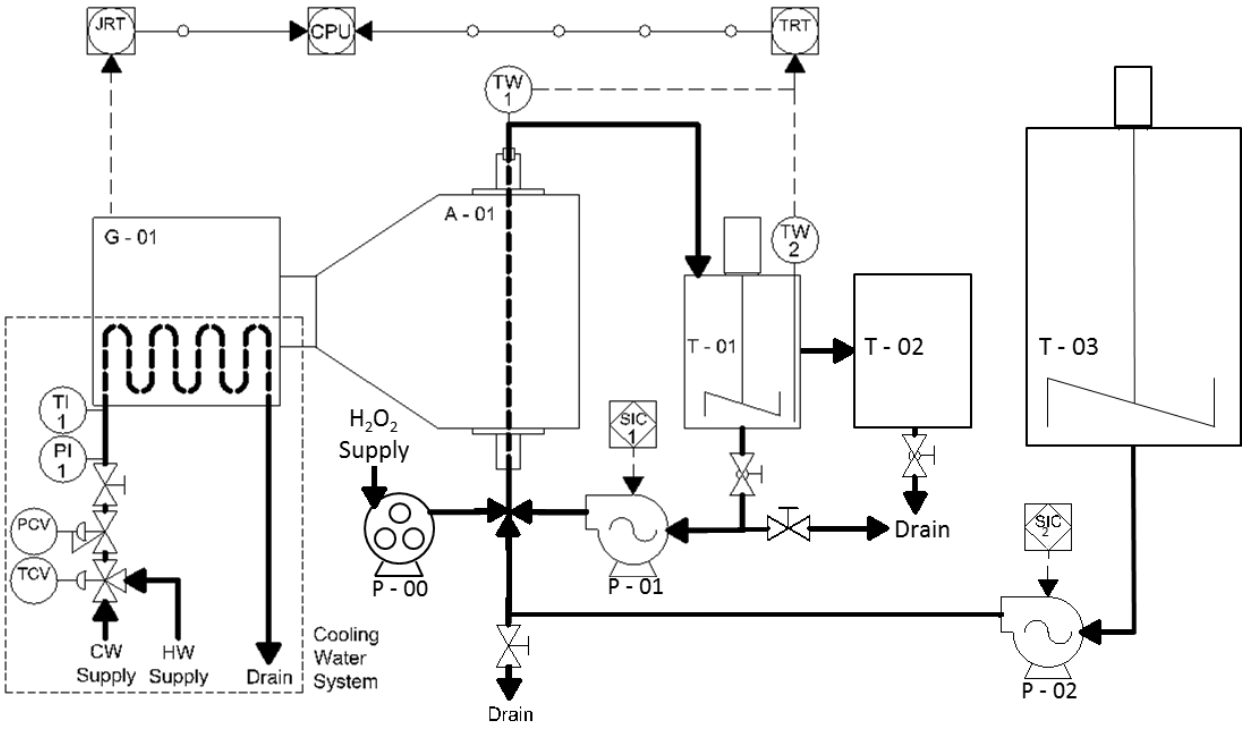

Figure 5: Continuous Reactor System Diagram

Fresh, room temperature liquid was introduced to the system by mixing it with hot liquid cycling from the semi-continuous reactor holding tank, immediately prior to entering the applicator. Having observed an average temperature rise per pass in semi-continuous experiments, a set of feed to recycle flow rate ratios were calculated and tested so that the drop in temperature resulting from cool, incoming feed was compensated by subsequent temperature rise in the applicator. In this way, the continuous system operated at a steady temperature with minimal adjustment.

3.1.3.3 Reactor Instrumentation and Monitoring

Temperature and process power consumption was monitored closely throughout experimental runs. Temperature was measured with fibre optic probes, which are unaffected by MW, and processed by a signal conditioner (Neoptix, Reflex). Two temperature probes were employed, one immersed in the bulk liquid of the reactor holding tank and one installed to measure liquid at the outlet of the applicator. Vigorous mixing ensures that the holding tank bulk liquid temperature closely matches the temperature of liquid entering the applicator. The difference between bulk and outlet temperature constitutes temperature rise per pass.

Input power and energy consumption was monitored at the supply outlet by power meter (Accuenergy, Accuvim-L). This measured all of the energy delivered and consumed by the generator, including draw for MW generation as well as cooling and control processes. The temperature processor and power meter communicated with a computer via USB, which was installed with the manufacturer's software, to log incoming measurements. Data was logged in 10-second intervals, which provided more than adequate resolution.

3.2 Operating Procedure

This section provides the details on the source and handling of experiment liquids, as well as experiment preparation, operation and the sampling regime.

3.2.1 Target Liquid Source

As previously mentioned, three different liquids were tested in the pilot-scale equipment: Vancouver tap water; liquid dairy manure from the UBC Dairy Research Centre in Agassiz, BC; and waste secondary sludge from UBC Civil Engineering's Staging Environmental Research Centre (SERC). Liquid dairy manure was collected from a sump following solid-liquid separation, on March 20, 2014, and stored in a refrigerator at 4°C, until use. Sludge was collected directly from the aerobic tank of train A at SERC. For reference, SERC train A is a University of Cape Town (UCT) biological phosphorus removal process with membrane solid-liquid separation, operating a 25-day solids retention time at the time of experimentation. For semi-continuous experiments, sludge was collected from SERC the morning of experiments and treated within an hour or two. For continuous experiments, in order to obtain required volumes of sludge while minimizing impacts to ongoing experiments at SERC, sludge was collected over the course of 3 days. Stored volumes were refrigerated at 4°C, and then mixed and acclimated for 1 hour prior to use.

3.2.2 Operating Variables

Given its' scale and modularity, there are a range of adjustable options available for the 915 MHz MW system. These include generator forward power, volume of target liquid to be treated, as well as liquid recycle and continuous flow rates. Preliminary experiments revealed optimal operating settings for each. This section reports standard values for these variables.

3.2.2.1 Forward Power

For this research, the fastest bulk liquid heating rate was desired, which required the highest possible forward power. The maximum generator output is 5 kW, however, at low liquid temperatures it was observed that setting forward power at 5 kW caused reflected power to be higher than 2 kW, resulting in an 'RP Limitation' warning on the generator display. This indicated that the isolator water reservoir was absorbing large amounts of energy, and despite attempts, this could not be resolved by tuning. While it did not directly interrupt operation, it was speculated to contribute to water cooling system faults. It was found that reflected power could be kept below 2 kW by employing a 4.5 kW forward power. This became the operating standard. As it turned out, this offered additional benefits to process control flexibility when the system was used to hold a liquid at a certain temperature. Forward power could be adjusted up or down to control the temperature rise per pass, and as a result, the bulk liquid heating rate.

3.2.2.2 Volume of Target Liquid

Like forward power, target liquid volume affects the bulk liquid heating rate. For semi-continuous experiments with forward power set at 4.5 kW, preliminary runs showed that the MW system could heat 12 L of liquid to 90°C, hold it there for five minutes, and total run time would be about 30 minutes. In half an hour, the heating rate was slow enough that sampling and H_2O_2 delivery were adequately spaced and easily managed. On the other hand, this relatively short processing time meant that set-up, target liquid preparation, treatment runs, clean up, some initial sample preparation and any necessary troubleshooting could be completed in about a day, with sample analysis performed in following days. Given these considerations, a volume of 12 L became the standard for semi-continuous experiments.

Three primary constraints guided the choice of volume for continuous experiments. First was the availability of sludge from SERC, which at the time was about 50 L/day. Two days storage, with experiment on the third day, was deemed acceptable, making 150 L of sludge available. This ensured that sludge was relatively fresh, and that collection and experiments were performed by mid-week, with initial sample preparation, preservation and more sensitive analysis complete by the end of the week. Second was the need for a large enough volume of hot liquid circulating in the reactor holding tank to maintain a stable temperature, given fluctuations introduced by cold feed. The objective was to keep temperature fluctuations small so they could be overcome by

adjusting input power, with recycle and feed flow rates held constant. Third was an expectation that a continuous system would take time to stabilize, requiring that the liquid in the reactor turn over several times. This was initially estimated as being three Hydraulic Retention Times (HRT). However, results from the first continuous experiment indicated that more time was needed. Five HRTs proved to be sufficient in subsequent experiments.

Various configurations were calculated from expected liquid temperatures and flow rates. Given the constraints, for continuous runs the reactor holding tank volume was set at 20 L. Altogether, 120 L of sludge was required to fill the reactor holding tank and provide enough feed volume for five HRTs.

3.2.2.3 Reactor Recycle Flow Rate

The reactor recycle flow rate, or the flow rate at which liquid was recycled through the applicator, served as both a dependent and independent variable in this research. Varied flow rate was investigated in water testing and semi-continuous sludge experiments. These results indicated an optimal flow rate for continuous sludge experiments, as will be described in detail in following chapters. Changing flow rate alters liquid residence time in the applicator, changing the temperature rise per pass. Theoretically, given a constant forward power and recirculating volume, a consistent amount of energy is supplied to the liquid. As a result, the bulk-heating rate should be minimally affected by recycle flow rate. However, higher flow rate did show some disadvantage for semi-continuous sludge runs. A recycle flow rate of 6.5 L/min proved optimal, without exerting observable stress on the pump.

3.2.2.4 Continuous Feed Flow Rate

Calculations performed to determine required reactor volumes for continuous experiments also informed continuous feed flow rates. Based on semi-continuous experiment observations of temperature rise per pass, the maximum feed flow rate was calculated as being about 0.6-0.7 L/min, independent of recycle flow rate. This is the highest theoretical feed flow attainable, while maintaining a stable reactor temperature and employing 4.5 kW forward power. Experimentation confirmed reactor temperature stability given these flow and input power settings.

3.2.3 Hydrogen Peroxide Addition

Hydrogen peroxide was delivered differently for manure, and both semi-continuous and continuous sludge experiments. In all cases, doses were calculated on the basis of a target liquid's total solids (TS) content: g H_2O_2/g TS.

For manure, H_2O_2 was dosed all at once following acidification. For semi-continuous sludge experiments, the dosed concentration was varied between runs. It was delivered at a continuous rate over the course of one overturn of liquid in the reactor tank, timing of which depended on the recycle flow rate. For all but the first run (which was dosed at the beginning of run for comparison), doses were added after bulk liquid reached 60°C, thereby avoiding catalase inhibition.

For continuous sludge runs: the reactor tank was dosed over one overturn of the reactor tank after liquid had reached 90°C. The dosing pump was then adjusted to deliver a dose corresponding to untreated solids in the incoming feed, and turned back on for the duration of the run.

3.2.4 Sampling

Only temperature and power data were collected for water experiments, whereas a suite of analyses were performed for manure and sludge, detailed in Section 3.3. Sampling regimes for manure and sludge are provided in Table 4.

Table 4: Experiment/Treatment Sampling Regime

Process and Target Liquid	Sample Volume (mL)	Sampling Increment	Sample Collection Regime
Semi-continuous Manure	500	10°C	60, 70, 80, 90°C and 90°C + 5 min
Semi-continuous Sludge	250	15°C	45, 60, 75, 90°C and 90°C + 5 min
Continuous Sludge	250	HRT	90°C, 1/2, 1, 2, 3, 4 and 5, HRT

3.2.4.1 Controls

All sampling sets included a raw, untreated control sample and, where necessary, an acidified raw control sample. To provide an oxidant treatment control sample, three separate raw sludge samples were subjected to H_2O_2 alone. For future reference, these did not vary significantly from raw samples. To provide a thermal treatment control, semi-continuous and continuous sludge experiments were performed using MW only.

3.2.4.2 Semi-continuous Process Sampling Regime

A standout benefit of this MW system was that samples could be drawn as temperatures rise, helping elucidate reaction kinetics as experiments proceed. From early stages of experiment design it was known that temperature would guide sampling. Initially for manure, samples were taken at 10°C increments, beginning at 60°C. Results showed that this 10°C increment provided unnecessarily high resolution, with significant overlap for several values. For subsequent sludge experiments, 15°C increments were used. Further, based on prior experiments and information from literature, 60°C was expected to be an inflection point where a significant shift in results would occur. This was not apparent for manure, but was clearly evident for sludge. An initial 45°C sample was drawn to illustrate sludge character before this 60°C inflection, followed by a 75 and 90°C sample. Finally, all semi-continuous experiments included a final sample taken five minutes after 90°C was reached. This was used to elucidate the benefits of holding samples at a constant, high temperature.

Once the bulk liquid had reached the predetermined temperature, samples were withdrawn from a drain at the bottom of the reactor holding tank. For manure, 500 mL was withdrawn for each sample. This provided more volume than necessary, which initially proved useful. Manure is very challenging to analyse, requiring substantial effort to filter and in some cases, 100 fold dilutions. Having more volume lent flexibility to developing analytical methods, allowing trial and error to hone accuracy and precision. However, it was recognized that drawing this much sample might have some overall effect on the process. Having honed analytical methods, 250 mL was drawn for subsequent sludge experiments.

3.2.4.3 Continuous Process Sampling Regime

Continuous sludge experiments used a markedly different sampling regime. Here, the aim was to find when results stabilized in a hot, 90°C reactor fed a continuous supply of cold sludge. As such, sampling was performed in increments of time, based on the HRT of the reactor holding tank: roughly 30 minutes. An initial 90°C sample was taken to establish a baseline expectation for treatment and this temperature was retained, ±2°C, for the duration of experiments. Subsequent samples were taken first at fractional HRT to elucidate trends as the process stabilized, then at complete turnovers, until five HRTs had elapsed. Samples of 250 mL were taken from the reactor tank overflow at times indicated.

3.3 Analysis

The following section provides information on quality assurance and control, centrifugation and filtering procedures, and the analytical methods employed.

3.3.1 Quality Assurance/Control

To ensure quality in analytical procedures, sensitive analyses were performed within one day of experimentation. This included prioritizing centrifugation and filtration for analyses requiring soluble sample and solids measurements, which might otherwise repartition in storage. During any break in analysis, samples were refrigerated at 4°C. Although analyses on total sample fractions took a lower priority, they were complete within a few days of experimentation.

For every analysis that required a preparation step, where the experimenter or sample heterogeneity could introduce error, samples were run in triplicate. For analyses that would primarily involve equipment error, such as pH or conductivity readings, a common deviation, based on three or more initial measurements was determined.

Sample mean and standard deviation was calculated for each triplicate. For every data point, no more than 10% error was accepted (based on the ratio of standard deviation divided by mean). Where error in excess of 10% occurred, triplicate samples were evaluated for outliers. Outliers were identified as those samples that were either below or above a ratio of 0.85 or 1.15, respectively, when divided by the next closest value. This is based on the observation that, when data falls in this range, calculated error does not typically exceed 10%. If the other two samples in the triplicate were within 0.85 or 1.15 of each other, the outlier was screened and these were taken as representative. If this evaluation failed, where possible, analysis was repeated.

3.3.2 Statistical Analysis

For statistical analysis one-tailed t-tests and analysis of variance (ANOVA), both with 95% confidence intervals, were used. These tests determine if differences in treatment are distinguishable from sample standard deviations. If not, the null hypothesis (μ_0) is confirmed: samples represent the same population so treatments are the same. This occurs where differences between treatments are insignificant, or for total portion samples where differences would only

result from sampling error, substantial boiling or volatilisation. Experiments were conducted below the boiling point of water, so boiling was expected to be insignificant.

Where means were determined to be equivalent, all sample means and deviations were pooled together for use in later calculations. For total portions, on the rare occasion where means proved to be different, the highest mean was used for subsequent calculations, expecting that this would report the most conservative result.

3.3.3 Soluble Samples

Solubility was assessed as liquid portions that passed through a 0.45 μm cellulose filter. More intensive preparation of the target liquids proved helpful in accelerating filtration. Manure, being difficult to separate, was spun in a high-speed centrifuge at 15,000 RPM for 20 minutes. Sludge was spun at 2500 rpm for 20 minutes. Following centrifugation, both liquids were coarse filtered through glass microfiber (Whatman 934-AH 47 mm). They were then passed through the smaller pore cellulose filters.

3.3.4 Dilutions

Table 5 provides dilution factors for each analytical method. Dilutions were developed to optimally utilize the available range of each method, most often to avoid exceeding an upper limit. The dilution method was also considered. For dilution factors below 10, dilutions could be performed with minimal error by directly pipetting sample and diluent water to test containers. For factors above 10, significant error was observed to result from direct pipette. These dilutions were performed in volumetric flasks, transferring a minimum sample volume of 0.5 mL by pipette.

Table 5: Analyte Dilution factors and Upper Limits of Accuracy for each Method

Analyte	Method Upper Limit (mg/L)	Dilution Factor			
		Manure		Sludge	
		Soluble	Total	Soluble	Total
PO_4^{-3}	25	10	n/a	4	n/a
TP	1 mg total mass	3.33	5	0.5	1
NH_3	50	50	n/a	1	n/a
TKN	2 mg total mass	3.33	5	0.5	1
VFA	200	5	n/a	1	n/a
COD	900	20	100	5	20
Metals	1000	20	20	10	20

3.3.5 Analytical Methods

The following section provides details on analytical methods employed in the research. Aside from temperature and power measurements, settling was the only test performed at the time and temperature of sampling. All other samples were bottled and transported from the equipment location to the nearby Civil Engineering, Environmental Laboratory for analysis. Where necessary, samples were preserved according to Standard Methods (APHA, 2005)

3.3.5.1 Settling

A 100 mL graduated cylinder was filled with sludge and allowed to settle undisturbed for half an hour, after which results and observations were recorded.

3.3.5.2 Lab Temperature and pH

Lab temperature measurements are used to scale results of conductivity and ensure comparability for particle size distribution (PSD) and capillary suction timer (CST) results. The pH was measured to monitor changes introduced during treatment, as a substantial drop could affect downstream processes. Temperature and pH were measured simultaneously with a combination multimeter (Beckman (phi) 44 pH meter). It was two-point calibrated for pH with 4 and 7 pH buffer solutions (Ricca Chemical Company).

3.3.5.3 Conductivity

Ionic conductivity has substantial effect on MW absorption. It was measured to elucidate differences between samples and levels of treatment. Measurements were taken as close to 25°C as possible with a conductivity meter (Radiometer-Copenhagen, type: 3DM 3b). Where samples were not 25°C, readings were adjusted by 2% of the reading per degree (EPA, 1984). Prior to measurement, the instrument was calibrated to appropriate range with stock potassium chloride solutions (Hanna Instruments, HI 7030 12880 μS/cm and HI 7031 1413 μS /cm). A relationship of conductivity to salt concentration is provided for reference in Table 6.

Table 6: Relation of Salt Concentration to Conductivity

Sample Source	Salt Conc. (g NaCl/L)	Conductivity (μS/cm)
Tap Water	-	29
Stock Solution (Tap Water + NaCl)	1	1876
	2.5	4691
	5	8830
	10	17181
	20	32285

3.3.5.4 Hydrogen Peroxide Residual

A field test kit (HACH Hydrogen Peroxide Test Kit, 0.2-10 mg/L, Model HYP-1) was employed for initial residual measurements. This provided a rough result to inform the development of more accurate methods. Accuracy and precision were increased by using an idiometric titration method (US Peroxide, 2014). This method was verified by testing standard solutions of stock H_2O_2.

3.3.5.5 Phosphorus

In natural waters, phosphorus exists as phosphate (a.k.a. reactive phosphorus or orthophosphate), polyphosphate and organic phosphorus (APHA, 2005). Speciation was accounted for with the following methods.

3.3.5.5.1 Phosphate

Phosphate was measured from soluble sample using flow injection analysis (Standard Methods 4500-P G. Flow Injection Analysis for Orthophosphate). Flow injection analysis was performed on a Lachat Quikchem (Series 8000, Zellweger Analytics Inc.) equipped with XYZ auto-sampler (ASX-500 series) and a reagent pump (RP-100 series).

3.3.5.5.2 Total Phosphorus

Total phosphorus (TP) was partitioned to total and soluble fractions, and measured by two methods. Samples were first analysed according to an adjusted EPA (1974) method (mercury sulphate omitted), involving block digestion in a sulphuric acid solution and analysis by flow injection. Phosphorus was also analysed as a metal, described later.

Total phosphorus measurements are expected to account for phosphate, polyphosphate and organic phosphorus. However, results indicated that flow injection typically returned lower values than metals analysis (Inductively Couple Plasma – Optical Emission Spectroscopy), suggesting that current modes of block digestion may be ineffective in liberating more recalcitrant forms of phosphorus, perhaps organically bound. This method is currently undergoing review.

3.3.5.6 Nitrogen

In natural water, nitrogen exists as ammonia (NH_3), nitrate and nitrites (NO_x) and organic nitrogen. Speciation was accounted with the following methods.

3.3.5.6.1 Ammonia

Ammonia was analysed from soluble sample using flow injection analysis (Standard Methods, 4500-NH3 H. Flow Injection Analysis). It utilized equipment previously detailed for phosphate.

3.3.5.6.2 Nitrate and Nitrite (NO_x)

Samples were analysed for total NO_x, also by flow injection analysis. Preliminary results indicated minimal concentrations, near the limits of detection. As such, nitrate and nitrite measurements were discontinued.

3.3.5.6.3 Total Kjeldahl Nitrogen

Total Kjeldahl Nitrogen (TKN) was partitioned to total and soluble fractions. Samples were analysed according to a (US EPA, 1993b) method, involving block digestion in a sulphuric acid solution and analysis by flow injection.

Digestion recovers nitrogen as ammonia from compounds of biological origin, such as amino acids, proteins and peptides. It may not recover nitrogen compounds of some industrial wastes such as amines, nitro compounds, hydrazones, oximes, semicarbazones and some refractory tertiary amines. Nitrates are not reported by this method.

3.3.5.7 Chemical Oxygen Demand (COD)

Chemical oxygen demand (COD) was performed for soluble and total samples by colorimetry (Standard Methods, 5220 COD D. Closed Reflux, Colorimetric Method). High range COD vials were used for every sample, given appropriate dilutions. High range accurately reports results between 20-900 mg/L. Digestion was performed in a HACH COD reactor (model 45600) for 2

hours at 120°C. Absorbance was measured by spectrophotometer at 600 nm (HACH DR 2800) and calibrated with two blanks containing reagent and 2 mL of distilled water. The zero point was set with an undigested blank and the reagent quality was confirmed by measuring a digested blank. No reagent effect was observed in any of the digested blanks.

3.3.5.8 Total and Volatile Solids (TS/VS)

Total and volatile solids were measured according to Standard Methods (2540 Solids B. Total Solids Dried at 103-105°C and E. Fixed and Volatile Solids Ignited at 550°C). Samples were held on aluminium weighing dishes (Fisherbrand cat. No. 08-732-101: low form, aluminium, fluted, 1 3/8 fl. Oz./42 mL). Total solids samples were measured after baking in an oven (Fisher Scientific Isotemp Oven or VWR scientific 1350 FM Forced Air Oven) at 105°C for a minimum of 8 hours. Volatile solids were measured after firing in a muffle furnace (Thermolyne 30400 Furnace or Lindberg (General Signal)) for at least one hour steadily at 550°C. Total solids were reported in % (w/v) or mg/L while VS was reported as the volatile fraction, % (w/w), of TS.

3.3.5.9 Total and Volatile Suspended Solids (TSS/VSS)

Total and Volatile Suspended Solids were measured according to Standard Methods (2540 Total Suspended Solids Dried at 103-105°C E. Fixed and Volatile Solids Ignited at 550°C). For each sample, 2 mL of sample was filtered through glass microfiber filters (Whatman 934-AH, 70 mm) and washed with distilled water. This test employed the same ovens used for TS and VS.

3.3.5.10 VFA

Volatile Fatty Acids (VFAs) were measured by Gas Chromatograph (Standard Methods, 5560 B. Gas Chromatograph Method).

3.3.5.11 Metals

Samples were digested in aquaregia and H_2O_2. They were then brought up to 20 mL with distilled, deionized water and measured by Inductively Coupled Plasma (ICP) with Optical Emission Spectroscopy (OES).

3.3.5.12 Particle Size Distribution

Particle Size Distribution was measured using a Mastersizer 2000 equipped with Hydro 2000S sample port and evaluated using Mastersizer software (Malvern Instruments). Settings included 1

rinse cycle, 3 measurement cycles – with the average being the result taken – sample measurement time of 20 s, at 20,000 snaps, and an obscuration of 15-25%, as advised by Mastersizer software.

3.3.5.13 Capillary Suction Timer

Capillary suction time was measured with a Komline-Sanderson device according to Standard Methods (2710 G. Capillary Suction Time).

4 Water Experiments

This section describes a series of preliminary water experiments designed to test the threshold operating conditions of the pilot-scale microwave (MW) system. These experiments helped to provide a foundational understanding of the observed behaviour of this novel system.

4.1 Problem Statement

This research is the first deployment of the pilot-scale 915 MHz MW system. The system is a custom design, with manual control of delivered power, tuning and recycle flow rates. Characterisation and optimisation of these variables was required to determine their effect on overall system operation and energy efficiency. One of the most important gaps in knowledge, hypothesized to have substantial effect on efficiency, was how the system would behave given differences in the composition or delivery of target loads. It was necessary to determine the conditions that maximized the energy transfer and subsequent heating rate of the target liquid, as well as the any conditions that might display suboptimal efficiency or instability.

4.2 Objectives

The objective of water runs was to determine if a change in a) recycle flow rate and subsequent temperature rise per pass or b) ionic concentration would contribute to more efficient energy transfer, as indicated by decreased energy consumption and increased heating rate (i.e. shorter heating time).

4.3 Results

Water runs were performed in two stages. Either recycle flow rate or ionic concentration was adjusted to a predetermined level, kept constant and a semi-continuous of 12 L of water was heated until the outlet temperature met 90°C. For each experiment, tuning was held at one setting and forward power was constant at 4.5 kW. For these experiments, only physical data was collected, including: reverse power, energy consumption and temperature, all measured with respect to time.

4.3.1 Recycle Flow Rate

Recycle flow rates tested were 1.75, 2.8, 4.5, 6.5 and 7.5 L/min, all with a sodium chloride (NaCl) dose of 1 g/L. The highest flow, 7.5 L/min, proved to be the physical upper limit of the pump configuration. At this setting, the pump motor displays excessive audible and visible

vibration, which should be avoided. The effect of different flow rates, on average heating rate, time and energy used, is provided in Table 7. A graphical representation of heating rate, time and temperature rise per pass for flow rate experiments is given in Figure 6. Results for reflected power over the course of flow rate runs are provided in Figure 8.

4.3.2 Ionic Concentration

Ionic concentrations tested were 1, 2, 3, 5, 10 and 20 g/L of NaCl, all at a flow rate of 6.5 L/min. The effect of ionic concentration on average heating rate, time and energy used are provided in Table 7. A graphical display for heating rate, time and temperature rise per pass is shown in Figure 7. Results for the effect of ionic concentration on reflected power is provided in Figure 9.

Table 7: Recycle Flow Rate and Ionic Concentration Tests: Heating Rate, Time and Energy Consumed

Experiment	**Range**	**Run Setting**	**Average Heating Rate**		**Heating Time** (min)	**Energy Used** (kWh)
			(°C/min)	(°C/pass)		
Flow Rate (L/min)	**25-70°C**	**1.75**	2.9±0.6	17±1.9	15.7	1.9
		2.8	2.8±0.6	9.8±2.5	16.2	2.0
		4.5	2.9±0.7	3.8±0.8	15.7	2.0
		6.5	2.9±0.6	2.5±0.3	15.5	1.9
		7.5	2.6±0.6	1.7±0.2	17.0	2.2
Ionic Conc. (g NaCl/L)	**25-85°C**	**1**	3.0±0.6	2.5±0.3	20.2	2.6
		2	3.4±0.6	2.8±0.3	17.7	2.3
		3	3.5±0.6	3.0±0.2	17.2	2.2
		5	3.5±0.6	3.0±0.3	17.0	2.2
		10	3.7±0.7	3.1±0.3	16.2	2.1
		20	3.7±0.7	3.3±0.3	16.0	2.1

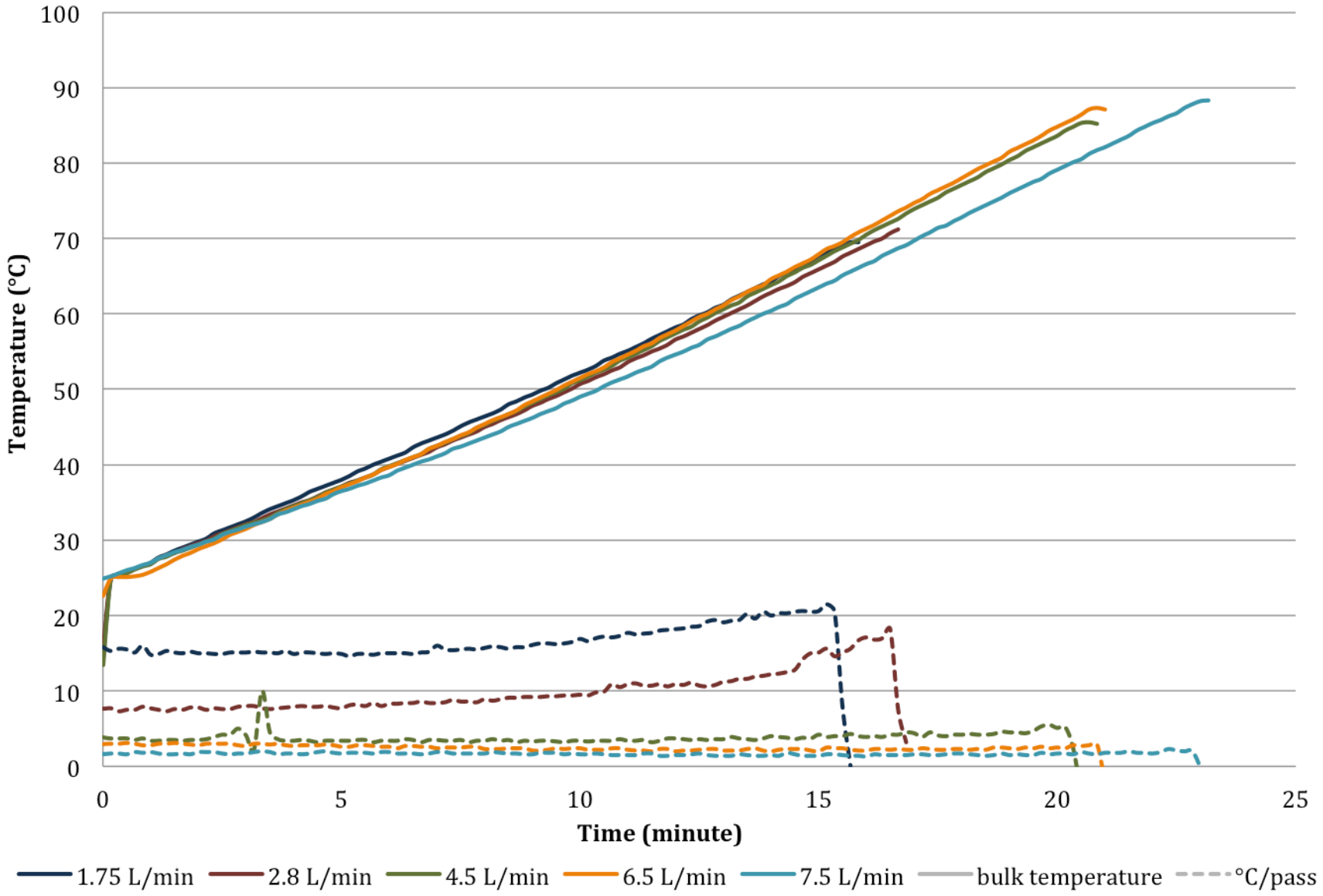

Figure 6: Effect of Recycle Flow Rate on Bulk Heating Rate and Temperature Rise per Pass

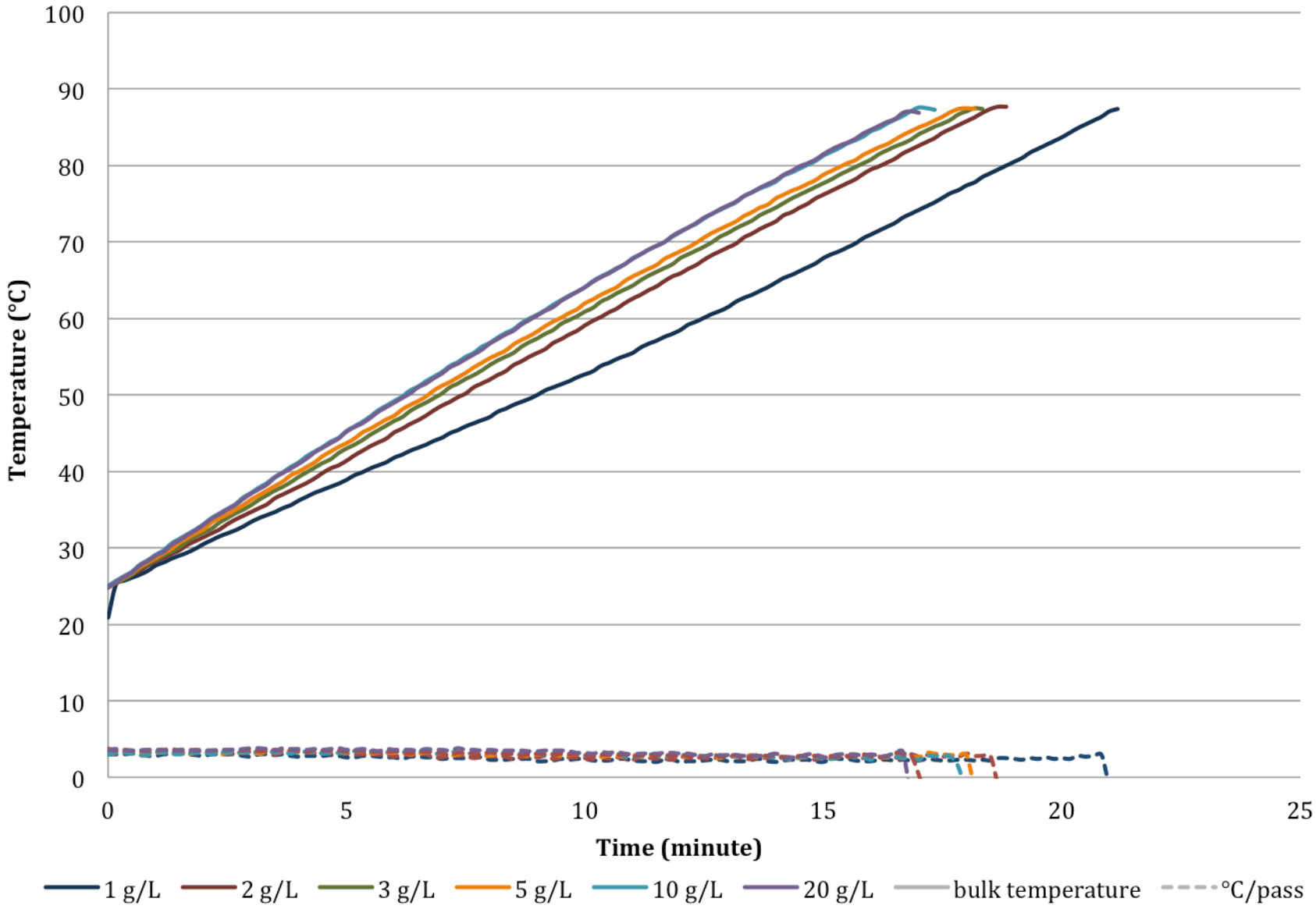

Figure 7: Effect of Ionic Concentration (NaCl) on Bulk Heating Rate and Temperature Rise per Pass

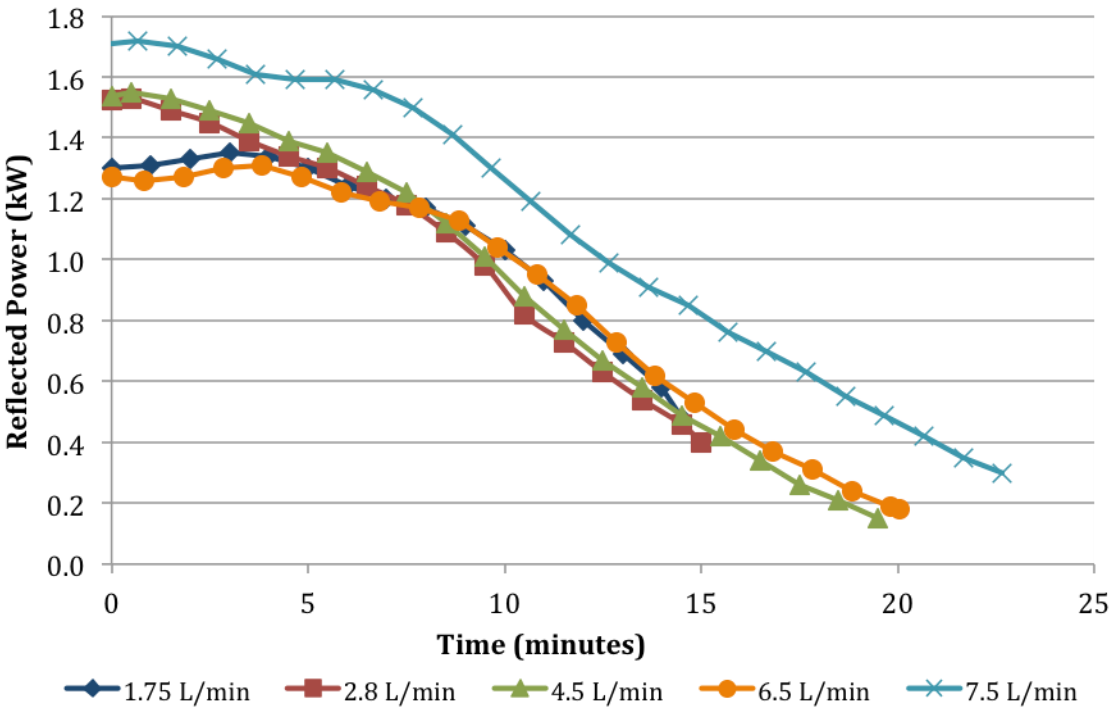

Figure 8: Effect of Recycle Flow Rate on Reflected Power versus Run Time

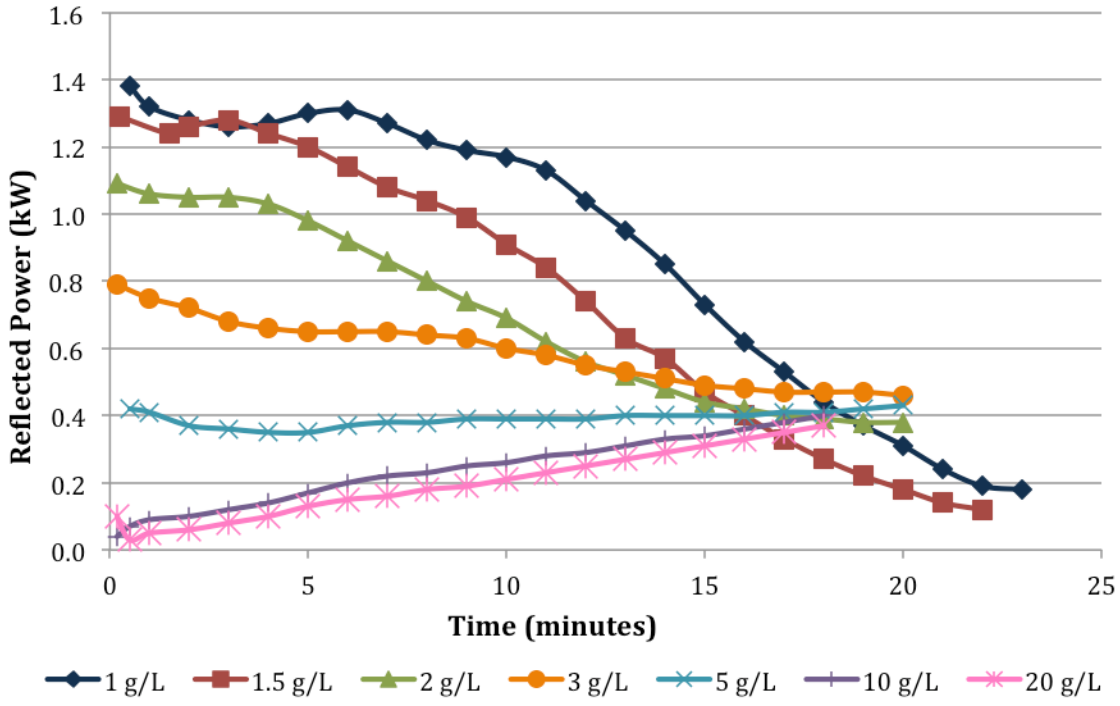

Figure 9: Effect of Ionic Concentration (NaCl) on Reflected Power versus Run Time

4.4 Discussion

In this section, results for each set of experiments are considered and discussed.

4.4.1 Recycle Flow Rate

In reference to Table 7 and Figure 6, the most drastic effect of different recycle flow rates was change in temperature rise per pass (°C/pass). The relationship is closely approximated by an exponential decrease in °C/pass, as flow rate increased. Regardless of increased °C/pass, for all flows but 7.5 L/min (which displayed a decline in heating rate) the average heating rates in terms of temperature rise per minute (°C/min) were statistically the same. Further, while an increased °C/min shows some relation to a decline in both heating time and energy consumed, there was no clear indication of a flow rate setting that optimizes these outcomes. Finally, given the similarity of the data, notable between 1.75 and 6.5 L/min, the result for the 7.5 L/min flow rate was aberrant and unexpected. It could not be attributed to any explicit cause, so is assumed to be a result of normal system variation.

There may be instances where a higher °C/pass is desired, such as for single pass pasteurisation or perhaps in operating a continuous system, where holding volume or number of passes is purposefully limited. However, given the current aims and operating scheme of this system, it may be a detriment. A higher average °C/pass includes higher inherent temperature deviation. As bulk fluid approaches its boiling point, localized temperatures in the target fluid may deviate enough to undergo isolated boiling. To read and respond to deviations in temperature, higher resolution measurement – more so than what is currently available – is needed to provide safe and effective process control. Given these concerns, paired with no discernible benefit to bulk heating rate: under the current operating scheme, changing recycle flow rate does not offer advantage.

In reference to Figure 8, as runs proceed and temperatures rise, a relatively consistent pattern in reflected power emerges: an initial plateau or shallow rate of decrease, followed by a steady, increased rate of decline. This change in reflected power is indication of transient, imbalanced impedance between the generator and load. It may arise from two factors: 1) a step-wise, ramp-up period observed in total input power delivered to the generator, and simultaneously, 2) rise in the target liquid temperature, which proportionally alters its dielectric properties. Total input power

eventually stabilized at 7.76 kW, a couple of minutes before the runs ended. Although power stabilized, temperature rose throughout the run. With a rise in temperature, the ionic conduction MW heating mechanism increases in strength – by an order of magnitude in some materials – and the load becomes proportionally more absorptive (Kappe, 2013). As runs progress, the ionic conductivity of the load increases, with the likely result of increased absorption of delivered power and consequently, decreased reflected power. Ultimately, reflected power did not reach a constant value, likely because power and temperature were not simultaneously constant at any time in the run. If both power and temperature are held constant, reflected power might reach a constant value.

4.4.2 Ionic Concentration

In reference to Table 7 and Figure 7, the results for ionic concentration tests display a couple of clear trends. As concentration increased, heating rate, in terms of both temperature rise per minute (°C/min) and per pass (°C/pass), increased in a logarithmic pattern, plateauing at concentrations above 5 g NaCl/L. Simultaneously, with increasing salt concentration, heating time and energy used showed an exponential decline. This suggests that, with increased ionic concentration, energy was more quickly and efficiently absorbed. The consistently low, reflected power results of higher concentration runs shown in Figure 9 help illustrate this efficiency: there are less reflected losses to the isolator, so it follows that more power is delivered to, and potentially absorbed, by the load. The spread of bulk temperature curves shown in Figure 7 shows how this increased absorption translates to an increased heating rate.

The reflected power results in Figure 9 illustrate the most substantial effect of different ionic concentration. For concentrations 1 and 2 g NaCl/L, the curves resemble reflected power patterns observed in flow rate tests: decreasing as the run proceeds, as total power stabilizes and temperature and ionic conductivity increase. At higher concentrations, reflected power was immediately minimal, likely because the ionic conductivity of the load was strong at the onset of the run. At the highest concentrations reflected power increased close to linearly as runs proceeded, although the gains remained in an acceptable range (i.e. 10% of forward power). This rise is likely correlated to the aforementioned ramp-up in total power. In support of this, for the 20 g NaCl/L run, between 25 and 85°C, reflected power rose in proportion to total input power at a consistent ratio of 4.3±0.3% over 18 available data points. This suggests that, at highest ionic concentration and at the set tuning, an optimal limit of load matching and power absorption has been achieved.

Under present conditions, it seems that ionic concentration meets this limit and does not confer any additional advantage at some point between 10 and 20 g NaCl/L.

4.5 Conclusion

In regard to the objective, recycle flow rate did not offer any benefit to heating rate or energy consumption. Observed variations could not be distinguished from standard deviation, so were assumed to result from normal system variation. As expected, lower recycle flow rate did result in higher temperature rise per pass (°C/pass). However, due to higher inherent deviation at higher temperature, increased °C/pass may pose a potential challenge to current modes of temperature monitoring and control. Since no standout setting was identified, and both higher and lower flow rates were potentially problematic, 6.5 L/min was chosen as the nominal recycle flow rate for subsequent experiments.

Increased ionic concentration did provide some benefit, showing a clear relation to increased heating rate and decreased energy consumption. The trend was logarithmic, with improvements plateauing as concentration was increased above 5 g NaCl/L. Under current conditions, benefits of high ionic concentration seem to reach an optimal limit at a point between 10 and 20 g NaCl/L. These findings are important for target substrates high in free ions, which may be an inherent substrate property or the result of acid-induced dissociation.

5 Dairy Manure Experiments

Dairy manure has been a focus of our research group in recent years, in effort to control its accumulation and waste, and capitalize on its rich nutrient content. The liquid portion of separated dairy manure was identified in previous studies as being most amenable for microwave (MW) treatment and subsequent processing or application, due to high concentrations of nitrogen, phosphorus, and magnesium (Chan et al., 2013). Both the study by Chan et al. (2013) and by Zhang et al. (2014) used virtually the same liquid manure used here, similarly acidified and microwaved in a flow through reactor. They provide ideal comparison studies. The study by Chan et al. (2013) indicates that thermal-oxidation treated dairy manure is not amenable to anaerobic digestion. Nevertheless, substantial nutrient release was achieved given certain pretreatment combinations. The study by Zhang et al. (2014) shows that, after decreasing the concentration of phosphate-competitive calcium, struvite can be recovered from treated liquid manure. To compliment these two studies, the experiments performed here focus on precursors of struvite recovery, including ammonia, phosphate, and magnesium concentrations, the ratio of calcium to magnesium, and settling as indication of liquid phase separation.

5.1 Problem Statement

Previous studies have identified benefits to nutrient recovery following the acidification and thermal-oxidative treatment of liquid dairy manure in MW reactors. However, these studies have all been evaluated at a frequency of 2450 MHz. Literature review confirmed that this study was the first time a 915 MHz system has been employed for manure. The higher energy wavelength and consequent increased penetration depth of this system may be more conducive to the high solids content of liquid manure. Comparative data was needed.

Further, no previous study has evaluated the overall efficacy of manure treatments weighed with respect to energy consumption. The system employed here is novel in that it is able to monitor power and energy in real time as treatment proceeds. Optimal treatment outcomes can be reported in terms of energy consumption for future comparison and improvement.

Finally, liquid dairy manure treated with oxidants, acid and heat is a very challenging substrate. When the reactor system is run with manure treated to these conditions, it is exposed to high potential for corrosion, acid attack and oxidation of rubber components, as well as pump wear caused by ligneous solids and grit. It was an additional aim of this experiment to determine the system's ability to withstand these stresses and identify trouble points.

5.2 Objectives

The objectives in experiments on dairy manure were to determine:

1) Optimal treatment combinations for struvite nutrient recovery
2) Improvements at 915 MHz in comparison to previous experiments by 2450 MHz and;
3) Most effective use of energy: i.e. minimum energy consumed to achieve an optimal treatment outcome

These are evaluated in terms of treatment indicators detailed in the literature review and methods section, excluding TSS/VSS, CST and PSD analyses performed for sludge experiments.

5.3 Tests Performed

All manure samples were acidified to a pH of 3.5. This pH was employed in previous studies with significant effect on phosphorus (Chan et al., 2013; Kenge et al., 2009; Zhang et al., 2014). Altogether, three manure experiment runs were performed. Each used 12 L of manure with a different dose of H_2O_2. In increasing order of dose, these were: Manure Run 1 (MR1): 0.5 g H_2O_2/g TS; Manure Run 2 (MR2): 1.0 g H_2O_2/g TS, and; Manure Run 3 (MR3): 1.5 g H_2O_2/g TS. Results represent analysis performed for: raw manure; manure treated with acid; manure treated with acid and H_2O_2, and; manure treated with acid, H_2O_2 and successive stages of thermal treatment.

5.4 Results

Results for each measured parameter are presented below. Where analysis of variance (ANOVA) or t-test indicates that a treatment level does not differ ($p = 0.05$), the null hypothesis (μ_0) is confirmed and data sets are truncated for brevity.

5.4.1 Total and Volatile Solids (TS/VS)

Total Solids (TS) and VS results for every treated sample were very similar, although ANOVA confirmed that the results differed. They are so similar that, for brevity, their pooled values are reported in Table 8. The difference in TS observed between raw and all subsequent acidified

samples is likely a result of added sulphuric acid, which has a density nearly twice water and a boiling point of 337°C. As such, it is likely that some form of residual sulphuric acid remains after baking samples at 105°C.

Table 8: Manure Run Total Solids (TS) and Volatile Solids (VS) Results (%)

Treatment	MR1		MR2		MR3	
	TS	VS	TS	VS	TS	VS
Raw	3.3±0.0	63±0.1	3.3±0.0	63±0.1	3.7±0.0	70±0.4
H^+	4.0±0.0	66±0.3	3.9±0.1	65±0.2	4.3±0.0	66±1.1
$H^+ + H_2O_2$	4.1±0.0	65±0.3	4.1±0.0	65±0.3	4.2±0.0	65±0.3
$H^+ + H_2O_2$ + MW	4.2±0.1	68±0.4	4.0±0.0	67±0.3	3.6±0.1	63±1.8

5.4.2 Settling

Settling data for treated manure is provided in Table 9. This data suggests the advantages of increase hydrogen peroxide dose on the bulk settling properties of liquid dairy manure.

Table 9: Treated Manure 30 minute Solids Settling Volume (mL/L)

Treatment	MR1	MR2	MR3
Raw	1000	1000	1000
60°C	1000	960	900
70°C	1000	880	820
80°C	980	820	750
90°C	970	790	690
90°C + 5 min	950	800	640

5.4.3 Chemical Oxygen Demand (COD)

Table 10 gives COD results. At every level of treatment, TCOD results confirmed μ_0. For SCOD results excluding acid alone, every level of treatment confirmed μ_0. Soluble COD results are provided to indicate instances where treated results increased beyond the raw value.

Table 10: Treated Manure COD (g/L)

Parameter	Treatment	MR1	MR2	MR3
Total COD	-	36±4.2	37±4.0	40±3.2
Soluble COD	**Raw**	11±0.1	11±0.1	12±0.3
	H^+	8.7±0.3	8.7±0.3	9.3±0.8
	$H^+ + H_2O_2$	10±0.5	13±0.1	14±0.1
	60°C	11±0.7	12±0.4	15±1.0
	70°C	10±0.6	12±0.2	15±0.9
	80°C	12±0.5	12±0.1	15±0.5
	90°C	11±0.1	13±0.3	16±1.0
	90°C + 5 min	11±0.0	12±0.3	16±0.5

5.4.4 Volatile Fatty Acid (VFA)

Results for VFA, adjusted to report as total acetic acid, are provided in Table 11. For all runs, thermal treatments confirmed μ_0. Any trend to increasing thermal treatment was minor or inconsistent.

Table 11: Treated Manure Volatile Fatty Acids (VFA) as acetic acid (g/L)

Treatment	MR1	MR2	MR3
Raw	3.9±0.0	3.9±0.0	3.5±0.3
H^+	3.3±0.2	3.3±0.2	3.5±0.0
$H^+ + H_2O_2$	3.9±0.1	3.9±0.1	3.7±0.0
$H^+ + H_2O_2$ + MW	3.6±0.1	3.6±0.1	3.4±0.1

5.4.5 Phosphorus

Phosphorus results are presented in Table 12. Total phosphorus (TP) results for both MR1 and MR2 confirmed μ_0. For MR3, raw and acidified TP results were confirmed to be the same by t-test, though they differed from oxidant treated results. The difference in TP for MR3 is possibly a result of dilution by H_2O_2. To account for this, any subsequent calculations compare soluble raw samples to the raw TP, and soluble treated samples to the treated TP.

Thermal treated SP results within tests MR1 and MR2 confirmed μ_0, whereas results differed for MR3. Thermal treated phosphate results confirmed μ_0 for sets MR2 and MR3, but differed for MR1. Due to these complications, all the phosphorus data is provided in Table 12.

It is worth mentioning that while SP results in Table 12 and Table 14 largely agree in magnitude and trend, Kenge et al. (2009) notes that colorimetry can report results around 7% higher than ICP metal results for dairy manure. Additionally, solids content higher that 0.5 w/w% can introduce slight interfere in the accuracy of phosphate measurements. This is noted for reference.

Table 12: Treated Manure Phosphorus Results (mg/L)

Parameter	Treatment	MR1	MR2	MR3
TP	**Raw/H^+**	n/a	n/a	276±19
	Treated	258±28	262±33	225±16
SP	**Raw**	18±1.9	18±1.9	22±1.3
	H^+	192±2.2	192±2.2	166±6.6
	$H^+ + H_2O_2$	157±9.7	171±0.7	164±0.7
	60°C	171±6.1	157±1.7	170±1.8
	70°C	169±1.6	157±12	172±2.0
	80°C	185±18	150±3.2	178±2.1
	90°C	191±10	182±11	186±1.2
	90°C + 5 min	192±13	161±14	196±1.7
Phosphate	**Raw**	3.9±1.9	3.9±1.9	15±0.6
	H^+	166±4.0	166±4.0	168±4.7
	$H^+ + H_2O_2$	164±3.9	171±6.6	160±0.7
	60°C	177±1.4	181±12	160±4.2
	70°C	176±6.7	179±11	159±4.4
	80°C	185±5.8	165±9.3	160±8.3
	90°C	182±5.6	170±10	157±4.0
	90°C + 5 min	203±8.7	169±8.3	147±2.1

5.4.6 Nitrogen

Nitrogen results are presented in Table 13. Like TP, TKN results for MR1 and MR2 confirmed μ_0. For MR3, all oxidant treated results were statistically different from raw and acidified samples. As for TP, this may be a result of H_2O_2 dilution. Without exception, all SKN and ammonia results, from both raw and treated samples confirmed μ_0. Results for SKN and ammonia showed no obvious relation to increasing thermal treatment, with the exception of a minor upward trend in ammonia for MR3.

Table 13: Treated Manure Nitrogen Results (g/L)

Parameter	Treatment	MR1	MR2	MR3
TKN	**Raw/H^+**	-	-	2.6±0.2
	Treated	2.0±0.2	2.1±0.4	2.1±0.2
SKN	**Raw**	1.2±0.1	1.2±0.1	1.5±0.0
	H^+	1.3±0.1	1.3±0.0	1.6±0.1
	$H^+ + H_2O_2$	1.2±0.1	1.3±00	1.6±0.0
	$H^+ + H_2O_2$ + MW	1.3±0.1	1.2±0.1	1.6±0.1
Ammonia	**Raw**	1.1±0.0	1.1±0.0	1.3±0.1
	H^+	1.3±0.0	1.3±0.0	1.5±0.1
	$H^+ + H_2O_2$	1.2±0.0	1.2±0.1	1.5±0.1
	$H^+ + H_2O_2$ + MW	1.2±0.0	1.1±0.0	1.4±0.0

5.4.7 Metals

Results for selected metals of interest are presented in Table 14. Thermally treated soluble results for calcium, magnesium and potassium confirmed μ_0, with no observed trend. For phosphorus, MR1 confirmed μ_0, while MR2 and MR3 did not. Due to this, all phosphorus results are provided.

Table 14: Treated Manure Select Metals Results (mg/L)

Parameter	Fraction	Treatment	MR1	MR2	MR3
Phosphorus	Total	Raw	284±23	284±23	248±11
	Soluble	Raw	18±1.7	18±1.7	20±0.9
		H^+	181±2.6	181±2.6	141±4.3
		$H^+ + H_2O_2$	157±5.6	166±1.3	139±8.2
		60°C	157±4.5	132±3.9	131±2.4
		70°C	165±15	138±1.9	137±5.2
		80°C	170±2.0	142±1.1	141±6.9
		90°C	186±2.5	154±2.0	153±7.4
		90°C + 5 min	188±6.7	156±3.0	165±4.1
Magnesium	Total	Raw	394±36	394±36	383±16
	Soluble	Raw	198±8.7	198±8.7	193±12
		H^+	371±8.5	371±8.5	356±15
		$H^+ + H_2O_2$	359±13	300±1.3	342±21
		$H^+ + H_2O_2$ + MW	349±13	277±5	311±14
Calcium	Total	Raw	1127±91	1127±91	1066±52
	Soluble	Raw	120±7.0	120±7.0	239±14
		H^+	833±15	833±15	899±31
		$H^+ + H_2O_2$	935±34	784±5.2	911±58
		$H^+ + H_2O_2$ + MW	917±34	732±14	859±34
Potassium	Total	Raw	1758±149	1758±149	2154±54
	Soluble	Raw	1765±58	1765±58	2095±131
		H^+	1770±32	1770±32	2186±84
		$H^+ + H_2O_2$	1721±59	1406±5.8	2109±131
		$H^+ + H_2O_2$ + MW	1640±62	1300±24	1866±83

5.4.8 Temperature and Energy

The dairy manure bulk temperature, as well as MW forward and reflected power over the duration of experimentation, is provided in Figure 10. Run characteristics including average heating rate (°C/minute) and temperature rise per pass (°C/pass), as well as total heating time from 25-90°C, are provided in Table 15.

Table 15: Manure Run Temperature and Power Characteristics

Characteristic	MR1	MR2	MR3
Average Heating Rate (°C/minute)	4.1±0.7	3.4±0.4	3.9±0.9
Average Temperature Rise per Pass (°C/pass)	11±4.9	6.2±1.0	7.0±1.6
Total Heating Time: 25-90°C (minutes)	16.2	16.8	15.0
Total Energy Consumed: 25-90°C+5 min			
kWh	2.6	2.6	2.5
kJ/g TS	24	24	22

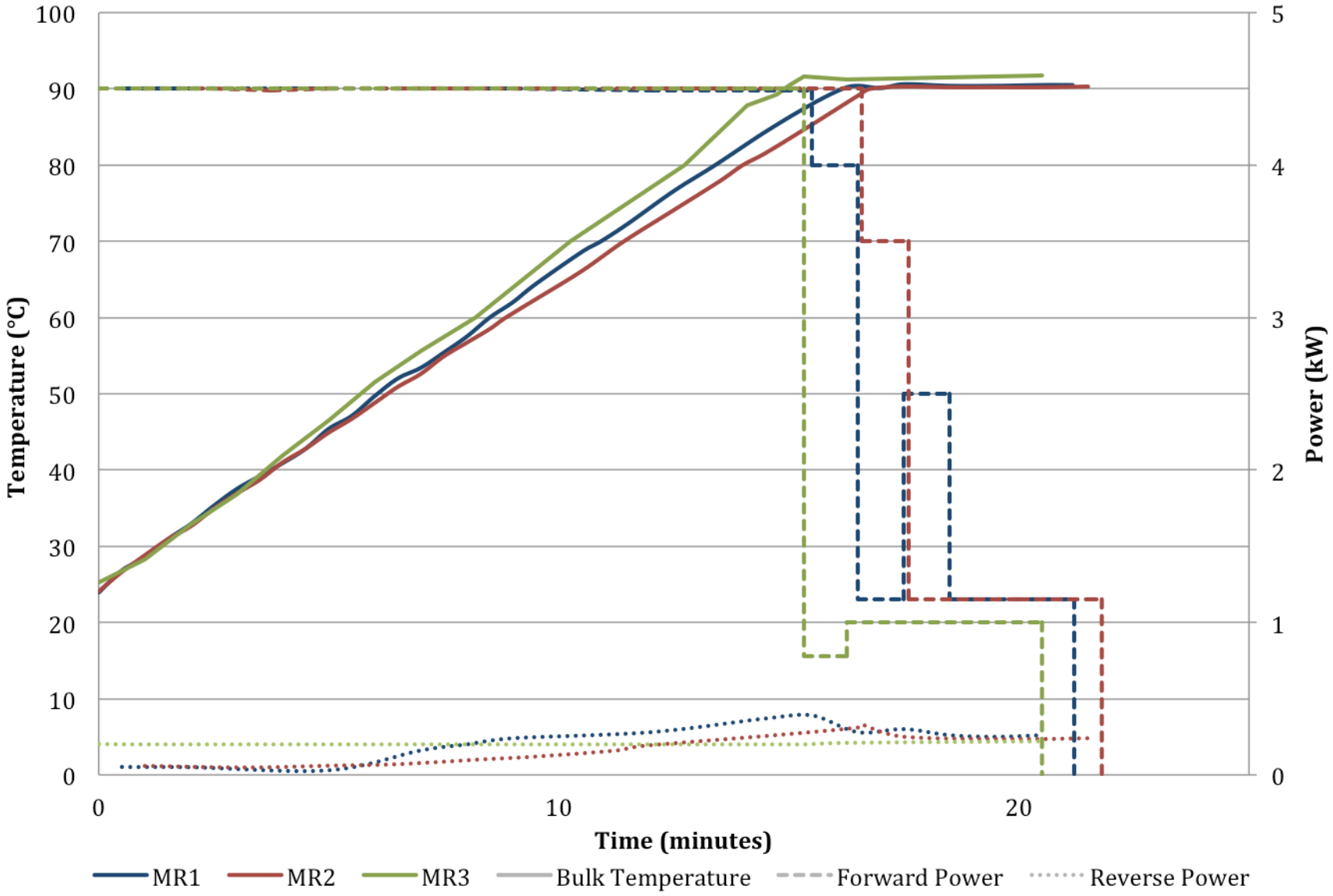

Figure 10: Manure Heating Rate, Forward and Reflected Power

5.5 Discussion

Many of the results reflect the immediate and substantial effect of acid treatment (pH = 3.5). The data indicates two general trends, which can be roughly categorized as affecting organic or inorganic constituents. Organic constituents are considered for their role in in solids settling as well as anaerobic digestion, despite previous evidence of minimized methane potential. Inorganic constituents are given focus for their value in nutrient recovery processes. Next, aspects of nutrient recovery are discussed. Finally, an assessment of energy is presented.

5.5.1 Organics: Resultant Concentrations and Settling

The solubilisation of organic components in manure is reported in part by ammonia and SKN: representing primarily free ammonia, urea and protein, the latter from enzymes and indigestible forage; and VFA: indicative of digestive by-products. The SCOD measure encompasses both, measuring all soluble carbohydrates, proteins and fats. Ammonia results showed little change with treatment. The VFA results for runs MR1 and MR2 showed a decline, while the MR3 result was inconclusive, due to high deviation in the raw sample. Following acidification, SCOD results showed a significant decline.

Most of the results indicate acid-induced, conglomeration of organics, as typical for humic aggregates, resulting in their filtered removal from soluble samples. In explanation, Liao et al. (2007) reported that manure contains organic hemicellulose, lignin and cellulose, arranged in order of increasing resistance to hydrolysis. When subjected to acid or thermal hydrolysis, these materials undergo varying degrees of accumulation (understood as meaning conglomeration) or degradation depending on the severity of the treatment. Generally, a more severe treatment favours degradation. The decrease in soluble organic concentrations reported here suggests that acid treatment was too moderate to initiate substantial degradation. This is in contrast to much more drastic acid hydrolysis procedures employed elsewhere, which specifically target the release of soluble sugars from lignin and cellulosic material (Liao et al., 2006; W. Liao et al., 2007)

The next stage of treatment severity, the addition of H_2O_2, induced a slight increase in degradation in relative proportion to the dose. For MR1, acid and oxidant treatment did not raise SCOD concentration above the raw result. Thermal treatment increased the concentration,

resulting in minimal (~10%) yet significant increase over the raw value at 80°C. For MR2, acid and oxidant treatment provided statistical advantage over both raw and most thermal treated samples, save for a match at 90°C. In MR3, thermal treatment to 80, 90 and 90°C + 5 minutes provided a slight yet significant increase of roughly 7-14% over acid and oxidant treatment, totalling roughly a 25-33% increase, relative to the raw value. Altogether, results indicate that acid treatment alone was too moderate to favour the degradation of organics, instead resulting in conglomeration; an increased dose of H_2O_2 provided an advantageous boost in degradation; subsequently, thermal treatment displayed a minimal benefit in addition to acid and oxidant treatment, or none at all.

Comparable COD results here are at most 11±0.3% different from samples in the work by Chan et al. (2013), and suggest similar patterns. In that study, acidification to pH of 3.5 showed a similar decrease in SCOD. In fact, in all cases, it seemed acidification detracted from the full potential of COD solubilisation. Even after a full suite of treatment – including acidification, H_2O_2 and MW – results were statistically indistinguishable from both raw and MW only. In that study, only treatment with 0.3 g H_2O_2/g TS, heating to 96°C and no acid increased the SCOD result with statistical relevance past the starting raw value.

Regardless of minor SCOD release, an important result of increasing thermal and oxidative treatment is increased settling. Results here agree with those reported previously by Zhang et al. (2014); improvements to settling are achieved by treatment with H_2O_2 and heat. It is worth noting that TS reported in that study was 0.8-2 w/w%, compared to the 3.3-3.6 w/w% reported here. This helps to explain differences in results. In that study, a control confirmed that acid alone did not induce settling. Further, increasing H_2O_2 dose from 0.3 and 0.5 g H_2O_2/g TS did not appreciably improve settling. Here, increasing the H_2O_2 dose from 0.5 to 1.5 g H_2O_2/g TS displayed considerable effect on settling. Where Zhang et al. (2014) reported settling of about 600 mL/L for a H_2O_2 dose of 0.5 g H_2O_2/g TS after 30 minutes, given the same conditions here, very minimal settling was achieved (950 mL/L). Here, a H_2O_2 dose in excess of 1 g H_2O_2/g TS and temperature above 80°C showed substantially improved settling. Clear supernatant is challenging to achieve in liquid dairy manure, but is an imperative precursor to nutrient recovery (Zhang et al., 2014). As such, it is an important outcome of acidification and thermal-oxidative treatment.

5.5.2 Inorganics: Phosphorus and Metal Partitioning

Previous studies have identified that a large portion of the total phosphorus in dry dairy manure is water extractable and exists primarily as inorganically bound phosphate (He et al., 2004). Results here confirm this finding and show, as would be expected, that acidification induces substantial dissociation and solubilisation of this inorganic phosphate. As shown in Table 12, with acidification alone, the fraction of soluble phosphorus (SP) to total phosphorus (TP) increases roughly ten-fold in all three runs, from an initial value of 7-8% to 73-74%. Further, after acidification, 86±2.3% to roughly all of this SP exists as phosphate. Simultaneously, Table 14 illustrates a roughly 4-7 fold increase in soluble calcium and roughly 2 fold increase in soluble magnesium following acidification. This supports the anticipated acid dissociation of inorganics, such as di- and octo-calcium phosphate, newberyite and struvite (Zhang et al., 2014). Finally, by deduction, remaining minority fractions of SP and TP not accounted for by phosphate must represent organic phosphorus and perhaps remnant recalcitrant polyphosphate (APHA, 2005).

The effects of successive stages of treatment on phosphorus partitioning vary, though a few general trends are apparent. First, SP showed a decline after the addition of H_2O_2, which is more pronounced at a lower dose. Phosphate did not display this same decline. This suggests that the change in SP is from conglomeration and filtered removal of non-phosphates, perhaps with complexation or enmeshment in conglomerating organics. Magnesium and potassium also displayed a decline following the addition of H_2O_2, while magnesium, potassium and calcium results indicated a significant decline with thermal treatment. This is further indication of reintegration into particulate solids by conglomeration or enmeshment.

In succeeding stages of thermal treatment, SP showed a steady, visible increase in MR1 and MR3, but remained relatively constant for MR2. Phosphate consistently constituted roughly 100% of the SP for MR1 and MR2. For MR3, the ratio of phosphate to SP declined from roughly 100% after acidification, to 75±1.3 % at 90°C + 5 minutes. In the same interval, the ratio of phosphate to TP decreased from 75±5.7 to 65±4.7%. For MR1, following acidification, increasing SP and phosphate suggests that particulate TP is dissolving. From acid addition to 90°C + 5 minutes, the ratio of phosphate to TP increased from 64±7.2% to 80±9.3%. This indicates the favoured release of phosphate. For MR3, it seems the opposite is true. Increasing SP and a simultaneous decrease

in phosphate suggests that the formation of soluble polyphosphates or organic phosphorus compounds may be favoured at high H_2O_2 dose. In MR2, phosphate and SP results do not increase appreciably with treatment.

Zhang et al. (2014) do not report the same effect of increasing H_2O_2 dose causing a reduction in phosphate. At a pH of 3.5, they reported a slight increase in phosphate as H_2O_2 increases from 0.2 to 0.5 g H_2O_2/g TS. Here, phosphate for the 0.5 g H_2O_2/g TS dose increased from acidified raw, while the highest dose of 1.5 g H_2O_2/g TS displayed a relative decrease. Results here may recommend a threshold, where increasing H_2O_2 is ultimately detrimental for phosphate release, though more data is required. Further, Zhang et al. (2014) report that the highest ratio of phosphate to TP achieved was roughly 100% at a pH of 3.5 and dose of 0.5 g H_2O_2/g TS. Here, the same conditions resulted in a ratio of phosphate to TP of 80±9.3%. Again, the difference in TS between these two studies might help explain this discrepancy.

There is much more similarity between the results here and those reported by Chan et al. (2013). In that study, both SP and phosphate for acidified manure were statistically indistinguishable from results for manure treated with acid, MW to 96°C, and H_2O_2. Here, although phosphate showed an increase, results reported the same trend and nearly the same values in SP for treatment with acid, 90°C + 5 minutes and 0.5 g H_2O_2/g TS. That study also reported an increased SP, while phosphate reduced slightly yet significantly, when comparing manure treated with MW and acid, and treatment with combined MW, acid and H_2O_2. Barring improvements to settling, this indicates that in some instances, H_2O_2 is unnecessary or even detrimental to phosphate release from dairy manure.

5.5.3 Potential Nutrient Recovery: Optimal Treatment for Struvite Recovery

Struvite forms in a 1:1:1 molar ratio of soluble magnesium, ammonium (NH_4^+) and phosphate (Bhuiyan et al., 2008). Reviewing the treated concentrations for these core constituents: ammonia (molar equivalent to ammonium) and magnesium were in excess, with respective molar concentrations in the range of 61-83 mmol/L and 8.1-15 mmol/L, compared to phosphate which fell in a range of 1.5-2.2 mmol/L. Phosphate is the limiting nutrient, and by necessity, becomes the focus in evaluating struvite recovery.

The best phosphate release was achieved in MR1. Compared to raw sample, acid treatment released roughly 42 fold more soluble phosphate than was initially present. Thermal treatment to 90°C + 5 minutes achieved an additional release, for a roughly 53 fold increase compared to raw, and an overall ratio of phosphate to TP of 80±9.3%. However, this run also resulted in the poorest settling. In application, without achieving liquid-solid separation, phosphate cannot be recovered. Taking a different perspective, phosphate load can be considered, otherwise defined as the product of phosphate concentration (mg/L) and the volume of available supernatant (L). At a treatment level of 90°C + 5 minutes, phosphate load was roughly 10, 34 and 53 mg for MR1, MR2 and MR3, respectively. Despite declining availability of phosphate with treatment, the improved settling and higher theoretical load of phosphate in MR3 gives the best option for struvite recovery.

For MR3 at 90°C + 5 minutes magnesium and ammonia were in required excess. In addition, calcium was in excess to magnesium at a molar ratio (Ca:Mg) of roughly 1.7. As noted by Zhang et al. (2014) – who reported a similar post-treatment ratio of 1.6 – struvite formation is hindered when Ca:Mg exceeds 0.25. To favour the formation of struvite, calcium must be removed from solution. To this effect, Zhang et al. (2014) reported that at a Ca:Mg ratio of 1.6, oxalic acid added in molar ratio to calcium at 1.5 can reduce the calcium concentration by approximately 85%, with minimal effect on magnesium. Applying the same removal efficiency to results here, the molar ratio of Ca:Mg could be reduced from 1.7 to just over 0.25, in theory, favouring effective recovery of struvite. Ultimately, these results need to be substantiated with empirical data.

5.5.4 Energy Requirement

Due to a high concentration of free ions, acidified dairy manure is very MW absorbent. This is illustrated in Figure 10 by low reflected power, which is consistently less than 10% of the forward power. Compared to initial water runs, although both the heat capacity and loss tangent of manure differ, it displayed the same high heating rate and relatively short heating time of water, with a 5-10 g/L concentration of salt.

Results from MR3 indicate the best available outcome for struvite recovery, making it the focus of energy evaluations. Coincidentally, it also resulted in the shortest heating time and consumed the least energy. This may be due in part to aging of the manure or slight differences in handling – MR3 was performed 2 days before both MR1 and MR2. This is suggested by higher raw TS and

soluble raw concentrations of calcium and potassium seen in MR3. It may also be due to the increased dose of H_2O_2, providing enhanced disruption and liberation of free ions. This is suggested by calcium and potassium results following H_2O_2 addition and heat, which are, for the most part, similar or higher than comparative values for MR1 and MR2. Finally, it may also be due to observed, day-to-day fluctuations in MW system performance.

Assuming liquid dairy manure has a density similar to water, for MR3, treating 12 L to 90°C + 5 minutes, gives a specific energy consumption of 810 J/kg liquid manure for MW energy alone. On a solids basis, this is 22±0.0 kJ/g TS. Total wastewater flow from the UBC Dairy Farm was estimated in 2014 as being 38 m^3/day (Srinivasan et al., 2014). Although the current pilot-scale MW system can only handle around 0.600 m^3/day, the full flow provides an interesting base for comparison. Again assuming liquid dairy manure has a density similar to water: using the current system, total energy use per day would be roughly 31 MJ or 8.5 MWh.

The above values are hypothetical and are assumed accurate only to order of magnitude. They incorporate total energy input into the system, including functions of the MW unit ulterior to heating, such as magnetron cooling and control. As identified in the next chapter, once the system stabilizes, these secondary functions amount to roughly half of the required energy. In higher energy units (≥75 kW), it can be expected that the entire system, including these functions, operate with improved efficiency including lower extraneous energy draw and losses. As such, provided values likely overestimate energy requirements of a full-scale MW system.

5.6 Conclusion: Dairy Manure Experiments

Liquid dairy manure is a complex and challenging wastewater, due in part to its high solids content, which is rich in recalcitrant carbohydrates. Despite this, certain treatment configurations employed here displayed benefit to precursors of struvite nutrient recovery. The optimal treatment, resulting in the highest available load of phosphate directly recoverable from settled supernatant, was achieved in MR3 following acidification to pH = 3.5, an oxidant dose of 1.5 g H_2O_2/g TS and thermal treatment to 90°C + 5 minutes. Other treatments that were employed resulted in significantly higher concentrations of phosphate, although they did not produce adequate settling.

Comparison to previous studies on a 2450 MHz flow-through MW reactor showed comparability, indicating similar improvements and outcomes. The most similarity existed between results for the lowest H_2O_2 dose employed here and results reported by Chan et al. (2013); pH, H_2O_2 dose, and TS were nearly identical, with a difference in thermal treatment of only 6°C. Some similarity in trend and magnitude was observed in the results of Zhang et al. (2014), except that study reported a higher resultant ratio of phosphate to TP and markedly improved settling at a lower H_2O_2 dose. These differences were thought to arise from the lower solids content of liquid dairy manure used in that study.

Experiment MR3 stood out as being optimal in terms of potential nutrient recovery, and, considering comparable results for MR1 and MR2, required relatively less energy. Through a combination of factors, perhaps involving increased disruption of organically bound ions by higher H_2O_2 dose, manure in MR3 displayed steady and efficient absorption of MW energy, which gave lower overall energy consumption and a shorter heating time.

Overall, a decisive result of these experiments was settling. Certain treatment configurations resulted in higher concentrations of phosphate, but provided minimal supernatant from which to collect it. Settling is an important outcome of thermal-oxidative MW treatment, however, to confirm its importance and success in nutrient recovery from manure, other modes of liquid-solid separation might be explored.

6 Waste Activated Sludge Experiments

The treatment of Waste Activated Sludge (WAS) has been the subject of substantial research, with several targeted outcomes. The focus has been primarily on nutrient recovery, enhancements to anaerobic digestion, and solids reduction. The overall aim is to economize wastewater treatment, whether through production and sale of products of nutrient recovery and anaerobic digestion, or by reducing the quantity of byproduct waste solids, thereby reducing handling costs. The work here is an assessment of a relatively new thermal-oxidative WAS treatment, evaluated in regard to these aims, adding dewaterabilty due to its importance as a precursor of nutrient recovery. Overall focus is given to the challenges and opportunities of scaling up the technology for this treatment. The work was performed on pilot-scale equipment, on a path towards full-scale deployment.

Experiments were performed in two stages. The first stage of experimentation was semi-continuous operation, where target sludge was cycled from a holding tank until an endpoint of 90°C + 5 minutes, with no fresh feed added. This simulates the operation of a sequencing batch reactor. The second stage of experimentation was continuous operation, which maintained the same recycling configuration of the semi-continuous system, adding a fresh feed. Semi-continuous WAS experiments helped to establish a set of baseline expectations for the system, including the effect of flow rate, H_2O_2 dose and acidification on sludge treatment outcomes. This identified optimal conditions and a range of expected outcomes, to which the continuous operation system could be tested and compared.

6.1 Problem Statement

Literature has all but confirmed the reproducible advantages of thermal-oxidative treatment, including benefits specific to microwave (MW) heating. So far, the majority of studies employing MW seem to have been performed at bench-scale, in either laboratory or household grade units. These studies have been pivotal in proving the advantages of MW treatment; however, little work has been done to explore how this process would be scaled to handle full-scale sludge volumes. More information is needed to confirm the efficacy of larger scale systems, including further evaluation of the benefits of different operating modes, potential treatment limitations, required additions, opportunities to improve efficiency, and safety concerns. More information is also needed regarding system power requirements, the distribution of power draw, as well as modes

and mechanisms of energy delivery and absorption. A deeper exploration and understanding of the physical characteristics of MW treatment can help direct advances in scale-up.

6.2 Objectives

The two stages of sludge treatment had the same objectives, assessed separately. The objectives of sludge experiments were to determine:

1) Optimal treatment combinations for:
    a. Solids reduction
    b. Potential biogas production
    c. Dewatering
    d. Potential nutrient recovery
2) Improvement with pilot-scale 915 MHz technology or process design in comparison to previous experiments on bench-scale 2450 MHz systems
3) Most effective use of energy, identified as:
    a. Minimum energy consumed to achieve an optimal treatment outcome
    b. Improvements resulting from choice of operating mode

6.3 Semi-continuous Run (SR) Experiment Results

Results are presented below. These represent analyses performed for raw WAS, as well as several different treatment combination, which are described in Table 16. Runs were performed in sequential pairs, comparing the same sludge which was collected just prior to experimentation. The only exception is sludge samples used for SR3 and SR4, which were collected a day apart. Experiment SR1 and SR2 differ only in timing of H_2O_2 addition, at start of run and 60°C, respectively. For all subsequent experiments, H_2O_2 was added at 60°C. As noted in Table 16, runs 3 and 4 investigate the effect of different recycle flow; runs 5 and 6 investigate the outcomes of using MW only and of acid addition; runs 7 and 8 investigate the effect of different H_2O_2 dose.

As previously mentioned, where analysis of variance (ANOVA) or t-test indicates that a set of treatments are indistinguishable (95% CI), the null hypothesis (μ_0) is confirmed and data sets are truncated for brevity.

Table 16: Waste Activated Sludge Semi-continuous Run Legend

Parameter	SR1	SR2	SR3	SR4	SR5	SR6	SR7	SR8
Recycle Flow Rate (L/min)	6.5	6.5	4.5	2.5	6.5	6.5	6.5	6.5
H2O2 Dose (g H_2O_2/g TS)	0.3	0.3	0.3	0.3	n/a	0.3	0.2	0.5
Acid Dose (v/v %)	n/a	n/a	n/a	n/a	n/a	0.5	n/a	n/a

6.3.1 Total and Volatile Solids (TS/VS)

Total solids for different treated samples were very similar, although results confirmed that they are statistically different. Pooled values are provided for brevity. For every run except SR6, VS results confirmed μ_0. This exception, as well as differences in TS observed between raw and SR6 treated samples, is assumed to result from the addition of sulphuric acid, which likely leaves a residual after baking to 105°C. Results for TS and VS are reported in Table 17.

Table 17: Semi-continuous Treated WAS Total and Volatile Solids (TS/VS)

	TS (g/L)		**VS** (%)	
Run	**Raw**	**Treated**	**Raw**	**Treated**
SR1	8.2±0.1	7.9±0.3	78±0.1	77±0.3
SR2	8.2±0.3	7.7±0.2	78±0.1	77±0.4
SR3	6.7±0.3	7.5±0.0	77±0.2	76±0.6
SR4	7.5±0.0	7.3±0.1	77±0.1	76±0.5
SR5	7.6±0.1	7.3±0.1	79±1.3	79±0.5
SR6	7.6±0.1	16±0.6	79±1.3	72±5.0
SR7	8.0±0.1	7.5±0.1	78±0.7	77±0.5
SR8	8.0±0.1	7.2±0.3	78±0.7	77±0.9

6.3.2 Total and Volatile Suspended Solids (TSS/VSS)

Results for TSS and VSS are provided in Table 18. Except for SR4, VSS results within each run confirm μ_0, indicating that as TSS disintegrates the proportion of volatile solids remains constant. Further, VSS results compared between runs also confirm μ_0, indicating consistency in the source sludge. The aberrant results for SR4 indicated a slight, inconsistent rise in VSS fraction, which may be the result of localized hot spots and vaporisation, demonstrated by erratic outlet temperatures. These results do not elucidate a trend, so pooled values are given for brevity.

Table 18: Semi-continuous Treated WAS Total and Volatile Suspended Solids (TSS/VSS)

Run	TSS (g/L)						VSS (%)
	Raw	45°C	60°C	75°C	90°C	90°C + 5 min	Pooled
SR1	7.9±0.2	6.5±0.1	6.1±0.1	6.1±0.2	6.3±0.2	6.0±0.2	87±2.3
SR2	7.9±0.2	7.2±0.1	6.3±0.2	4.8±0.3	4.1±0.1	3.5±0.2	85±2.6
SR3	6.8±0.2	6.2±0.2	5.5±0.2	4.2±0.2	3.8±0.0	2.9±0.3	84±3.6
SR4	7.0±0.2	6.2±0.1	5.4±0.2	5.1±0.1	3.8±0.0	3.5±0.1	86±4.4
SR5	7.7±0.2	7.0±0.2	5.8±0.3	5.7±0.3	5.8±0.0	5.6±0.4	88±3.9
SR6	7.7±0.2	6.0±0.0	5.8±0.1	5.6±0.1	5.6±0.1	5.4±0.0	89±6.0
SR7	7.2±0.2	6.6±0.1	5.6±0.1	5.0±0.4	4.2±0.2	3.4±0.0	94±5.2
SR8	7.2±0.2	7.2±0.1	5.7±0.1	4.6±0.3	3.1±0.3	2.2±0.2	82±7.2

6.3.3 Chemical Oxygen Demand

Chemical Oxygen demand (COD) results are given in Table 19 and Table 20. Except for SR6 and SR8, treated TCOD results for each run confirmed μ_0. For SR6 and SR8, following H_2O_2 addition, TCOD results were significantly different. This is explained by the augmentative effect of H_2O_2 on COD readings (Kang et al., 1999). This is expected for SR8, which used the highest H_2O_2 dose; however, SR6 used a nominal dose. For SR6, it is speculated that acidification increased the augmentative effect of H_2O_2.

Table 19: Treated WAS Total and Soluble COD (g/L): Semi-continuous Runs (SR) 1-4

Parameter	Treatment	SR1	SR2	SR3	SR4
Total COD	**Raw**	8.4±0.4	7.6±0.8	8.2±0.4	8.3±0.3
Soluble COD	**Raw**	0.1±0.0	0.1±0.0	0.1±0.0	0.1±0.0
	45°C	0.3±0.0	0.2±0.0	0.2±0.0	0.2±0.0
	60°C	1.0±0.0	1.0±0.0	1.0±0.0	1.1±0.0
	75°C	1.3±0.1	3.0±0.2	2.9±0.0	2.5±0.0
	90°C	1.5±0.1	3.7±0.3	3.7±0.0	3.7±0.2
	90°C + 5 min	1.5±0.0	4.1±0.2	4.0±0.0	3.5±0.0

Table 20: Treated WAS Total and Soluble COD (g/L): Semi-continuous Runs (SR) 5-8

Parameter	Treatment	SR5	SR6	SR7	SR8
Total COD	**Raw**	8.4±0.1	8.0±0.3	8.6±0.1	8.8±0.5
	Raw+H2O2	n/a	9.6±0.1	n/a	10±0.6
Soluble COD	**Raw**	0.1±0.0	0.3±0.0	0.1±0.0	0.1±0.0
	45°C	0.1±0.0	0.4±0.0	0.2±0.0	0.2±0.0
	60°C	1.0±0.0	0.4±0.0	1.0±0.0	0.9±0.0
	75°C	1.3±0.0	2.1±0.2	2.6±0.1	4.0±0.1
	90°C	1.6±0.1	2.5±0.1	3.3±0.0	5.1±0.1
	90°C + 5 min	1.5±0.0	2.8±0.1	3.9±0.1	5.2±0.2

6.3.4 Volatile Fatty Acid (VFA)

Results for VFA are provided in Table 21. The data shows nearly unanimous increase in VFA concentration with increased thermal treatment, with the exception of SR7. This is thought to be the result of instrument contamination, which had been flushed out by SR7's third data point.

Table 21: Semi-continuous Treated WAS Volatile Fatty Acids (VFA) as acetic acid (mg/L)

Treatment	SR1	SR2	SR3	SR4	SR5	SR6	SR7	SR8
Raw	7.0±0.2	7.0±0.2	0.3±0.1	2.9±0.8	1.0±0.1	1.0±0.1	42±3.2	9.7±3.2
45°C	8.0±1.6	9.1±3.2	1.3±0.3	2.1±0.7	1.9±0.1	13±1.5	35±5.0	24±0.8
60°C	33±1.5	29±2.2	10±0.5	9.2±1.3	16±0.6	16±0.5	35±6.6	26±1.3
75°C	37±3.0	77±6.7	49±1.1	45±3.3	18±2.1	49±3.8	45±3.8	62±0.4
90°C	35±8.6	112±5.3	70±2.0	76±3.1	25±0.8	67±4.9	50±3.0	64±5.4
90°C + 5 min	45±11	119±9.8	79±4.0	74±8.1	22±1.3	73±1.7	56±5.2	74±3.8

6.3.5 Settling

Settling for treated WAS is given in Table 22. For SR6, acidified raw results are omitted, but can be described as bulking, with some solids floating and some sinking. Further, the supernatant of SR6 was completely transparent and virtually free of colour. Supernatant for all other runs was an opaque, brown liquid, taken to be visual indication of high suspended and dissolved COD.

Table 22: Semi-continuous Treated WAS 30-Minute Solids Settling Volume (mL/L)

Treatment	SR1	SR2	SR3	SR4	SR5	SR6	SR7	SR8
Raw	990	990	990	990	990	990	990	990
45°C	990	990	980	980	980	620**	980	970
60°C	950	950	970	970	980	420**	880	970
75°C	980	*	*	*	810	480**	*	580
90°C	980	750	600	600	800	440**	600	410
90°C + 5 min	980	550	430	440	820	440**	470	300

* Bulking Observed
** Observed approximately 5 mL of floating sludge

6.3.6 Particle Size Distribution (PSD)

Results for PSD, including graphical display and values for cumulative distribution ($d_{10\%}$, $d_{50\%}$ and $d_{90\%}$), are presented in Figure 11. Results represent raw sample or sample treated to 90°C + 5 minutes. Data is provided for SR6 acidified raw to illustrate the conglomerative effect of acid. Although raw sludge for semi-continuous runs 3 and 4 were collected a day apart, the average difference between data points was only 1%. As such, the raw sample for run 3 is provided here.

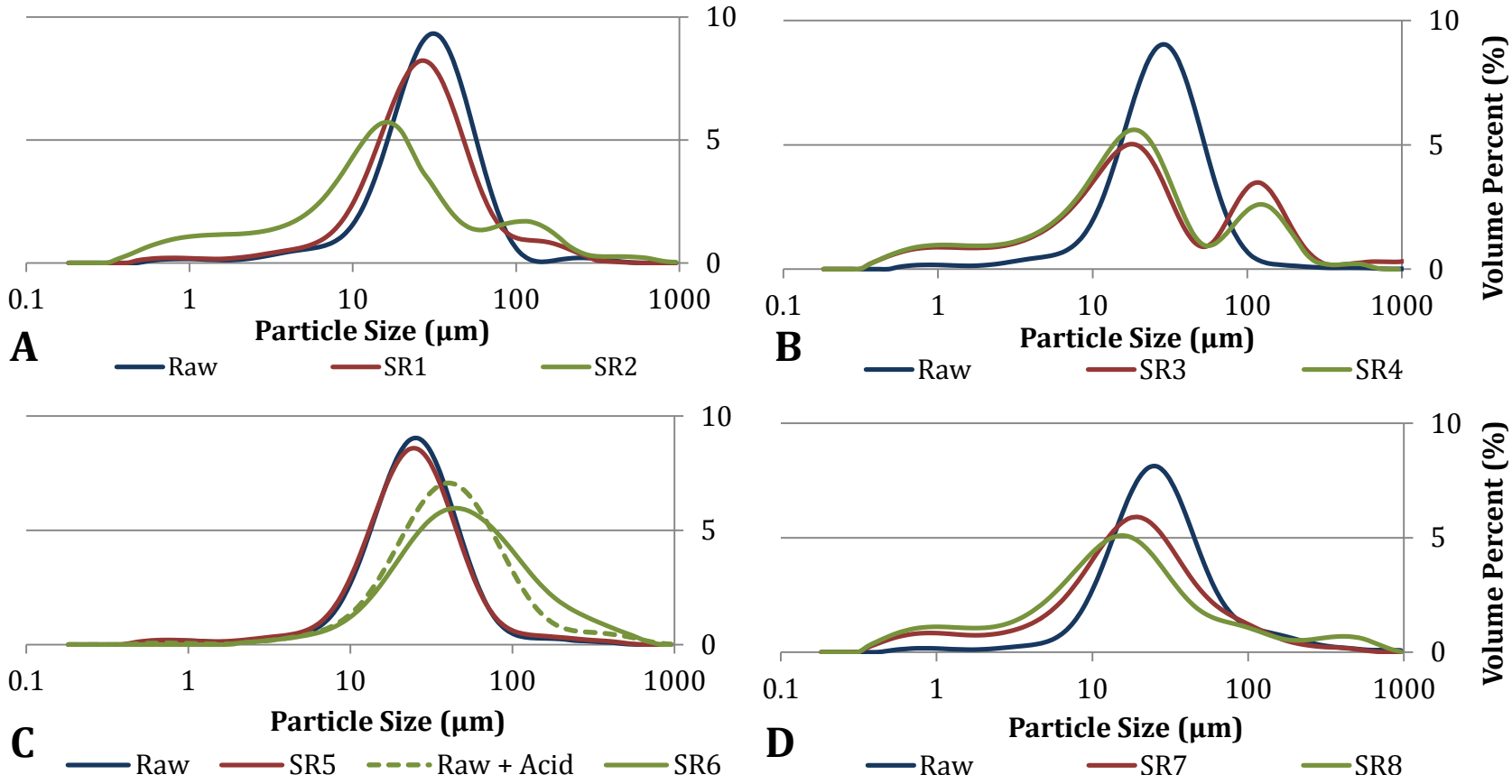

Figure		A			B			C				D		
Treatment		Raw	SR1	SR2	Raw	SR3	SR4	Raw	SR5	Raw + acid	SR6	Raw	SR7	SR8
Cumulative Distribution (µm)*	$d_{10\%}$	13	10	2.0	12	2.4	2.1	11	10	15	16	11	2.7	1.7
	$d_{50\%}$	31	28	17	29	21	19	26	26	43	52	27	19	15
	$d_{90\%}$	64	76	106	63	143	153	57	60	124	188	80	72	86

* Standard error for cumulative distributions: $d_{10\%}$ = 5%; $d_{50\%}$ = 5%, and; $d_{90\%}$ = 8%.

Figure 11: PSD for Semi-continuous Treated WAS: Graphical Display and Cumulative Distribution

6.3.7 Capillary Suction Timer (CST)

Results for CST are presented in Table 23. Results were taken when samples were between 20 and 25°C. Error inherent to measurements is expected to outweigh deviation caused by different temperature.

Table 23: Semi-continuous Treated WAS CST Results (seconds)

Treatment	SR1	SR2	SR3	SR4	SR5	SR6	SR7	SR8
Raw	136±26	136±26	76±15	58±2.5	42±1.3	42±1.3	42±0.6	42±0.6
Raw + H^+	n/a	n/a	n/a	n/a	n/a	27±1.2	n/a	n/a
90°C + 5 min	924±160	532±30	308±56	429±27	350±36	15±0.4	445±72	198±2.2

6.3.8 Phosphorus

Phosphorus results are presented in Table 24. All TP results confirmed μ_0. Note that metals results for runs SR5 to SR8 underestimate colorimetry results, which is unexpected given that the digestion for metals analysis is more severe. However, when converted to ratios of soluble to total phosphorus, both methods return comparable results. The discussion section will consider TP results from colorimetry.

6.3.9 Nitrogen

Nitrogen results can be found in Table 25. Like TP, TKN results unanimously confirmed μ_0.

6.3.10 Metals

Metals results are presented in Table 26. Sodium was also measured; however, treatment results did not differ significantly from raw, so they have been omitted.

Table 24: Semi-continuous Treated WAS Phosphorus Results (mg/L)

Parameter	Treatment	SR1	SR2	SR3	SR4	SR5	SR6	SR7	SR8
Total P	**-**	263±22	264±21	331±22	329±11	341±26	338±31	288±8.0	285±14
Soluble P	**Raw**	7.9±8.0	7.9±8.0	1.3±0.7	0.9±0.3	6.6±0.2	6.6±0.2	0.0±0.0	0.0±0.0
	45°C	55±0.9	14±0.7	22±0.3	31±0.4	34±0.2	105±10	31±1.9	19±1.7
	60°C	172±8.8	155±9.6	183±2.5	185±1.5	218±5.2	109±3.6	157±6.8	153±6.3
	75°C	192±3.3	144±6.2	186±6.3	186±4.5	231±11	155±5.0	146±3.8	136±5.8
	90°C	236±15	181±5.6	215±1.3	217±3.3	256±2.3	202±7.0	151±2.5	173±11
	90°C + 5 min	238±10	188±5.1	230±1.6	230±2.4	266±6.1	235±4.5	173±0.7	172±11
Phosphate	**Raw**	0.4±0.3	0.4±0.3	0.0±0.0	0.9±0.3	5.1±0.2	5.1±0.2	0.3±0.0	0.3±0.0
	45°C	26±0.3	11±0.0	22±1.1	19±1.0	36±0.5	58±1.5	30±0.4	17±0.1
	60°C	79±1.4	75±0.5	54±0.8	53±2.9	97±2.2	42±0.6	66±0.8	78±0.6
	75°C	38±1.3	18±0.1	16±0.5	16±0.2	54±1.2	45±1.4	19±0.3	16±0.5
	90°C	26±0.1	23±0.9	23±1.1	21±0.5	47±1.0	52±1.3	20±0.3	19±0.1
	90°C + 5 min	30±0.7	29±0.2	30±1.1	28±0.8	29±0.9	63±0.6	27±0.3	26±0.5

Table 25: Semi-continuous Treated WAS Nitrogen Results (mg/L)

Parameter	Treatment	SR1	SR2	SR3	SR4	SR5	SR6	SR7	SR8
Total KN	**-**	529±49	538±52	626±27	524±17	689±66	694±105	540±91	582±31
Soluble KN	**Raw**	15±0.7	15±0.7	0.0±0.0	0.0±0.0	12±0.9	12±0.9	6.7±1.2	6.7±1.2
	45°C	32±1.3	19±1.3	0.0±0.0	0.0±0.0	15±0.4	22±1.1	15±2.3	13±2.8
	60°C	115±6.5	91±10	38±1.0	108±6.4	77±3.5	26±0.4	64±3.8	60±4.4
	75°C	161±5.3	179±4.3	120±9.9	189±2.6	100±5.7	42±2.6	110±4.6	135±8.6
	90°C	160±6.9	260±12	234±5.3	331±5.4	112±7.0	52±1.1	142±1.8	269±18
	90°C + 5 min	173±14	305±11	298±5.3	339±0.8	134±11	84±5.7	216±0.7	308±11
Ammonia	**Raw**	0.1±0.0	0.1±0.0	0.1±0.0	0.1±0.0	0.5±0.0	0.5±0.0	0.2±0.0	0.2±0.0
	45°C	7.3±0.1	3.9±0.1	8.1±0.5	7.4±0.2	9.2±0.5	0.5±0.0	8.9±0.2	6.5±0.3
	60°C	6.1±0.0	6.5±0.1	7.7±0.1	6.1±0.2	11±0.2	0.6±0.0	6.1±0.0	6.0±0.1
	75°C	3.9±0.0	9.8±0.2	11±0.3	9.7±0.4	7.8±0.1	10±0.0	9.3±1.2	15±0.3
	90°C	2.8±0.0	12±0.1	13±0.3	13±0.6	4.6±0.1	11±0.1	12±0.2	17±0.4
	90°C + 5 min	3.1±0.0	14±0.1	16±0.7	17±0.3	4.6±0.1	12±0.1	14±0.3	18±0.2

Table 26: Semi-continuous Treated WAS ICP Metals Results (mg/L)

Parameter	Portion	Treatment	SR1	SR2	SR3	SR4	SR5	SR6	SR7	SR8
Phosphorus	Total	Raw	367±6.6	367±6.6	357±8.5	357±8.5	268±3.8	268±3.8	266±4.5	266±4.5
	Soluble	Raw	1.3±0.2	1.3±0.2	1.9±0.2	2.4±0.1	-	-	0.3±0.1	0.3±0.1
		45°C	53±0.6	14±0.8	25±0.6	30±1.3	30±0.4	82±1.9	29±0.2	18±0.1
		60°C	177±6.7	176±7.3	181±17	181±6.7	153±0.9	89±1.4	159±0.9	148±2.4
		75°C	201±6.4	163±3.5	192±2.8	180±1.0	174±2.1	119±1.3	156±6.1	148±1.1
		90°C	248±3.5	207±9.2	205±1.3	202±5.0	188±0.7	162±1.0	176±1.5	171±0.2
		90°C + 5 min	243±5.3	218±5.0	212±4.5	226±5.7	190±1.0	184±4.2	181±2.0	172±4.2
Magnesium	Total	Raw	84±1.8	84±1.8	79±1.6	79±1.6	71±2.4	71±2.4	71±0.8	71±0.8
	Soluble	Raw	3.0±0.1	3.0±0.1	2.8±0.0	2.8±0.0	-	-	0.3±0.0	0.3±0.0
		45°C	7.7±0.0	3.4±0.1	4.8±0.1	5.4±0.4	4.2±0.1	65±0.8	3.2±0.1	2.0±0.0
		60°C	34±1.3	35±0.8	35±1.5	35±1.0	33±0.7	66±0.9	35±0.6	32±0.2
		75°C	39±0.4	34±0.9	38±1.8	39±0.9	38±0.5	66±1.0	36±0.8	35±0.4
		90°C	48±0.7	44±2.1	44±2.4	45±0.5	44±0.6	70±1.4	43±0.6	44±0.4
		90°C + 5 min	47±1.0	48±2.0	50±2.2	52±1.8	46±0.7	70±2.1	47±1.6	47±1.3
Calcium	Total	Raw	81±1.6	81±1.6	74±0.9	74±0.9	68±1.5	68±1.5	65±1.0	65±1.0
	Soluble	Raw	9.1±0.5	9.1±1.6	8.4±0.4	8.4±0.2	-	-	5.9±0.2	5.9±0.2
		45°C	14±0.3	9.4±0.2	8.6±0.5	7.0±1.0	9.5±0.5	58±1.8	7.3±0.2	6.5±0.2
		60°C	20±0.7	22±0.4	22±1.0	22±0.2	20±0.5	61±1.5	23±0.7	19±0.2
		75°C	28±0.5	25±0.9	29±1.4	26±1.1	27±0.5	65±1.9	25±0.8	25±0.4
		90°C	35±1.0	33±1.5	32±1.5	31±0.6	32±0.2	67±1.2	32±0.8	33±0.5
		90°C + 5 min	32±0.6	36±1.8	35±1.7	36±0.8	32±0.6	71±4.2	34±1.1	36±6.1
Potassium	Total	Raw	123±5.6	123±5.6	101±5.9	101±5.9	84±3.9	84±3.9	60±0.1	60±0.1
	Soluble	Raw	18±3.8	18±3.8	19±1.8	21±8.2	-	-	6.6±0.2	6.6±0.2
		45°C	50±3.4	23±1.9	31±0.9	41±2.4	26±1.4	77±4.6	20±1.4	14±0.5
		60°C	82±1.7	72±1.4	65±1.3	71±3.2	56±1.6	78±4.7	46±1.7	44±0.6
		75°C	80±3.4	74±3.0	63±3.3	73±2.5	60±0.7	62±3.2	50±1.4	51±2.9
		90°C	86±1.1	80±2.2	65±4.0	73±2.1	62±0.8	63±1.8	52±1.0	54±0.9
		90°C + 5 min	84±1.9	78±4.2	70±1.7	76±3.0	65±0.8	61±2.1	53±2.9	55±1.9

6.3.11 Conductivity and pH

Conductivity and pH were measured in Semi-continuous Runs 5-8 to provide reference for subsequent continuous runs. These results are provided in Table 27. Hydrogen peroxide addition seems to have caused a decline in pH, perhaps due to the observed increase in VFAs.

Table 27: Semi-continuous Run (SR) 5-8: Conductivity and pH

Run	Treatment	Conductivity (μS/cm)	pH
SR5	**Raw**	480	6.9
	45°C	540	6.8
	60°C	750	6.5
	75°C	680	7.0
	90°C	690	7.1
	90°C+5 min	720	7.1
SR6	**Raw**	480	6.9
	Raw + Acid	32500	1.7
	45°C	32000	1.7
	60°C	30000	1.7
	75°C	31000	1.7
	90°C	30800	1.7
	90°C+5 min	30400	1.6
SR7	**Raw**	645	7.1
	45°C	-	-
	60°C	1014	6.8
	75°C	889	6.8
	90°C	-	6.5
	90°C+5 min	1017	6.0
SR8	**Raw**	645	7.1
	45°C	-	-
	60°C	952	6.9
	75°C	890	6.5
	90°C	-	5.9
	90°C+5 min	1136	5.5

6.3.12 Temperature and Energy

Run characteristics including average heating rate in °C/minute and °C/pass, as well as heating time and energy, are provided in Table 28. Illustrations of bulk temperature, as well as MW forward and reflected power over the duration of experimentation, are provided in Figures 12 and 13. Efficiency of delivered and absorbed energy is provided in Figures 14 and 15.

Table 28: Semi-continuous Run Temperature and Energy Characteristics: Heating Rate, Time and Energy Used

Run	Range	Average Heating Rate (°C/min)	Average Heating Rate (°C/pass)	Heating Time (min)	Energy Used (kWh)	Energy Used (kJ/g TSS)
SR1	**25-90°C+5 min**	3.2±0.7	4.9±2.2	25.4	2.9	110±2.8
	30-45°C		3.7±2.0	5.3	0.7	
	45-60°C		3.5±1.1	5.2	0.7	
	60-75°C		6.6±1.4	4.2	0.5	
	75-90°C		7.8±0.8	4.3	0.5	
SR2	**25-90°C+5 min**	2.6±0.7	4.0±2.6	30.4	3.5	133±3.4
	30-45°C		1.9±0.6	6.7	0.9	
	45-60°C		2.3±0.9	6.7	0.9	
	60-75°C		7.1±1.9	4.8	0.6	
	75-90°C		7.6±0.5	5.2	0.6	
SR3	**25-90°C+5 min**	2.4±0.7	5.1±2.4	32.7	3.8	168±4.9
	30-45°C		3.3±0.7	7.3	1.0	
	45-60°C		3.6±1.0	7.3	0.9	
	60-75°C		7.2±2.2	5.3	0.7	
	75-90°C		9.3±0.7	5.5	0.6	
SR4	**25-90°C+5 min**	2.6±0.7	11±4.3	32.5	3.4	146±4.2
	30-45°C		6.6±1.0	6.2	0.8	
	45-60°C		10.7±3.7	5.5	0.7	
	60-75°C		16.5±3.2	4.8	0.7	
	75-90°C		13.8±2.1	8.7	0.7	
SR5	**25-90°C+5 min**	2.7±0.7	3.8±0.4	29.0	3.1	121±3.1
	30-45°C		4.1±0.2	6.5	0.8	
	45-60°C		3.7±0.2	6.4	0.9	
	60-75°C		3.5±0.2	4.6	0.6	
	75-90°C		3.6±0.5	4.7	0.5	
SR6	**25-90°C+5 min**	3.7±0.7	7.6±0.8	22.5	2.6	101±2.6
	30-45°C		8.5±0.3	3.7	0.4	
	45-60°C		7.9±0.2	3.9	0.5	
	60-75°C		7.2±0.2	4.3	0.6	
	75-90°C		6.7±0.4	4.7	0.6	
SR7	**25-90°C+5 min**	2.8±0.7	6.1±1.6	28.3	3.3	138±3.8
	30-45°C		7.4±0.4	6.2	0.9	
	45-60°C		7.0±0.2	5.5	0.7	
	60-75°C		3.9±1.4	4.7	0.6	
	75-90°C		5.0±0.6	5.2	0.6	
SR8	**25-90°C+5 min**	3.0±0.6	6.3±2.1	26.9	3.1	129±3.6
	30-45°C		8.4±0.4	5.3	0.7	
	45-60°C		7.1±0.4	5.2	0.6	
	60-75°C		3.8±2.1	4.7	0.7	
	75-90°C		4.9±1.1	5.2	0.6	

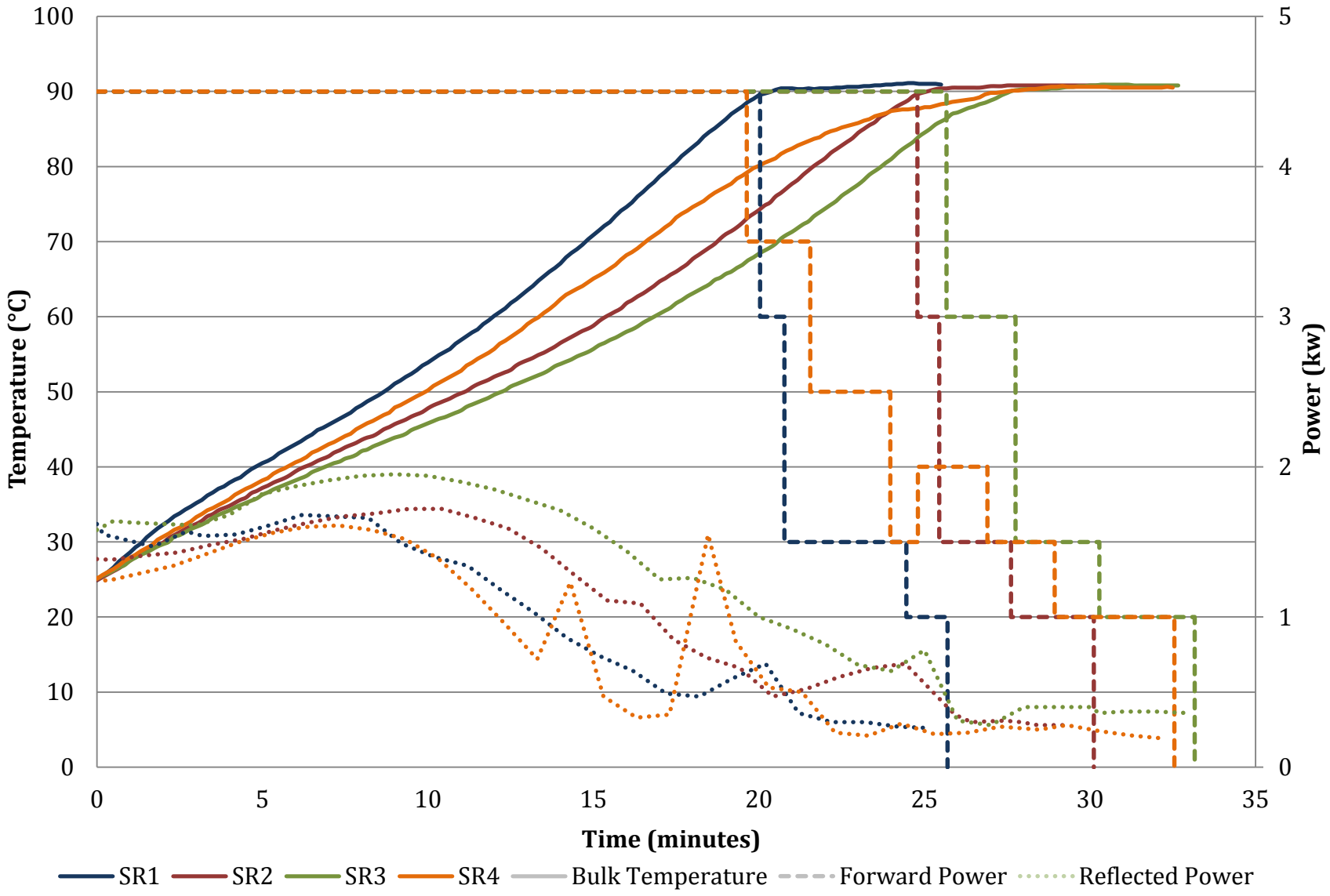

Figure 12: Semi-continuous Runs (SR) 1-4: Bulk Temperature, Forward and Reflected Power

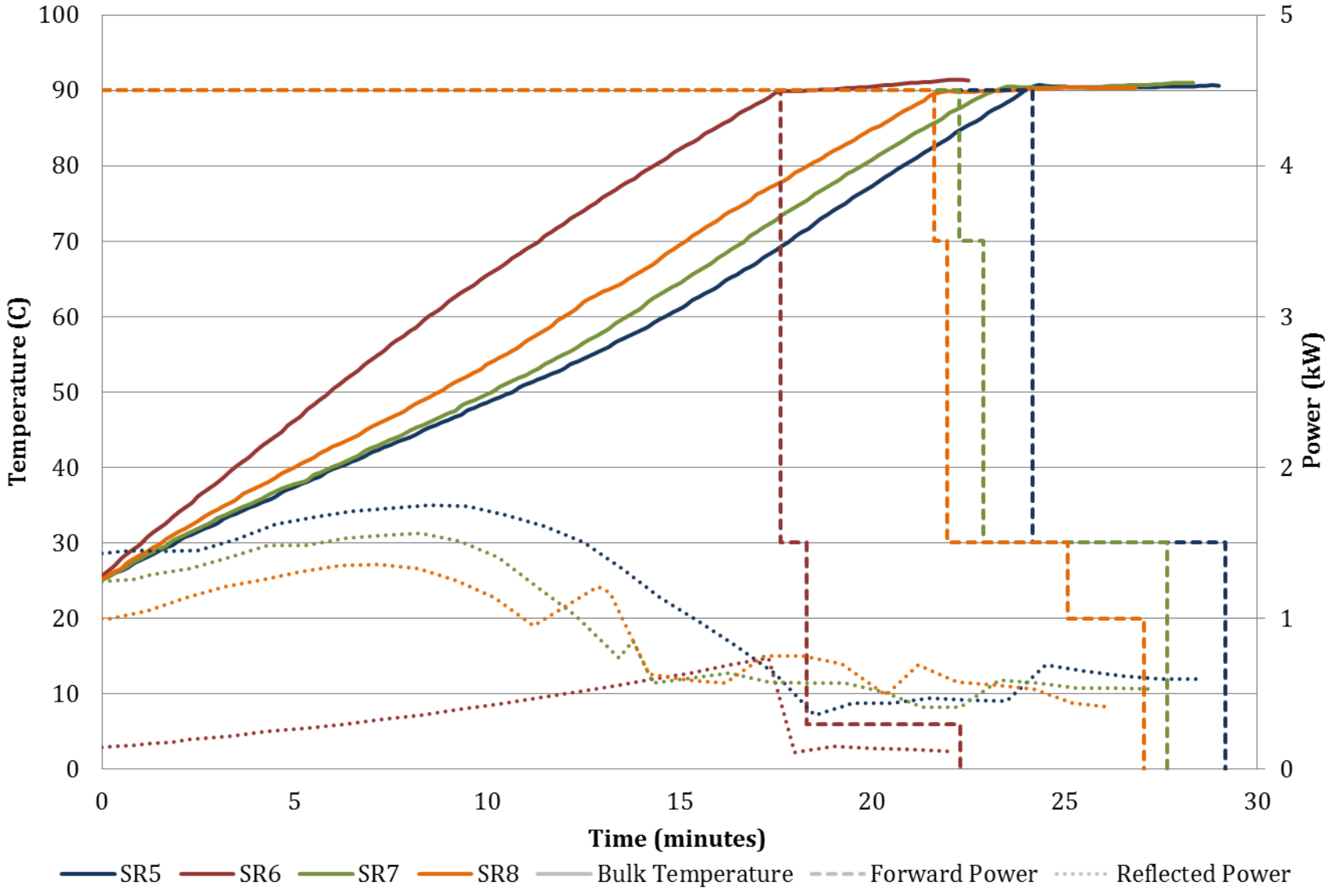

Figure 13: Semi-continuous Runs (SR) 5-8: Bulk Temperature, Forward and Reflected Power

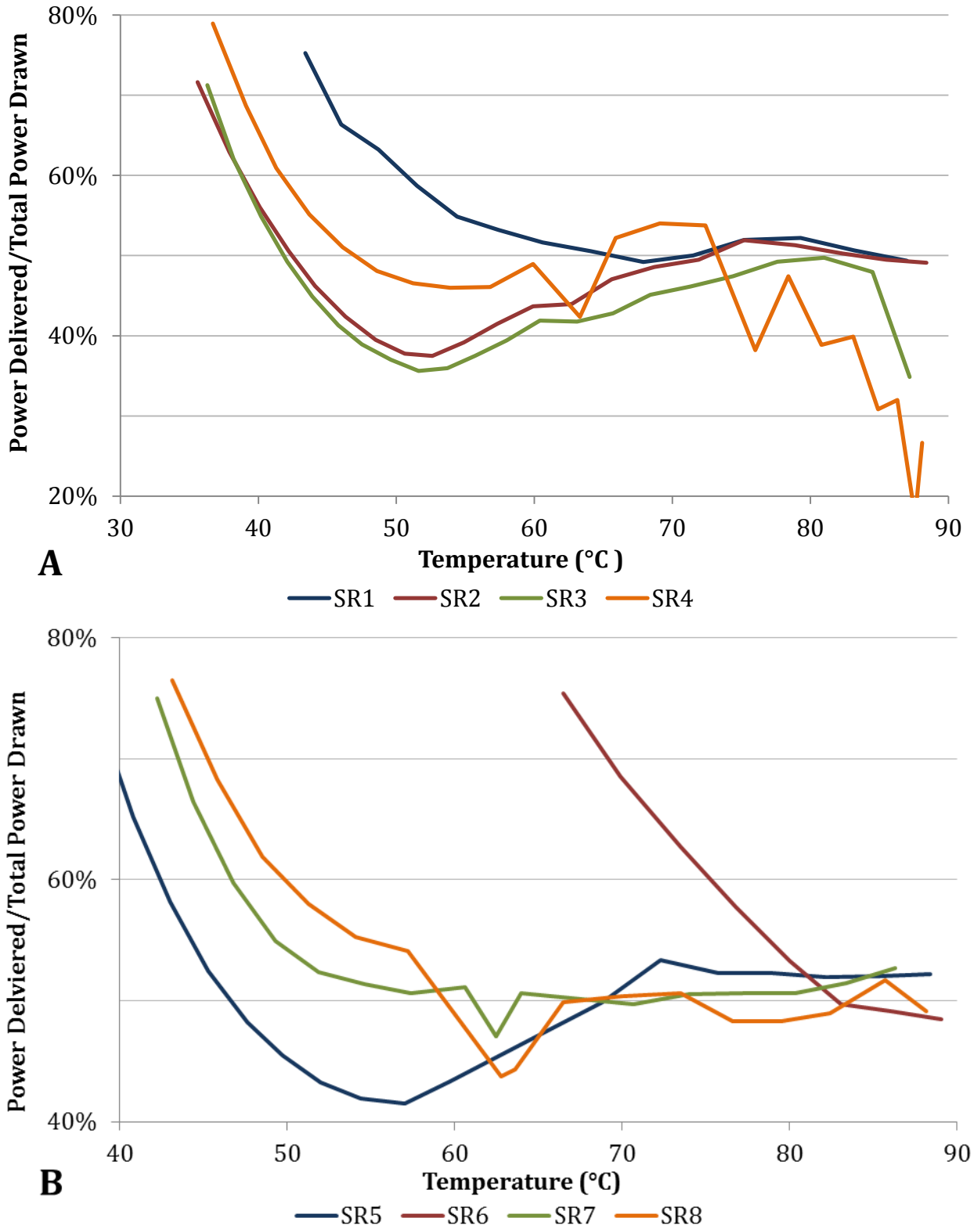

Figure 14: Power Delivered/Total Power Drawn over Duration of Semi-continuous Runs (SR): A) SR 1-4 and B) SR 5-8

Figure 15: Power Absorbed/Power Delivered over Duration of Semi-continuous Runs (SR): A) SR 1-4 and B) SR 5-8

6.4 Semi-continuous Run (SR) Discussion

The following section discusses results of semi-continuous testing. These results standalone, although they also establish a baseline for comparison with continuous operation tests discussed in the next section. This section discusses the outcomes of specific treatment aims, delimited as solids reduction, biogas production, dewatering and nutrient recovery. Each is described in reference to its representative results.

6.4.1 Reductions to Particulate Solids

There are minor changes in TS between raw and treated sample, with most – except SR3 and SR6 – displaying a decrease. This decline in concentration suggests slight mineralisation or volatilisation of solids during treatment or in TS preparation. It also indicates that the vaporisation of water was insignificant during treatment. The significant, aberrant increase in the TS of SR6 is assumed to be a result of residual acid, which has a boiling point above that reached in TS preparation.

Results for TSS show a substantial decline with increased temperature and H_2O_2 dose. For SR1, SR5 and SR6, a minimal decrease of 24-30% was observed, indicating that H_2O_2 added early, heat only and acidification had a similarly limited effect on suspended solids dissolution. For SR2, SR3, SR4 and SR7, which used similar H_2O_2 dose (0.2-0.3 g H_2O_2/g TS) added after 60°C, results for TSS at 90°C + 5 min displayed a reduction of 51 to 58%, compared to raw sample. For SR8, which used the highest dose of H_2O_2 (0.5 g H_2O_2/g TS), a statistically distinguishable decrease and the highest TSS disintegration was achieved, with a 69±4.7% reduction from raw. The VSS results, both within and between runs, were statistically indistinguishable. This suggests that total and volatile suspended solids dissolve proportionally as temperature and H_2O_2 dose increase. Notably, many of the results indicate a substantial decline in TSS at 60°C, the temperature range at which sludge proteins would be expected to denature (George et al., 2008).

The data suggests that mineralisation of solids was minimal. Instead, solids are disintegrated and reapportioned as soluble (<0.45 µm) fragments. This was supported by a concurrent rise in SCOD concentration.

6.4.2 Potential Biogas Production

Studies have shown that the solubilisation of organic material, indicated here by increased SCOD and heightened volatile fatty acids (VFA), has the potential to enhance biogas production (Appels et al., 2013). Pretreatment to hydrolyse organic material improves carbon availability, aiding the process of microbial hydrolysis, which is a rate-limiting step of digestion (Chang et al., 2011). Increasing the feed of VFA, especially acetic acid, aids and pre-empts both the acidogenesis and acetogenesis stages of digestion. The result is typically faster, occasionally higher quantity biogas production.

6.4.2.1 Soluble Chemical Oxygen Demand (SCOD)

Results for SCOD mirror the trends of TSS only in reverse, showing an increase in soluble organic matter when TSS declines. The SCOD results reflect the same beneficial effect of heat combined with the late addition of H_2O_2 on solids dissolution; the limited effect of H_2O_2 added early, heat only and acidification; and a noticeable rise in SCOD at 60°C, assumed to result from the denaturation of proteins.

The greatest dissolution of TCOD achieved, indicated by the ratio of SCOD to TCOD, is 54-59%, representing a statistical tie between SR2 at 90°C + 5 min and SR8 at both 90°C and 90°C + 5 min. In this instance, raising the oxidant dose from 0.3 to 0.5 g H_2O_2/g TS and holding 90°C for 5 minutes has minimal effect on SCOD release. The similarity in these results recommends a threshold in the efficacy of H_2O_2 dose and holding time, although the effects of inherent system variation and variability in starting material no doubt contribute to the outcome.

Solubilising COD is a prevalent focus in literature, and as such, there are many comparison studies available. The study by Wong et al. (2006a) also reported a positive correlation between improved SCOD release and increasingly severe treatment with heat and H_2O_2. In that study, oxidation dominated SCOD release, reaching roughly complete TCOD dissolution at the highest dose of 6 to 7 g H_2O_2/g TS. The higher solubilisation achieved in that study likely resulted from the substantially higher H_2O_2 dose used, in addition to the younger and less recalcitrant nature of the source sludge. The study by Eskicioglu et al. (2008b) also uses H_2O_2, adding a dose of 1 g H_2O_2/g TS to cold, thickened sludge (64 g TS/L), then subjecting it to MW heat to temperatures ranging from 60 to 120°C. Heat alone achieved an SCOD/TCOD ratio between 12 and 16%, with

a decline at 120°C, indicating solids mineralisation, while heat and H_2O_2 increased the ratio steadily with rising temperature, from roughly 15 to 25%. Comparing studies, it is interesting to note that heat treatments achieved a similar SCOD/TCOD, slightly higher here perhaps due to longer heating times. However, using heat and H_2O_2, this study doubles the COD solubilisation reported by Eskicioglu et al. (2008b), while using less H_2O_2. This is likely the result of adding H_2O_2 at 60°C, avoiding catalase inhibition and facilitating heat activated reactions. The lower dose of H_2O_2 and more effective reaction may also reduce its residual and associated issues.

Several other studies have been conducted using heat alone. A study by Bougrier et al. (2008) summarizes the results of their own thermal treatment experiments, as well as 5 other studies. According to their summary, thermal treatment to temperatures in excess of 150°C were required to meet the SCOD/TCOD ratio achieved here at 90°C, with late H_2O_2 addition. In this way, H_2O_2 helps to save energy required to superheat sludge, and also negates the need for pressure vessels.

6.4.2.2 Volatile Fatty Acids (VFA)

Results for volatile fatty acid (VFA) mirror some of the same trends as TSS and SCOD, although to different extent. Late addition of H_2O_2 and heat to 90°C achieved the best VFA release in SR2. Holding 90°C for 5 minutes showed insignificant effect for SR2, SR4, SR6, and significant, yet minor, effect for SR3. The early addition of H_2O_2 and heat alone – SR1 and SR5, respectively – displayed limited VFA release. Dissimilar to TSS and SCOD results, acidification in SR6 did not appear to be detrimental to VFA release. However, as shown in SR6 and all other runs with late oxidant addition, the reaction of H_2O_2 from 60 to 75°C accounted for roughly half or more of the total VFA release. This highlights the improved efficacy of heat activated H_2O_2 oxidation. In these runs, VFA continues to rise with temperature, likely due to continued thermal-oxidation, indicating significant advantage over the otherwise limited release achieved by low temperature H_2O_2 reaction and heat alone. However, the higher dose of H_2O_2 used in SR8 did not provide any advantage to VFA release. Overall, treatment below 100°C, with a dose of 0.3 g H_2O_2/g TS, resulted in the accumulation of VFAs, especially acetic acid. This is in contrast to more severe treatments, where they may be mineralised (Shanableh and Jomaa, 2001).

6.4.2.3 Treatment Recommended for Further Investigation

Treatment by SR2 to 90°C shows the best potential for enhanced biogas production, suggested by the high values of SCOD and VFA. The most substantial increments to SCOD and VFA are a result of high temperature reaction of sludge with an oxidant dose of 0.3 g H_2O_2/g TS. These treatments are recommended for future study.

6.4.3 Dewatering

Increasing temperature and late addition of H_2O_2 showed the best improvements to settling. Optimal settling was achieved in SR8, with treatment to 90°C + 5 min. However, acidification resulted in the most immediate settling, with the best result achieved before H_2O_2 addition at 60°C. In SR6, after 60°C, it may be that previously settleable particles disintegrate with oxidant addition. Heat alone achieves minimal settling, especially at treatment temperatures below 75°C. Finally, in SR1, the early addition of H_2O_2 proves detrimental to settling. This result requires further investigation.

Particle size distribution (PSD) results display one of three patterns relative to raw: no change; distribution spreading and decrease of the $d_{10\%}$ and mean diameter ($d_{50\%}$) with heat and H_2O_2; or spreading and increase of the $d_{10\%}$, $d_{50\%}$ and $d_{90\%}$ with acid. Results for heat only in SR5 showed insignificantly minor spreading. The early addition of H_2O_2 in SR1 achieved slight spreading, a minor decrease and minor increase in bimodality. The late addition of H_2O_2 in SR2, SR3, SR4, SR7 and SR8, resulted in substantial spreading of the distribution, a decrease in particle size, and, for most runs, considerable bimodality. This bimodality shows a majority of particles disintegrating to smaller size, and a minority conglomerating to form larger particles.

Microwave was shown to reduce sludge particle size in previous studies, said to result from the disruption of sludge floc polymer bonds, releasing smaller particles (Tyagi and Lo, 2012). This disruption seems to be aggravated by H_2O_2, demonstrating the heightened destabilisation and size reduction caused by oxidation. On the other hand, Yu et al. (2010) speculate that the formation of larger particles results from disruption of electric double layers by MW induced particle friction, causing coagulation. At higher temperatures, particles may also conglomerate in Maillard browning and caramelisation reactions. An increased fraction of particulates, indicated by decreasing soluble concentrations of sugars and amino acids, was attributed to these mechanisms

in the study by Eskicioglu et al. (2007a). Finally, the increased particle size caused by acidification further illustrates the acid conglomeration of humic substances. In heating acidified sludge, particle size continues to increase, perhaps due to further coagulation or complexation in browning and caramelisation reactions.

Most of the treatments decreased dewaterability, indicated by a roughly 4-11 fold increase in capillary suction timer (CST) results, relative to the raw samples. Acidification used in SR6 was the exception, showing an increased dewaterability with acid alone and further improvement with heat. It has been suggested that dewaterability is affected in part by the bulk surface area of solid particles in sludge (Vesilind, 1994): the smaller the particles, the higher the surface area and the harder the sludge is to dewater. Results here largely agree with this statement. Heat and H_2O_2 treatments show a mean particle size reduction and substantial increase to CST, whereas acidification shows mean particle size increase and CST decrease. Further, comparing treatment pairs (1/2, 3/4, 5/6, 7/8), where distributions in Figure 11 display a higher relative fraction of particles near or above 100 μm, dewaterability showed improvement.

However, this explanation does not fully elucidate differences in CST between similar treatments, or the decreased dewaterability of SR1 and SR5, which showed minimal change in PSD. In further opposition to the statement above, raw results showed a slight reduction in PSD, and improved CST, progressing from raw used in SR1 to raw in SR8. Another explanation is the distribution of water, which exists freely, in interstices, bound to surfaces or as water of hydration (Tsang and Vesilind, 1990). Liberating bound forms of water typically improves dewaterability. Changes in water distribution could result from inherent differences in the sludge at time of sampling, as is suggested by differences in raw CST. It could also change with the effects of different treatment. Free and interstitial water are the most easily affected, and the most readily separated (Vesilind, 1994). Water squeezed from interstices could explain particle size reduction and improved dewatering seen in the raw sample.

Severe treatment is required to disrupt surface bound and hydration water. Even when floc and microorganisms are destroyed, surface water can remain bound to residual particles (Vesilind, 1994). Smaller particles with retained surface water would increase CST. Decreased CST,

observed between SR7 to SR8, may illustrate the disruption and liberation of surface water by increased oxidation. Hydrogen peroxide might also exchange places with surface and hydration water, as suggested by Schumb et al. (1955), thereby decreasing CST. Results for SR1 and SR5, inexplicable from PSD data alone, could be the result of redistribution of water. Poor settling results support this, reflecting more water entrained in sludge solids.

The above discussion introduces some of the many factors affecting dewaterability. An experiment designed to focus on dewatering only, using identical starting sample, is needed to fully elucidate these factors.

6.4.4 Potential Nutrient Recovery

Nutrients of interest are phosphorus, nitrogen and magnesium, due to their role in potential struvite recovery. These are discussed below.

6.4.4.1 Phosphorus

The different species of phosphorus measured show different outcome with treatment. Soluble phosphorus (SP), which is a combined measurement of orthophosphate (reactive phosphate), polyphosphate and organic phosphorus, displayed nearly uninterrupted increase as treatment proceeded. For all runs except SR6, a substantial increase occured between 45 and 60°C. Within this range, the ratio of SP/TP increased 44-54%. The highest SP/TP achieved is 90±9.4% at 90°C in SR1, roughly 12% more than the next highest SP/TP achieved at 90°C + 5 min in SR5.

The remaining runs (SR2, SR3, SR4, SR7 and SR8) were similar in magnitude and trend, showing the same major release of phosphorus at 60°C, although less ultimate solubilisation than SR1. The late addition of H_2O_2 increased phosphorus solubility by only 6-14% between 60 and 90°C. Compared to SR1, this shows a reduced potential for phosphorus solubilisation. Overall, the results for SP indicate the dominant effect of temperature especially between 45 and 60°C, the relative detriment of late H_2O_2 addition and the insignificant effect of a 5 minute holding time on phosphorus solubilisation. Results reflect some of same trends found in other studies, including substantial release of phosphorus observed at 60°C, followed by a plateau of lesser increase when subjected to holding time or higher temperature (Danesh et al., 2008; Kuroda et al., 2002).

As mentioned previously, 60°C coincides with the denaturation of protein, which is a primary constituent of extracellular polymeric substances (EPS) (Comte et al., 2008; Liu and Fang, 2002). Due to their prevalence, the dissolution of protein strongly effects the integrity of EPS floc. Data indicating the solubilisation of suspended solids at 60°C supports this. Further, the impact of protein denaturation in this temperature range has been correlated to a rapid decline and cessation of faecal coliform enzyme and metabolic activity, with suspected cell damage at 60±3°C (Hong et al., 2004). The destruction of EPS is likely a rich source of phosphorus. Within EPS, phosphorus is bound in functional groups, in enzymes and their constituent proteins, and in other residual extracellular compounds, such as nucleic acids and phospholipids. An additional source would be polyphosphate, released from perforated or lysed phosphate accumulating bacteria (Danesh et al., 2008; Kuroda et al., 2002).

Considering phosphate, all treatments, save acidification in SR6, displayed a roughly parabolic peak concentration at 60°C, giving a value roughly double any other point in the run. At 60°C, SR1, SR2, SR5 and SR8 achieve the highest, statistically indistinguishable phosphate/TP ratio of 27-30%. Lower values were given by SR7 at 23±0.7%, and SR3 and SR4, which both averaged a 16%. Increased concentrations of phosphate would also result from the disintegration of EPS, which is typically rich in phosphate functional groups (Guibaud et al., 2005), from permeated or lysed cells and subsequent hydrolysis of intracellular polyphosphate (Kuroda et al., 2002), and cleaved from phospholipids (Saktaywin et al., 2005).

Another trend, unanimous to all runs with late H_2O_2 addition, save SR6, and absent from SR1 and SR5, was a marked reduction in phosphate as well as visible, yet insignificant, decline in SP concentration at 75°C, following oxidant addition. This indicates that some product of the reaction of sludge and H_2O_2 reduces the availability of free phosphorus, primarily phosphate. Explanations could include complexation with the substantially increased concentration of SCOD, or as a byproduct of improved settling, enmeshment in settled solids. In any case, late H_2O_2 displayed detriment to phosphate solubilisation.

The work by Wong et al. (2006b) provides an excellent comparison study. They used the same sludge source as the present study, although at the time, the source had a shorter retention time and

a TS of 3.5 to 4 g/L. Using MW and H_2O_2 over a range of temperatures, they observed peak phosphate solubility at 60°C. Compared to the present study, they reported a higher ratio of phosphate/TP, reflecting the younger, less recalcitrant nature of the sludge. Regardless, they observed the same minimal and, in some cases, detrimental effect of H_2O_2 on phosphate solubilisation. Kuglarz et al. (2013) reported a similar trend in phosphate concentration with increased thermal treatment, though they reported a peak at 70°C and a relatively minor decline at higher temperatures. It is worth noting that their study used very different sludge, thickened to TS of approximately 5.3%, as compared to the 0.8% used here. Altogether, this repeating trend suggests that, while phosphate is released up until about 60-70°C, at higher temperature, liberated phosphate is transformed or reintegrated into non-reactive form or enmeshed in settled solids. The virtually undeterred increase of SP suggests that these new forms remain soluble as polyphosphate or organic complexes.

Acid treatment in SR6 had a very different effect on phosphorus. The difference likely derives from the rigid, tightly packed conglomerates formed in acidification of humic solids, evidenced in SR6 by clear supernatant, low CST and good solids settling. For instance, SP results for acidified raw (not shown), 45 and 60°C data points were statistically indistinguishable, averaging an SP/TP ratio of 29-32%. This suggests an initially fixed release of phosphorus following acidification, with subsequent resistance to thermal degradation. On the other hand, phosphate declines from 45 to 60°C. The static concentration of SP indicates that this lost phosphate either remains soluble, perhaps due to binding or enmeshment with byproducts of denatured and dissolving EPS, or joins particulates, while a commensurate amount of TP dissolves.

In SR6, only after 60°C and H_2O_2 addition did SP increase, with the ratio of SP/TP increasing by an approximate 10-14% per data point from 60 to 90°C + 5 min. Phosphate also increased, though minimally by only 1-4% per point. This suggests that, while oxidation is successful in liberating phosphorus from conglomerated solids, freed forms are mostly polymers or organic complexes. From 45 to 90°C + 5 min, SP/TP increased from 31±4.1% to 70±6.5%, an end result similar to other oxidized runs, while phosphate increased insignificantly, and was never higher than 17±1.6% to 19±1.7%.

6.4.4.2 Nitrogen

Nitrogen was solubilised in trends similar to phosphorus, which was expected, given that they are both abundant components of EPS. Considering heat alone in SR5, raising temperature from 45 to 60°C accounted for roughly half of the total Soluble Kjedhal Nitrogen (SKN) released, concurrent to protein denaturation, with the remaining half achieved between 60 and 90°C + 5 min. Similar to SP, acidification in SR6 seemed to limit the release of SKN until after the addition of H_2O_2, although acid subdues SKN release even more than is observed for SP. This is likely the result of protonation of ammonia under acidic conditions, giving it higher affinity to solids. In contrast to SP, the early addition of H_2O_2 in SR1 resulted in a comparatively minor SKN increase, plateauing at 75°C, and climbing insignificantly with rising temperature. The late addition of H_2O_2 had a profound effect on SKN release, reflecting the propensity of H_2O_2 to react with nitrogenous compounds (Schumb et al., 1955). In contrast to SR1 and SR5, where temperature appears dominant, the late addition of H_2O_2 achieved the majority of SKN released and overall, with the exception of SR6, the highest ratios of SKN/TKN ranging from 40-63% at 90°C + 5 min.

Comparing runs involving the late addition of H_2O_2, there is some evidence of proportionality between oxidant dose and SKN release. Of the runs employing oxidation, the lowest dose, 0.2 g H_2O_2/g TS, achieved the lowest SKN/TKN ratio of 40±6.7% at 90°C + 5 min. This proportionality breaks down between medium and high dose, 0.3 and 0.5 g H_2O_2/g TS, respectively, which gave statistically indistinguishable results between 48-57%. Further, the highest SKN/TKN achieved was 65±2.1% at 90°C + 5 min in SR4, which used a medium dose and the lowest recycle flow rate. It is speculated that the erratic outlet temperatures observed in this run were indication of isolated boiling, and that heightened temperature and local boiling increased SKN release.

Ammonia release is minimal, with the ratio of ammonia/TKN never exceeding roughly 3.2%. Considering heat to 60°C, ammonia solubility peaked early, and without H_2O_2 addition, declined as temperatures rise. Following patterns seen previously, acid seemed to fix the ammonia concentration until H_2O_2 was added. Following the addition of H_2O_2, ammonia more than doubled in concentration from 60 to 90°C + 5 min, resulting in the highest releases. The relation of H_2O_2 dose to ammonia release is unclear: SR2, SR4 and SR8 were statistically indistinguishable, resulting in the highest average ammonia/TKN ratio of 3.0-3.2%.

The study by Wong et al. (2006b) also relates the importance of H_2O_2 to nitrogen solubilisation, with clear indication of a positive relation between ammonia solubility and oxidant dose. However, that study displayed higher ultimate yields of ammonia, likely due to the higher dose of H_2O_2 of 1 to 2 mL or approximately 3 – 7 g H_2O_2/g TS.

6.4.4.3 Magnesium and Other Metals

Total concentrations of magnesium, calcium and potassium declined from SR1 to SR8, reflecting the changing quality of starting sludge. These metals all underwent substantial solubilisation from 45 to 60°C, likely a result of EPS disruption, wherein metals are adsorbed and bound in matrices (Danesh et al., 2008). Additional sources include accumulation in cell cytoplasm and adsorption to cell walls (Shumate and Strandberg, 1985). The release at 60°C accounts for the majority of solubilised magnesium and potassium and roughly half of the solubilised calcium. Comparing all runs except SR6, at 90°C + 5 min, magnesium and calcium results showed no significant difference with different treatments. This shows that temperature may be more important to calcium and magnesium solubilisation, more so than the timing and dose of H_2O_2. However, acidification achieved the highest release, solubilising roughly 85 and 92% of the total calcium and magnesium, respectively, by 45°C. By 90°C, roughly all of the calcium and magnesium measured was soluble.

Potassium displayed a different trend. Although the total concentration in raw samples decreased from SR1 to SR8, in most cases the ratio of soluble to total potassium increased. Beyond this reduction, for all runs save SR6, the impacts of treatment were indiscernible. A single, major release of potassium occurred at 60°C, with minor or insignificant increase achieved with rising temperature and H_2O_2 dose. In every run except SR6, potassium release generally increased with temperature. In SR6, results at 45 and 60°C showed that following acidification, potassium was roughly 100% soluble. After H_2O_2 addition, the ratio of soluble to total potassium declined to a static value between 73-75% for the remainder of the run. This may be the result of complexation or enmeshment with oxidized, dissolved solids, induced to agglomerate under the acidic conditions.

The study by Wong et al. (2006a) supports the conclusion of temperature having highest impact on metals solubilisation; higher concentrations of soluble metal seemed to correlate to higher temperature. They report releases similar, though slightly lower, than results here, perhaps reflecting the lower TS of that study. They also reported the minor or inconsistent effect of H_2O_2 on metals solubilisation, with heat alone showing release similar to paired heat and oxidation.

6.4.4.4 Treatment Recommended for Further Investigation

Struvite is recovered in basic solutions containing equal 1:1:1 molar proportions of soluble magnesium, ammonium and phosphate. Table 29 gives the resulting molar ratios of magnesium:ammonim:phosphate for semi-continuous experiments, each normalized to phosphate, with instances where the molar ratio is satisfied, highlighted in green. For the most part, phosphate is limiting. However, under certain conditions ammonium, and less often, magnesium, are limiting. Most problematic is the unanimously limited ammonium at 60°C, at which point most runs reported peak phosphate concentration.

Table 29: Struvite Molar Ratios Given as Magnesium:Ammonium:Phosphate

Treatment	SR1	SR2	SR3	SR4	SR5	SR6	SR7	SR8
45°C	1.2:1.5:1	1.2:1.9:1	0.9:1.9:1	1.1:2.1:1	0.5:1.3:1	4.4:0.0:1	0.4:1.6:1	0.5:2.0:1
60°C	1.7:0.4:1	1.8:0.5:1	2.5:0.8:1	2.6:0.6:1	1.3:0.6:1	6.1:0.1:1	2.1:0.5:1	1.6:0.4:1
75°C	4.0:0.5:1	7.4:2.9:1	9.3:3.6:1	9.5:3.2:1	2.8:0.8:1	5.7:1.2:1	7.4:2.6:1	8.6:4.9:1
90°C	7.2:0.6:1	7.5:2.8:1	7.5:3.0:1	8.4:3.3:1	3.7:0.5:1	5.3:1.1:1	8.4:3.2:1	9.1:4.7:1
90°C + 5 min	6.1:0.5:1	6.5:2.5:1	6.5:2.8:1	7.3:3.2:1	6.2:0.8:1	4.3:1.0:1	6.8:2.7:1	7.1:3.7:1

A further problem is the milky brown supernatant witnessed in all runs except SR6. As has been noted, struvite formation is inhibited when supernatant suspended solids (SS) are high (Bhuiyan et al., 2008). While supernatant SS was not directly measured in these experiments, SCOD measured soluble and suspended organics and was identified as closely accounting for dissolved TSS. For every run, either temperature in excess of 60°C, or H_2O_2 treatment, resulted in high SCOD. The lowest SCOD was reported for SR1 and SR5, although these runs also displayed the poorest settling. The next lowest SCOD was reported by SR6, which achieved the best settling. A further advantage of SR6 is that magnesium was largely solubilised by acid, and remains so throughout the run. Furthermore, unlike any of the other treatments, there is consistent, positive correlation between ammonia and phosphate concentrations as treatment progresses. However, ultimate ammonium and phosphate concentrations are low, or average, compared to other runs.

Of the treatments employed, SR6 seemed to best satisfy requirements for immediate struvite recovery, such as an easily separable, clear supernatant, and adequate molar ratios of magnesium, ammonium and phosphate. However, treatment in SR6 to 90°C + 5 min has the potential to recover a maximum of 19±1.7% of TP as struvite-bound phosphate. Furthermore, acidification adds complication and cost to processing, especially in advance of struvite recovery, where caustic is used to aid precipitation. Ultimately, only empirical testing can determine whether the sludge treatments used here are amenable as pretreatment to struvite precipitation.

The benefits of thermal-oxidative pretreatment to biogas production are clear and simple, whereas advantages to nutrient recovery are more difficult to discern, or require increasingly complex additions. If maximum phosphorus recovery is the aim, it may be best to pursue recovery of SP, where recovery may be as high as 90±9.4% of TP, as achieved at 90°C in SR1. However, due to observations of poor settling, advanced solids separation would be required. Further, hydrolysis of soluble polyphosphate and organic phosphorus, perhaps by enzyme attack (Monbet et al., 2007), may be desired to liberate reactive phosphate.

An area of study requiring further exploration is the application of thermal-oxidative treatment, in advance of anaerobic digestion, to improve biogas production, with evaluation of digester outflows for phosphorus recovery. This seems especially feasible, given that digester supernatant is a conventional source of struvite phosphate (Bhuiyan et al., 2008; Britton et al., 2005). Further, though thermal-oxidative treatment of digester solids was shown to be detrimental to phosphate recovery in previous studies (Kenge, 2008), further study might be pursued to evaluate alternative and untested treatment configurations.

6.4.5 Energy Efficiency

Energy data conveys several trends, indicated by results in Table 28 and by visual representation in Figures 12 to 15.

6.4.5.1 Energy Absorption and Heating Profile

Most of the data indicated a positive correlation between heating time and energy consumed. This holds true for increments where MW forward power (FP) was held constant at 4.5 kW. Slight inconsistency in this correlation is explained by the resolution (0.1 kWh) of energy measurements.

An exception and obvious inconsistency is seen in SR4 between 75-90°C, where more active adjustment of the FP was required to prevent boiling.

For most runs, heating time and energy used was higher between the low temperature increments of 30-45°C and 45-60°C. This is speculated to result from at least three contributing factors. The first is that MW input power – the total power drawn by all systems in the MW generator – has a ramp up cycle, which begins when FP is initiated. This is an inherent function of the equipment, likely a protective measure for the magnetron and related to the increasing activity of cooling and monitoring systems. It is likely that as long as this power is increasing, the generator impedance is inconstant, which could contribute to imbalanced load matching and suboptimal energy transfer. The other two factors involve free ionic concentration. First is that MW absorption by ionic conduction becomes increasingly strong as temperatures rise, with a concurrent rise in energy absorption efficiency. Second, for most runs, treatment to 60°C coincides with a considerable release of soluble ions, as indicated by metals and conductivity data, which would further improve energy absorption. The effect of these three factors is displayed by reflected (unabsorbed) power data in Figure 12 and 13, which, except for SR6, declines as runs progress and temperatures rise.

A notable exception to declining reflected power (RP) was a slight rise following the addition of H_2O_2 at 60°C. This is likely a result of foaming observed following the addition of H_2O_2, which could affect the density of fluid in the MW reactor. This rise in RP was visible to different degrees in every run that used late H_2O_2 addition, except SR6, and was absent in SR1 and SR5. It seemed to be aggravated by: lower recycle flow rate in SR4, where fresh fluid is slower to replenish and higher temperatures are reached in a single pass; and higher H_2O_2 dose in SR8, where intensified reaction is likely to incur more foaming. Another rise in RP was apparent in SR4, around where the fluid temperature reached 75°C. At this point temperature rise per pass (°C/pass) was measured as being as high as 22.7°C, and may have been higher (though readings were limited by equipment resolution). Indicators of boiling, such as an excess of steam and erratic outlet temperatures, were observed. In the instance of boiling, entrained vapour in the fluid stream would result in immediate detriment to energy absorption. Additional disturbance in RP occurred whenever FP was altered, as the system normalized to changed impedance.

The fastest heating coincided with lowest energy used, and was achieved in SR6, followed in order by SR1 and SR8. In explanation, observing data in Figure 12 and 13, a trend is obvious. Runs with the lowest and least disturbances to RP, correlating to minimal reflected losses and optimal energy absorption, were the fastest to heat. Low RP might result from inherent differences in starting sludge or normal generator variability, illustrated by SR7 and SR8 prior to 60°C. Here, sludge and treatment conditions are virtually identical but RP profiles differ. More drastic differences in RP, illustrated by SR6, are likely the result of increased free ion activity. This is confirmed by conductivity results for SR6, which, after acidification, are roughly 30 fold higher than any other run. An early increase in free ion concentration may also have helped to reduce the heating time in SR1. This is supported by higher initial soluble potassium results. Conductive absorbance may have increased just enough to save a few minutes of heating time.

6.4.5.2 Power Distribution

Power distribution is illustrated in Figures 14 and 15. Figure 14 displays the ratio of power delivered over the total power drawn, calculated as:

$$P_{sys} = \frac{(FP - RP)}{Total\ Power\ Drawn}$$

Total power drawn is the power measured at the outlet by the installed meter and includes cumulative draw from the generator and its supporting systems. This ratio indicates how much of the total power consumed by the system is actually directed into the applicator, with potential to be absorbed. Because the input power is initially low, increasing as the run proceeds, the ratio initially exceeds 100%. As input power levels stabilizes, power delivered settles to approximately 50% of total power drawn. In other words, once the system has stabilized, roughly half of the power drawn is directed to heating, half powers auxiliary systems, and some is unavoidably lost. Fluctuations from this 50/50 distribution, especially apparent for SR4, are the result of abrupt changes in RP values, seen in Figure 12 and 13.

Figure 15 illustrates the ratio of power absorbed over the power delivered, and is calculated as:

$$P_{abs} = \frac{(\dot{m} C_p \Delta T)}{(FP - RP)}$$

To clarify, $\dot{m}$ is the mass of fluid in the reactor at any moment, divided by the time it spends in the reactor in a single pass. This is required for use in conjunction with ΔT which represents the change in temperature from inlet to outlet of the reactor (°C/pass). This ratio indicates how much of the power delivered to the applicator is converted to measurable temperature rise. Overall, it provides characterisation of the energy absorption efficiency of sludge as achieved by the chosen system configuration and tuning.

Because data reflects the compounded variation of both RP and temperature measurements, trends in Figure 15 are relatively more variable. Temperature dominates fluctuations in this graph: the difference of FP and RP never exceeded a magnitude of 4.5, while reported ΔT (°C/pass) climbed to as high as 16.5. Regardless of fluctuation, certain trends are discernible. Figure 15 A shows a clearly heightened energy absorption efficiency at higher temperature. Disregarding noise, absorption efficiency below 60°C averaged roughly 40 to 60%, while at higher temperatures it increased to 60 to 100%. This increase traced the unanimous increase of °C/pass as temperatures increased in runs SR1 to SR4. Also notable is a decrement in absorption efficiency following H_2O_2 addition at 60°C, visible in varying degree for SR2, SR3, and SR4. Absorption efficiency in Figure 15: *B* does not reflect the same drastic temperature dependence, with SR5 and SR6 showing a slight overall decline with rising temperature. This reflects the decline in °C/pass with temperature rise witnessed for these runs. However, a similar drop in absorption efficiency coincided with H_2O_2 addition at 60°C for SR7 and SR8, with more drastic decline for the latter, higher H_2O_2 dose.

An important implication of power distribution graphs in semi-continuous experiments is that energy absorption patterns trace variations in impedance, as temperatures rise and electrical and mechanical properties of the target fluid change, including foaming caused by H_2O_2 addition. A process designed with stable temperature and steadily administered additions may result in more constant and efficient energy absorption.

6.5 Continuous Run (CR) Experimental Results

Results for each measured parameter are presented below. Results represent analysis performed for raw WAS, as well as one of three treatment runs, which are detailed in Table 30. Experiment CR1b was performed last, after noting that, following 3 HRT cycles, phosphate results in CR1a indicated an upward trend and required further investigation. Being a repeat run, some analyses were omitted from CR1b, for brevity and assuming the results of CR1a are representative.

Table 30: Waste Activated Sludge Continuous Run Legend

Parameter	CR1a	CR1b	CR2
Recycle Flow Rate (L/min)	6.5	6.5	6.5
Feed Flow Rate (L/min)	0.65	0.65	0.65
H2O2 Dose (g H_2O_2/g TS)	n/a	n/a	0.2
Run Time (HRT)	3	5	5

6.5.1 Total and Volatile Solids (TS/VS)

Results for TS and VS are given in Table 31. Treated TS results confirmed μ_0 for CR1a, but differed slightly for CR2, showing a slight increase as the run progressed. Due to their close similarity, they are pooled here for brevity. Volatile solids results unanimously confirmed μ_0. A single measurement was taken for CR1b, with the expectation that it would be representative of the run. The higher TS for CR1b is the result of an upset at the Staging Environmental Research Centre. Finally, a sample was drawn at the end of CR2 as the reactor volume was drained. The TS from this sample was 9.2±0.1 g/L, significantly higher than any of the outlet samples. This is taken as indication that a fraction of solids were being retained as sludge flowed up through the reactor.

Table 31: Continuous Treated WAS Total and Volatile Solids (TS/VS)

Parameter	Treatment	CR1a	CR1b	CR2
TS (g/L)	**Raw**	8.2±0.3	9.4±0.2	7.9±0.5
	Treated	8.3±0.2	-	7.9±0.2
VS (%)	**Raw**	80±0.3	81±0.1	79±0.5
	Treated	81±1.5	-	79±0.5

6.5.2 Total and Volatile Suspended Solids (TSS/VSS)

Results for TSS and VSS are provided in Table 32. All VSS results confirmed μ_0, whereas treated TSS changed as the run progressed.

Table 32: Continuous Treated WAS Total and Volatile Suspended Solids (TSS/VSS)

Parameter	Treatment	CR1a	CR1b	CR2
TSS (g/L)	**Raw**	7.6±0.1	8.8±0.2	7.6±0.1
	90°C	5.6±0.2	6.7±0.1	5.7±0.1
	90°C + H_2O_2 + 5 min	n/a	n/a	5.6±0.1
	½ HRT	5.3±0.2	-	5.3±0.3
	1 HRT	5.3±0.1	7.4±0.1	5.6±0.1
	2 HRT	5.9±0.0	7.4±0.1	4.8±0.2
	3 HRT	6.1±0.1	7.5±0.1	5.5±0.1
	4 HRT	n/a	8.0±0.1	4.6±0.1
	5 HRT	n/a	7.6±0.1	4.6±0.3
VSS (%)	**Pooled**	91±4	89±2	91±4

6.5.3 Settling

Settling results are provided in Table 33. Only CR2 showed any substantial settling. Both CR1a and CR1b remained at 970±20 mL/L. Similar to semi-continuous runs, supernatant liquid was an opaque milky-brown, suggesting substantial dissolution of solids.

Table 33: Continuous Treated WAS 30 minute Solids Settling Volume (mL/L)

Treatment	CR2
Raw	990
90°C	880
90°C + H_2O_2 + 5 min	600
½ HRT	440
1 HRT	390
2 HRT	360
3 HRT	380
4 HRT	380
5 HRT	370

6.5.4 Particle Size Distribution (PSD)

Both CR1a and CR1b used thermal treatment exclusively. Similar to SR5, this did not affect a substantial change in particle size, so results are omitted. With H_2O_2, CR2 showed significant change in PSD. Graphical results for PSD as well as values for cumulative distribution, are provided in Figure 16. Standard error for cumulative distributions are as follows: $d_{10\%}$ = 5%; $d_{50\%}$ = 5%, and; $d_{90\%}$ = 8%.

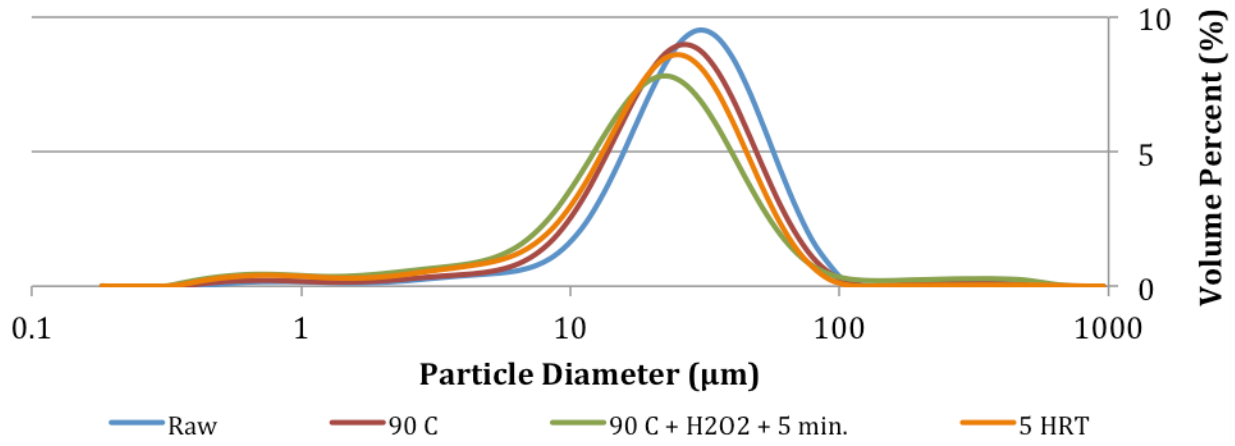

Treatment		Raw	90°C	90°C + H_2O_2 + 5 min	5 HRT
Cumulative Distribution (µm)	$d_{10\%}$	13	10	5.9	7.1
	$d_{50\%}$	30	27	22	24
	$d_{90\%}$	60	56	53	50

Figure 16: PSD for Continuous Treated WAS: Graphical Display and Cumulative Distribution

6.5.5 Capillary Suction Timer (CST)

Results for CST are given in Table 34. The results for CR1a show no significant change in CST between 90°C and 3 HRT. Similar results were expected for CR1b, so CST measurements were not taken.

Table 34: Continuous Treated WAS CST Results (seconds)

Treatment	CR1a	CR2
Raw	5.4±1.6	43±5.4
90°C	464±42	370±33
90°C + H_2O_2 + 5 min	-	440±19
1 HRT	-	262±24
3 HRT	473±39	254±12
5 HRT	-	233±22

6.5.6 Chemical Oxygen Demand (COD)

Table 35 shows the results for Chemical Oxygen demand (COD). Results for TCOD confirm μ_0.

Table 35: Continuous Treated WAS Total and Soluble COD (g/L)

Parameter	Treatment	CR1a	CR1b	CR2
Total COD	**Raw**	8.8±0.5	9.5±0.1	8.7±0.3
Soluble COD	**Raw**	0.1±0.0	0.1±0.0	0.0±0.0
	90°C	2.1±0.1	1.9±0.0	2.3±0.1
	90°C + H_2O_2 + 5 min	n/a	n/a	3.1±0.1
	½ HRT	1.7±0.0	-	2.9±0.1
	1 HRT	1.5±0.1	1.8±0.0	3.1±0.1
	2 HRT	1.4±0.0	1.6±0.0	3.3±0.1
	3 HRT	1.4±0.0	1.7±0.0	3.1±0.1
	4 HRT	n/a	1.6±0.0	2.9±0.1
	5 HRT	n/a	1.6±0.0	3.1±0.1

6.5.7 Volatile Fatty Acid (VFA)

Results for VFA are provided in Table 36.

Table 36: Continuous Treated WAS Volatile Fatty Acids (VFA) as acetic acid (g/L)

Treatment	CR1a	CR2
Raw	14±2.3	4.4±0.6
90°C	21±0.8	15±1.1
90°C + H_2O_2 + 5 min	n/a	31±4.4
½ HRT	21±1.2	36±2.5
1 HRT	21±1.4	46±2.4
2 HRT	20±1.1	46±2.7
3 HRT	24±1.2	50±2.5
4 HRT	n/a	55±0.5
5 HRT	n/a	58±5.0

6.5.8 Phosphorus

Phosphorus results are presented in Table 37. Results for TP unanimously confirmed μ_0.

6.5.9 Nitrogen

Nitrogen results are provided in Table 38. Like TP, TKN results unanimously confirmed μ_0.

6.5.10 Metals

Selected metals results are presented in Table 39.

Table 37: Continuous Treated WAS Phosphorus Results (mg/L)

Parameter	Treatment	CR1a	CR1b	CR2
Total P	-	360±14	294±22	270±17
	Raw	8.2±0.2	20±0.4	5.4±0.2
	90°C	249±2.1	223±6.1	222±1.5
	90°C + H_2O_2 + 5 min	n/a	n/a	206±14
	½ HRT	235±6.4	-	134±16
Soluble P	**1 HRT**	-	192±11	125±3.3
	2 HRT	227±3.5	206±4.5	117±5.3
	3 HRT	225±7.0	202±2.8	126±13
	4 HRT	n/a	192±10	136±3.4
	5 HRT	n/a	207±7.0	154±13
	Raw	5.8±0.2	4.2±0.0	4.7±0.1
	90°C	33±0.4	49±0.2	38±0.3
	90°C + H_2O_2 + 5 min	n/a	n/a	49±0.4
	½ HRT	39±0.3	-	53±0.3
Phosphate	**1 HRT**	44±0.6	58±0.4	50±0.3
	2 HRT	51±0.5	65±0.9	49±0.7
	3 HRT	59±0.8	68±1.4	50±0.5
	4 HRT	n/a	69±0.3	50±0.5
	5 HRT	n/a	66±0.6	50±0.3

Table 38: Continuous Treated WAS Nitrogen Results (mg/L)

Parameter	Treatment	CR1a	CR2
Total KN	-	768±28	587±45
	Raw	9.2±6.6	4.5±0.2
	90°C	148±2.5	157±1.9
	90°C + H_2O_2 + 5 min	n/a	212±7.4
	½ HRT	130±8.5	181±1.1
Soluble KN	**1 HRT**	-	165±7.3
	2 HRT	109±9.1	161±9.5
	3 HRT	108±4.7	161±1.1
	4 HRT	n/a	197±9.9
	5 HRT	n/a	257±2.5
	Raw	1.3±0.1	0.6±0.0
	90°C	4.2±0.1	3.6±0.3
	90°C + H_2O_2 + 5 min	n/a	21±1.0
	½ HRT	2.8±0.3	12±0.5
Ammonia	**1 HRT**	3.0±0.3	15±1.6
	2 HRT	2.6±0.4	17±1.6
	3 HRT	2.9±0.1	15±1.1
	4 HRT	n/a	17±0.7
	5 HRT	n/a	18±1.5

Table 39: Continuous Treated WAS ICP Metal Results

Parameter	Fraction	Treatment	CR1a	CR1b	CR2
Phosphorus	Total	Raw	359±3.3	374±5.3	339±6.4
	Soluble	Raw	9.2±1.0	30±2.5	6.9±3.5
		90°C	259±3.0	247±3.1	248±5.8
		90°C + H_2O_2 + 5 min	n/a	n/a	291±11
		1 HRT	245±2.2	251±4.3	190±3.5
		3 HRT	247±3.3	237±4.1	188±3.2
		5 HRT	n/a	241±4.2	189±6.1
Magnesium	Total	Raw	93±2.2	97±5.7	87±1.3
	Soluble	Raw	0.0±0.0	0.0±0.0	0.0±0.0
		90°C	61±0.4	56±0.9	58±0.8
	Soluble	90°C + H_2O_2 + 5 min	n/a	n/a	65±4.1
		1 HRT	56±0.6	46±1.5	49±1.8
		3 HRT	56±0.9	53±1.5	50±1.0
		5 HRT	n/a	54±2.4	54±5.3
Calcium	Total	Raw	261±14	281±23	255±2.2
	Soluble	Raw	5.1±3.5	63±21	10.1±3.9
		90°C	124±0.5	124±1.9	131±4.2
		90°C + H_2O_2 + 5 min	n/a	n/a	228±1.7
		1 HRT	101±1.7	72±5.6	103±7.4
		3 HRT	81±2.8	94±4.5	116±7.1
		5 HRT	n/a	94±4.5	125±2.8
Potassium	Total	Raw	151±3.4	153±5.3	133±3.5
	Soluble	Raw	25±1.5	37±5.8	19±1.4
		90°C	118±2.7	118±3.5	112±4.0
		90°C + H_2O_2 + 5 min	n/a	n/a	130±8.0
		1 HRT	118±2.7	133±0.3	121±3.5
		3 HRT	125±4.5	125±3.6	124±4.3
		5 HRT	n/a	124±4.4	125±0.9

6.5.11 Conductivity, pH and Hydrogen Peroxide Residual

Conductivity, and pH are provided in Table 40. As before, patterns reported for CR1a are assumed to be representative of CR1b.

Hydrogen peroxide residual for CR2 is provided in Table 41. Samples were taken over the course of the run, as well as four points at runs end to determine the degree of H_2O_2 accumulation and dissipation at all stages of processing. The expected standard deviation is ±14 mg/L.

Table 40: Continuous Run (CR) Conductivity and pH

Run	Range	Conductivity (μS/cm)	pH
CR1a	**Raw**	529	6.5
	90°C	1120	6.5
	1 HRT	1047	6.6
	2 HRT	968	6.7
	3 HRT	1061	6.7
CR2	**Raw**	511	6.5
	90°C	751	6.9
	90°C + H_2O_2 + 5 min	905	5.8
	1 HRT	980	5.4
	2 HRT	1036	5.3
	3 HRT	1102	5.3
	4 HRT	1061	5.2
	5 HRT	1059	5.2

Table 41: Hydrogen Peroxide Residual over Duration of CR2

H_2O_2 Treatment Stage	Treatment	H_2O_2 Residual (mg/L)
Theoretical Dose	-	1660
Background H_2O_2	**Raw/90°C**	0.0
Semi-continuous Reactor Residual	**90°C + H_2O_2 + 5 min**	857
Continuous Overflow Residual	**1 HRT**	661
	2 HRT	652
	3 HRT	671
	4 HRT	643
	5 HRT	643
Time after Continuous Feed Dosing Terminated (minutes)	**1**	571
	2.5	535
	5	485
	7.5	349

6.5.12 Temperature and Energy

The heating time and energy used for continuous runs is summarized in Table 42. These are given for the preheating stage, the entire run and averaged over each cycle of the HRT. Figure 17 gives profiles for heating, as well as forward and reflected power. Figure 18 Figure 19 provide the power distributions for continuous runs. The visible discontinuity for CR2 in Figure 19 represents the 5 minutes of holding time at 90°C, where forward power was either off or on at minimal setting to maintain temperature.

Table 42: Continuous Run Temperature and Energy Characteristics

Run	Range	Heating Time (min)	Energy Used (kWh)	Energy Used (kJ/g TSS)
CR1a	**25-90°C**	44	5.8	137±1.8
	25°C-end	137	16.9	400±5.3
	Per HRT	31	3.7±0.1	88±2.6
CR1b	**25-90°C**	51	6.7	137±3.1
	25°C-end	207	26.3	538±12
	Per HRT	31	3.9±0.1	80±2.5
CR2	**25-90°C**	46	6.0	142±1.9
	25°C-end	211	25.7	609±8.0
	Per HRT	31	3.8±0.1	90±2.6

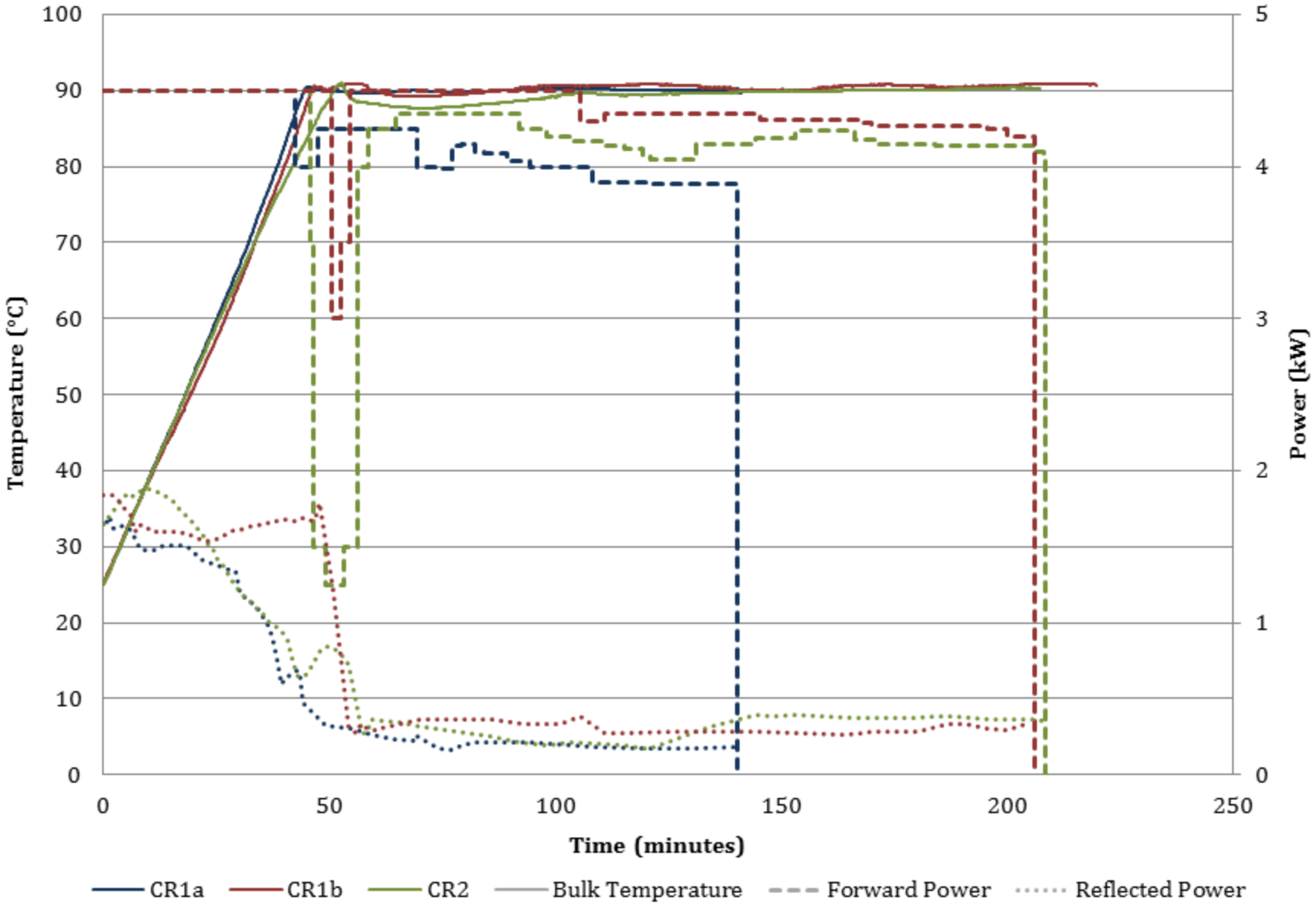

Figure 17: Continuous Run Bulk Temperature, Forward and Reflected Power

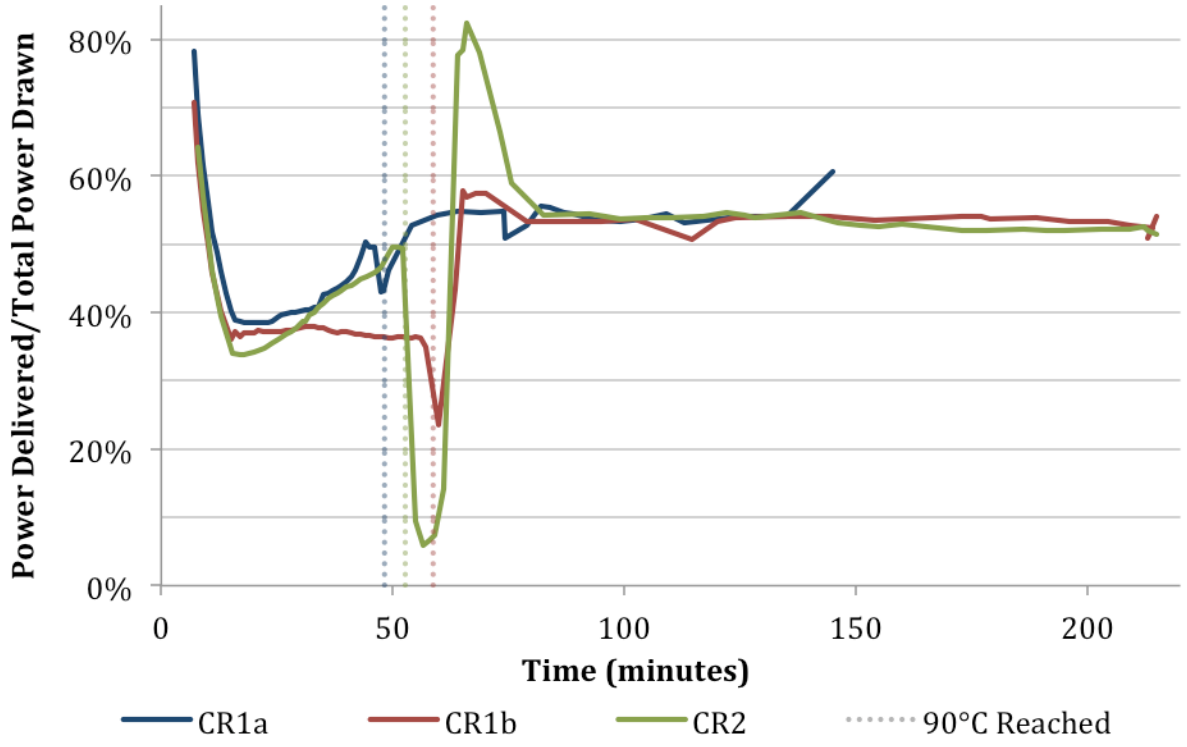

Figure 18: Power Delivered/Total Power Drawn over Duration of Continuous Runs

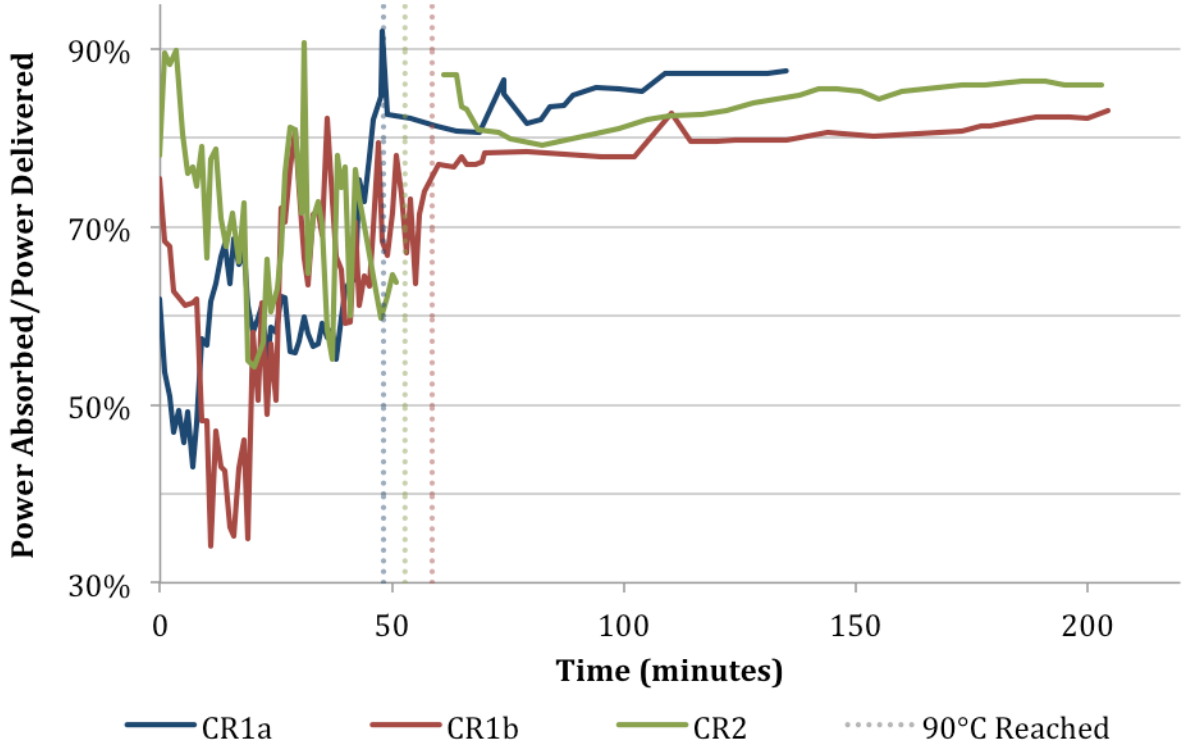

Figure 19: Power Absorbed/Power Delivered over Duration of Continuous Runs

6.6 Continuous Run (CR) Discussion

Results of continuous treatment are discussed below, divided in terms of solids reduction, potential biogas recovery, dewatering, potential nutrient recovery and energy efficiency.

6.6.1 Reductions to Particulate Solids

Continuous treatment had little effect on total and volatile solids in CR1a. A minor but significant increase was observed from start to finish in CR2, with a slight dip in between. This may be the result of some fraction of solids being retained in the up flow section of the reactor, which was indicated by a slightly higher solids concentration measured in a sample of reactor bound sludge, taken post-run. Retained solids may have been intermittently released as the run progressed.

In continuous runs, treatment to 90°C gave a TSS reduction very similar to results achieved by semi-continuous heat treatment in SR5. For all runs, TSS reduction at 90°C fell between average of 24 and 26%. This is the highest reduction achieved by CR1a and CR1b. After fresh feed was introduced, reductions to TSS declined to 20±0.4% for CR1a and 14±0.4% for CR1b, by the end of each run. These values are both lower than the comparable semi-continuous run, SR5, which displayed TSS reduction of 25±3.0% with heat treatment to 90°C. Inversely, the addition of H_2O_2 in CR2 reduced TSS as the run proceeded. By the end of the run, TSS reduction reached 39±1.0%. This is also less than the comparable semi-continuous run, SR7, which used the same H_2O_2 dose, and achieved a TSS reduction of 41±4.0% at 90°C.

Both semi-continuous and continuous treatments raised sludge to an ultimate temperature of 90°C. As such, the lower solids dissolution achieved in continuous operation must result from other factors than temperature. Holding time has been identified both here and in other studies as having less influence than temperature (Wong et al., 2007; Y. Yu et al., 2010), although it still plays a role. Continuous treatment differs primarily from semi-continuous runs, in terms of sludge retention. In the present continuous configuration, a fraction of the reactor holding tank volume is fresh feed, which had only been at 90°C since undergoing irradiation. It had much less time at that temperature than other sludge recirculating in the holding tank, yet some fraction of it invariably short circuits to become part of the sampled volume. An additional difference between the two

process designs is the dosing scheme for both sludge and H_2O_2. It involved more steps, more equipment and therefore more deviation. Further, an ever present source of deviation is differences in starting sludge.

Regardless, all results indicated that mineralisation of TS was minor. Solids disintegrated, but were not destroyed, as suggested by TSS results and visual observation of an increasingly opaque, milky supernatant, as treatment proceeds.

6.6.2 Potential Biogas Production

Precursors of enhanced biogas production include increased soluble COD and VFA. Hydrogen peroxide residual is also discussed for its potentially inhibitive effect. These are discussed below.

6.6.2.1 Soluble Chemical Oxygen Demand (SCOD)

Continuous SCOD results confirm the benefits of combined heat and H_2O_2 indicated in semi-continuous experiments. Further, runs CR1a and CR1b gave results similar to heat alone in SR5. Like for TSS, results for SCOD/TCOD ratio peak at 90°C, giving an average of 20-24%. After fresh feed was initiated, this ratio fell to a consistent average of 16-19%. Treatment in CR2 doubled the SCOD, giving values comparable to SR7 and higher H_2O_2 dosed SR4. The SCOD/TCOD ratio climbed from an average of 26% at 90°C to between 33-38%, following H_2O_2 addition and fresh feed initiation. The stability of SCOD results within continuous runs, and the similarity between semi-continuous and continuous results, gave further indication that retention time, the biggest difference between the two configurations, had less influence on COD solubilisation than temperature. This similarity also suggests that continuous treatment may respond well to an increased H_2O_2 dose.

The work by Y. Yu et al. (2010), which used the same sludge source as the present study (although with an SRT of 10 days), provides an excellent comparison. That study used a continuous flow 2450 MHz MW with varying configurations of pre- and post-MW heating, combined with different MW retention times and an inlet dose of H_2O_2 of about 0.2 g H_2O_2/g TS. Similar to this study, they reported that the ratio of SCOD/TCOD increased dramatically as a result of paired MW and H_2O_2 treatment. Further, preheating prior to H_2O_2 addition gives improved solubilisation, with their maximum of 60°C, proving optimal for all treatment configurations. Post-

heating holding time produced a small increase in COD solubility, although like this study, treatment temperature was found to be more dominant than holding time. With preheating to 50°C, Y. Yu et al. (2010) reached similar outlet temperatures as achieved here – around 90°C. With this configuration, SCOD/TCOD results were remarkably similar, falling in the range of 30-35%, compared to 33-38% found here. This similarity provides confirmation of comparability between 915 and 2450 MHz frequencies.

6.6.2.2 Volatile Fatty Acids (VFA)

Continuous run VFA results are also very similar to semi-continuous experiments. Heating to, and retention at 90°C in CR1a, gave results that closely resembled heat to 90°C in SR5. As elsewhere, VFA results for CR1a are taken to represent the trends of CR1b. Further, although SR7 was found to be erroneous, VFA results achieved there at 90°C are comparable to CR2, confirming the higher temperature outcomes of SR7. In CR2, VFA concentration increased as treatment proceeded, plateauing after about 3 HRT. As for semi-continuous runs, the addition of H_2O_2 was responsible for the release of half or more of the total VFA increase. This is further evidence of the improved efficacy of high temperature H_2O_2 addition, although adding H_2O_2 at either 60 or 90°C showed no definitive benefit to VFA.

6.6.2.3 Hydrogen Peroxide Residual

Hydrogen peroxide residual may be a concern for digestion, due to the inhibitory effect of oxidants on anaerobic bacteria. As such, it is important to determine if it accumulates in continuous operation, and whether further action is needed to remove it, prior to digestion. As can be seen in Table 41, H_2O_2 had a consistent residual, but it did not accumulate. Further, after terminating continuous dosing, and maintaining 90°C, this residual declined to half its original value in under ten minutes.

Residual measurements also denote reaction efficiency of H_2O_2. Of the theoretical dose of 1660 mg/L, only about half of the initial semi-continuous holding tank dose is utilized when given 5 minutes reaction at 90°C. During continuous operation, the theoretical dose remained at 1660 mg/L, although it is added in proportion to solids in the incoming continuous feed flow (which is 10% of the total flow, with the remaining 90% being recirculated semi-continuous holding tank fluid). The lower residual in continuous operation is speculated to result from the reaction of H_2O_2

with both fresh feed and any susceptible compounds remaining in the recirculating feed, in addition to the effects of extended reaction holding time. In continuous operation, roughly 60% of the dosed H_2O_2 was consumed, leaving the remainder as residual.

6.6.3 Dewatering

Settling in CR2 was improved in comparison to many of the semi-continuous runs, with relative stability reached after only 2 cycles of the holding tank HRT. It showed improvement at 90°C relative to CR1a and CR2b, which returned negligible settling, indicating some improvement inherent to the starting sludge. However, as for semi-continuous runs, settling did not result in a clear supernatant.

As indicated by PSD results for CR2, particles underwent substantial size reduction at 90°C following H_2O_2 addition and 5 minutes holding time. Unlike semi-continuous PSD trends, continuous treatment in CR2 did not result in a bimodal distribution. After 5 HRT cycles of continuous fresh feed dosed with H_2O_2, PSD increased back towards raw and 90°C results, although it maintained a visibly wider spread distribution. This may be a result of the relatively short time a fraction of fresh feed spends in the reactor, mentioned previously. It could also be the result of conglomerative browning and caramelisation, enhanced in sludge that is retained in the reactor and subjected to high heat and extended holding time.

Considering CST results, CR1a showed insignificant change from 90°C to the end of run at 3 HRT, confirming that thermal treatment and holding time alone do not effectively improve dewatering. These results were comparable to previous semi-continuous runs, notably SR4 and SR7. In CR2, treatment to 90°C achieved results similar to SR5, while 90°C plus H_2O_2 addition and 5 minutes holding time gave results indistinguishable from SR7. Following this, continuous heat treatment and relatively low H_2O_2 dose achieved considerable improvement to dewatering, nearly matching the best CST results achieved in semi-continuous runs.

Previously, semi-continuous results suggested a trend between an increased particle size, particularly in the observed upper modal of PSD, and improved CST. Results for CR2 verified this in an inverse trend. In CR2, a decrease in particle size from raw to 90°C, then to 90°C plus H_2O_2 and 5 minutes, coincided with impaired CST. In further corroboration, an increased particle size

at 5 HRT improved CST. Notably, although PSD at 5 HRT was visibly similar to results at 90°C, it showed substantially improved dewaterability. This indicates that changes to dewaterability are more complex than PSD alone can describe. For CR2, from 90°C to 5 HRT SCOD and PSD results change only slightly, yet CST and settling improved substantially. This is clear evidence that heat and H_2O_2 treatments simultaneously disintegrate and reconfigure solids. This is especially true at sustained high temperatures, which would enhance rates of browning and caramelisation, as well as altering the distribution of interstitial and bound water. In any event, treatment by CR2 attained considerable improvement in dewaterability using a relatively low dose of H_2O_2, indicating a unique effect and potential advantage of continuous treatment.

6.6.4 Potential Nutrient Recovery

Phosphorus, nitrogen and magnesium are discussed below for their role in potential struvite recovery.

6.6.4.1 Phosphorus

The highest SP/TP ratios were returned at 90°C, with 69±2.8%, 76±6.0% and 82±5.2% for CR1a, CR1b and CR2, respectively. After the initiation of fresh feed, SP/TP for CR1a and CR1b declined to a statistically consistent average, similar in magnitude to SR5, at 63-65% and 65-70%, respectively. This decline may be the result of retention patterns in continuous treatment, discussed in the solids section. Results for CR2 showed more drastic change. Initially, the SP/TP declined insignificantly with holding tank H_2O_2 addition. However, during continuous feed and H_2O_2 dosing, SP/TP declined considerably, from 76±7.1% at 90°C + H_2O_2 + 5 min, to within 43 and 57% in successive samples. As discussed for semi-continuous phosphorus results, this decline may be the result of initially liberated phosphorus reforming recalcitrant organic or insoluble complexes under maintained heat and extended oxidant reaction time. However, further exploration is needed.

Phosphate results were more stable as runs progressed. In contrast to SP, phosphate was lowest at 90°C for all runs. Following this, in CR1a the ratio of phosphate/TP climbed slightly from 11 to 16%, by the end of the run. On the other hand, phosphate/TP for both CR1b and CR2 stabilized at 20-23% and 18-19%, respectively, with no consistent climb or decline displayed after about 1 HRT. The difference in the average between CR1b and CR2 was slight, yet statistically distinguishable. The similarity indicates that, while H_2O_2 does not confer positive benefit to

phosphate in continuous configuration, it does not suppress its release to the degree observed in semi-continuous processing. It is likely that after heating to 90°C, the compounds targeted by subsequent H_2O_2 attack, and the products of oxidation, are different than at 60°C.

Comparing CR1b and CR2, the former showed largely improved release of SP and slight, yet significantly improved phosphate. In CR2, after continuous feed and H_2O_2 dosing was initiated, SP reduced drastically, while phosphate remained relatively steady. Soluble phosphorus compounds appear to be more sensitive to this altered treatment configuration, forming particulate (>0.45 µm) or unmeasured organic compounds. Ultimately, treatment by CR2 has the additional benefit of improved settling, making phosphate more available to recovery (although the high suspended solids observed in the supernatant may be an inhibitive obstacle).

The results of Y. Yu et al. (2010) help to corroborate the findings for phosphate release seen in both semi-continuous and continuous experiments performed here. In support of semi-continuous runs, they showed an absolute optimum release of phosphate following preheating to 50 or 60°C. With subsequent continuous MW and H_2O_2 treatment, phosphate concentrations showed considerable decline, especially when subjected to longer MW retention and higher exit temperature. Again, considering preheating to 50°C, which gave an exit temperature close to 90°C, ratios of phosphate/TP were remarkably similar to findings reported here. Y. Yu et al. (2010) report phosphate/TP between 18-25% following MW and H_2O_2, while here, under similar conditions, this ratio is 18-20%. They report that holding outlet temperature up to 120 minutes had relatively minor effect on phosphate release. Their study did not include a control for MW only, so comparative results for CR1a and CR1b are not available. However, results from both studies indicate that H_2O_2 had little, positive impact on phosphate solubilisation, in continuous thermal-oxidative treatment.

6.6.4.2 Nitrogen

Heat to 90°C accounted for the majority of SKN release, giving an SKN/TKN of 19±0.8% and 27±2.1% for CR1a and CR2, respectively. After continuous feed was initiated, this ratio declined in CR1a, from 17 to 14% by 3 HRT. As seen previously, H_2O_2 had the most profound effect on nitrogen release. In CR2, after H_2O_2 addition and 5 minutes reaction, SKN/TKN increased to 36±3.0%. With continuous feed and H_2O_2 dosing, the ratio initially declined, although it was never

lower than an average of 27%. Ultimately, it increased as the run proceeded, to a peak ratio of 44±3.4% by 5 HRT.

Similar to semi-continuous runs, ammonia release represented a minor portion of TKN. Ammonia results for CR1a remained low, never higher than 0.5% of TKN, and lower than any previous semi-continuous run. On the other hand, the addition of H_2O_2 in CR2 achieved the highest release of ammonia. At 90°C + H_2O_2 + 5 min, ammonia/TKN peaked at 3.6%, higher than any semi-continuous run result. This may reflect the improved, higher heat reaction of H_2O_2 with nitrogenous compounds when added at 90°C. After initiating continuous feed and H_2O_2, ammonia underwent an initial drop, then reached stability, maintaining a ratio of ammonia/TKN of 2.6-3.1% from 1 HRT onwards.

6.6.4.3 Magnesium and Other Metals

Phosphorus, measured as metal, returns consistently higher values than colorimetry (TP) results. This is expected, given that the metals digestion procedure is more severe. However, when metals results are converted to a ratio of soluble to total phosphorus, they are largely indistinguishable from the ratios reported by colorimetry. A notable exception is soluble phosphorus measured after semi-continuous tank dosing of H_2O_2: metals results increase, where colorimetry reports a decrease. This may be an indication of increased polymerisation or organic binding of phosphorus following oxidation. Analysis by colorimetry could miss these compounds, whereas metals digestion may more effectively liberate and measure them. A detailed study on the partitioning of phosphorus during thermal-oxidative treatment would help elucidate these outcomes.

Converting magnesium results to a ratio of soluble to total magnesium, it becomes apparent that the results of continuous runs were very similar to one another, displaying statistical parity at an average of 55-62% from 3 HRT's onward. This confirmed the findings of semi-continuous runs, where no difference between treatment was noted, suggesting that oxidation has a minor impact on magnesium solubilisation. The exception is a slight increase in soluble magnesium for CR2 at 90°C + H_2O_2 + 5 min. However, this is followed soon after by decline, and stabilisation, to results indistinguishable from CR1.

Converting calcium to a ratio of soluble/total, CR1a and CR1b were indistinguishable at an average of 31-33% at 3 HRT. Unlike semi-continuous results, oxidation in CR2 initially increased soluble calcium, showing a peak of 89±1.0% at 90°C + H_2O_2 + 5 min. After initiating continuous feed and H_2O_2 dosing, this average droped to 40-49%. As stated previously, at a higher temperature, oxidation either reacts through different pathways or different reactants are available to attack. In continuous runs, the result is oxidation increasing calcium solubility, in contrast to semi-continuous runs.

Potassium showed results similar to calcium. Results for CR1a and CR1b stabilized to an indistinguishable average of 81-83% from 3 HRT's onward. In CR2, oxidant addition gave a slight boost to soluble potassium, resulting in a statistically consistent average of 91-98% from 90°C + H_2O_2 + 5 min, until the end of the run.

6.6.4.4 Treatment Recommended for Further Investigation

Table 43 gives the resulting molar ratios of magnesium:ammonim:phosphate for continuous experiments. Each value is normalized to phosphate, highlighting instances where the molar ratio is at least 1:1:1 in green. Phosphate and magnesium are consistently in excess, while ammonia is limiting. Comparing the two runs, and from 90°C to after the addition of H_2O_2, it is evident that oxidation is necessary to release the ammonia necessary to satisfy molar ratios.

Table 43: Struvite Molar Ratios Given as Magnesium:Ammonium:Phosphate

Treatment	CR1a	CR2
90°C	7.2:0.7:1	6.0:0.5:1
90°C + H_2O_2 + 5 min	-	5.2:2.3:1
1 HRT	5.0:0.4:1	3.8:1.6:1
3 HRT	3.7:0.3:1	4.0:1.6:1
5 HRT	-	4.2:1.9:1

However, as in the semi-continuous runs, the supernatant was milky brown and opaque in all continuous runs. Soluble TSS was not directly measured; however, high SCOD results suggest high suspended solids, which may inhibit struvite formation. If continuous treatment is employed immediately prior to struvite precipitation, acidification (or some other form of solids/liquids separation) may be required to settle inhibitory solids. Ultimately, only empirical testing can

determine whether the sludge treatments used here are amenable as a pretreatment to struvite precipitation.

As recommended previously, at this stage in processing, to recover maximum phosphorus, it may be advantageous to recover all the available SP. Hydrolysis of soluble polyphosphate and organic phosphorus, perhaps by enzyme attack (Monbet et al., 2007), could liberate reactive phosphate for struvite recovery. Otherwise, treatment in advance of anaerobic digestion for potential improvements to biogas production, with phosphorus recovery from digester effluent, may be more practical. Further study is required to evaluate alternative and untested treatment configurations.

6.6.5 Energy Efficiency

Energy data for continuous runs is provided in Table 42, with visual representation given in Figures 17 and 19.

6.6.5.1 Energy Absorption and Heating Profile

Continuous runs also indicated a correlation between heating time and energy consumed, athough relative to semi-continuous runs, both are inherently higher in magnitude, with proportionally higher deviation.

In reference to Figure 17, a few trends are apparent. In the initial ramp heating stage of continuous runs – in the first, approximately 50 minutes of the run – reflected power (RP) started high and declined as temperatures increased and stabilized. This pattern matches semi-continuous runs, and is expected to be a result of magnetron ramp-up and changes in energy absorption determined by ionic conduction. Reflected power for CR1b followed this same general trend, but displayed higher RP. Further, it was also somewhat slower to heat, taking an additional 5 to 6 minutes to reach 90°C. Both of these outcomes are perhaps the result of higher sludge TS content in CR1b. Tuning was not adjusted or optimized for this higher density sludge, with the likely result of higher RP.

Regardless, for all runs, after sludge had reached 90°C, and all adjustments and H_2O_2 additions had been made, RP stabilized to a value consistently below 10% of the forward power (FP), until

the end of run. The addition of H_2O_2 incurred the most substantial jump in RP, while changes to FP caused slight and negligible disturbance. The chosen design of 20 L recirculating volume and the flow ratio of 10% fresh feed to 90% recirculated feed was adequate to ensure stable operating temperatures. Any change in temperature was slow enough that FP was easily adjusted to compensate. Further, FP was held consistently below the default 4.5 kW setting, allowing increase when needed, otherwise helping to lower power draw. Overall, the energy absorption patterns of continuous treatment was characterized by stability

In reference to Table 42, from the initiation of fresh feed to the end of the run, continuous runs all resulted in similar energy draw at 3.7-3.9 kWh per HRT cycle, treating 20 L of sludge per HRT.

6.6.5.2 Power Distribution

Power distribution for continuous runs is provided in Figures 18 and 19, calculated as described previously in the semi-continuous run discussion.

Referring to Figure 18, in the start-up phase of continuous runs, the ratio of power delivered over total power drawn displays the same initially rapid decline as in semi-continuous runs, as total power drawn increases to steady operating power. The ratio then increased for CR1a and CR2 as RP declined, while for CR1b it plateaued, due to stable RP. From 90°C on, FP adjustments incurred a slight fluctuation, with eventual recovery and stabilisation. For CR2 the drastic fluctuation observed is a result of a reduction in FP, coincident with the addition of H_2O_2 and a rise in RP. The data, following adjustments at 90°C and disruption from oxidation, eventually stabilized and remained very consistent. It did not falter more than about 5%, from an average of 54%, until the end of the run. In other words, in continuous operation, approximately 54% of the total power drawn by the magnetron, including all associated auxiliary systems, is consistently directed into the applicator for heating

In Figure 19, prior to 90°C, data was chaotic, in much the same way as the semi-continuous runs. As before, the ratio of power absorbed over power delivered was dependent on changing temperature, RP, and, unique to continuous runs, variable FP. The ratio is subject to all the variations observed in these parameters. Before 90°C, the only discernible trend was an overall rise in power absorbed for CR1a and CR1b, as temperature increased. As mentioned, the curve

break in CR2 coincides with the 5 minute H_2O_2 reaction time, where ΔT was effectively zero. Following 90°C, oxidant addition, and the initiation of fresh feed, ΔT is assumed to be constant at 6.4°C – a value predetermined by mass balance. As such, any fluctuation observed after this point is the result of variation in RP and FP. As observed, power absorbed over power delivered was very consistent. Since the system was tuned for sludge solids observed in CR1a and CR2, these achieve the highest absorption, stabilizing to 87 and 86%, respectively, by the end of the run.

The most important outcome displayed in power distribution for continuous operation is that, when temperature and oxidant additions are held constant and the system is allowed to develop stability, energy transfer is steadier and consistently more efficient than semi-continuous operation.

6.7 Conclusion: Semi-continuous and Continuous Waste Activated Sludge Treatment

This chapter provides data and discussion on semi-continuous and continuous thermal-oxidative treatment of WAS. Many trends are identified, cooperative and competitive, in achieving the objectives of treatment. A majority of the results indicated a threshold at 60°C, at which point the measured benefits of treatment increased drastically. This is speculated to result from heat denaturation of proteins, which drastically alters the mechanical and chemical characteristics of sludge floc EPS. This liberates soluble organic material, nutrients (such as nitrogen and phosphorus), and various metals. A coincident benefit is the inactivation of catalase, which will otherwise quench H_2O_2. Results indicated that, when adding H_2O_2 after 60°C, the impact and efficacy of oxidation was increased.

Some comparative results are available between treatments employed in this study and other published works. Despite different operating frequencies, process configurations, MW applicator modes and other variations, results in this study were comparable to results reported elsewhere. This helps to confirm the continuity of different forms of thermal treatment, recommending the dominant and determinant effect of temperature. In some instances, results here showed improvement over certain previous studies. Standing out is the addition of H_2O_2 above 60°C, which makes more effective use of the oxidant, resulting in improved solubilisation of COD and VFA. Details are discussed in the following sections.

6.7.1 Solids Reduction

In terms of solids reduction, both semi-continuous and continuous treatment had little impact on TS results. This shows that mineralisation and volatilisation, which would result in respective decline or concentration of solids, are both minor. On the other hand, while not strictly destroyed, TSS are dissolved. The best reduction in TSS was shown in SR8 at high heat, with largest dose and late addition of H_2O_2. Comparing similar semi-continuous and continuous runs, namely SR7 and CR2, semi-continuous operation showed advantages for TSS dissolution. This may be due to the potential for flow to short circuit in the continuous configuration, in effect granting semi-continuous processing a longer effective retention time. Although retention time is consistently identified as being less determinant to treatment outcomes, its effect may be enough to explain the differences observed in semi-continuous and continuous results.

6.7.2 Potential Biogas Production

Using WAS as a feedstock, many studies have identified that an increased availability of soluble COD and VFA can augment the quantity and rate of biogas produced by any subsequent anaerobic digestion process. Results here mirror this: high temperature and the late addition of H2O2 results in the highest VFA and ratios of SCOD/TCOD. These results are summarized in Figure 20, given together with specific energy, which is calculated at 90°C + 5 min for semi-continuous runs and per HRT for continuous runs.

For semi-continuous runs, the best SCOD/TCOD result achieved was a statistical tie between SR2 and SR8 at 90°C or 90°C + 5 min. The best VFA is achieved in SR2, again tied at 90°C and 90°C + 5 min. This indicated either that: an increased dose of H_2O_2 and holding time of 5 minutes gives minimal additional benefit to COD and VFA release; or that differences in treatment are buried in variability in operation, starting material or sampling error. In continuous runs, H_2O_2 again proves vital, with CR2 achieving the best COD and VFA release, after continuous feed and H_2O_2 dosing were initiated.

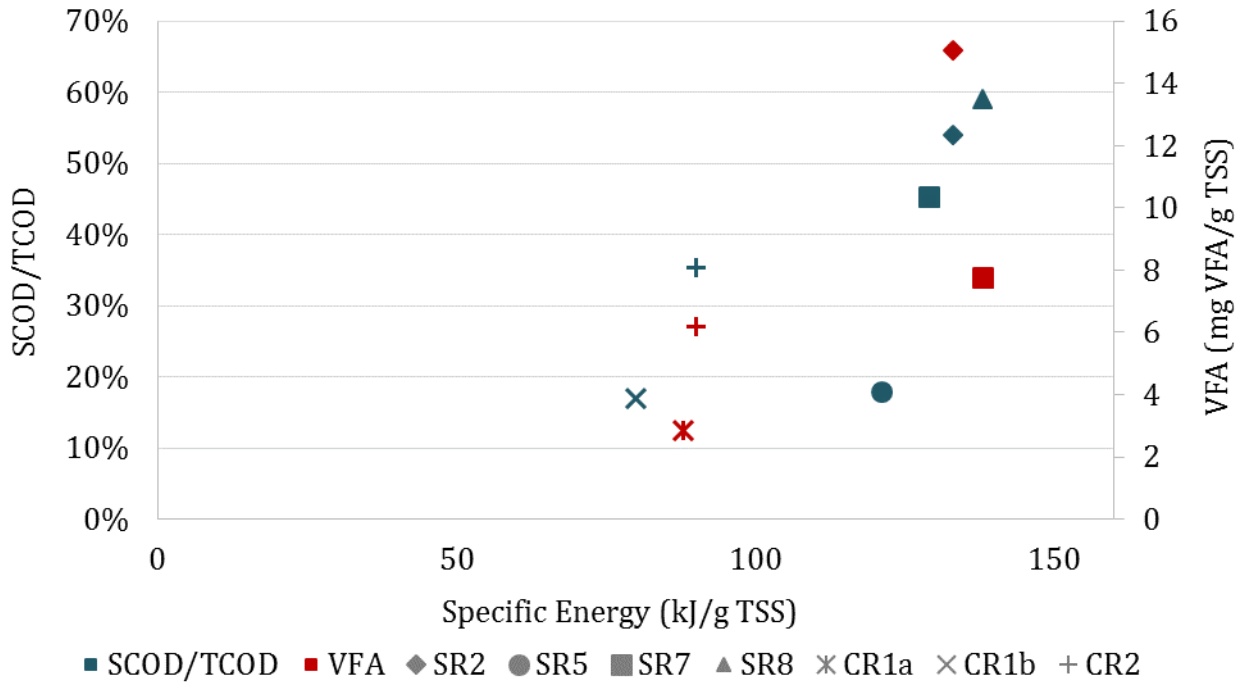

Figure 20: SCOD/TCOD and VFA versus Specific Energy for Select Runs

Figure 20 illustrates two strong trends: a higher H_2O_2 dose gave higher SCOD/TCOD and VFA results; and continuous operation consistently used less specific energy. Considering comparable pairs in semi-continuous and continuous runs – namely SCOD/TCOD for SR7 and CR2, SR5 and CR1b, as well as VFA for SR7 and CR2 –the continuous results were similar, although slightly lower than semi-continuous runs. Taken together, the data suggests that an increased dose of H_2O_2 in continuous operation could augment SCOD and VFA concentrations, while retaining energy savings. This is suggested for further study. Tests with actual, operating anaerobic digesters are required to confirm the benefits of treatment.

6.7.3 Dewatering

Dewatering is pivotal to economic solids/liquids separation and the recovery of nutrients. The present study gives settling, PSD and CST as indicators of dewaterability. The best overall settling was achieved in SR8 at 90°C + 5 min, indicating the advantages of late addition of H_2O_2 at high dose, as well as holding time. Settling in CR2 was better than the comparable semi-continuous run, SR7, and used less specific energy. However, in all cases save SR6, the settled supernatant of heat and oxidation treatments was an opaque brown. This is visual indication of high suspended solids, which could inhibit nutrient recovery (Srinivasan et al., 2014). Acidification in SR6 was

the only treatment that gave a clear supernatant, in addition to the most immediate settling, optimal at 60°C.

Heat and the late addition of H_2O_2 reduceD overall PSD, in some instances causing a bimodality to emerge, while acidification causeD an overall increase. Particle size in CR2 initially showed trends similar to semi-continuous runs. However, following the initiation of fresh feed, PSD again increased. This is taken as evidence of the retention pattern of continuous operation, namely the short-circuiting of some portion of the fresh feed. Heat only, as well as the early addition of H_2O_2, had a minimal effect on both settling and PSD.

Only SR6 improved dewaterability relative to the raw result. All other treatments gave CST values roughly an order of magnitude higher than the raw. Overall, a rough trend was observed between PSD and CST. Runs that displayed an increased particle size, whether overall such as in SR6, or due to an increased upper modal witnessed in other semi-continuous runs, also showed a relative improvement to dewaterability.

6.7.4 Potential Nutrient Recovery

Phosphorus is a primary target of nutrient recovery efforts. Treatments used in this study have a varied effect on different species of phosphorus found in WAS. The ratio of SP/TP was highest in SR1, following the early addition of H_2O_2 and heat to 90°C. Heat to 60°C displayed the most drastic increase in SP for all semi-continuous tests, save SR6. Only slight gains are achieved by holding 90°C for 5 minutes, indicating the dominant impact of temperature. Considering continuous operation, heat treatment by CR1b gave the highest SP, although lower than semi-continuous runs. Except in SR1, the addition of H_2O_2 did not increase SP concentration, relative to the results of heat treatment alone.

In semi-continuous operation, phosphate displayed peak concentrations at 60°C. The highest phosphate/TP was a statistical tie between SR1, SR2 and SR5 all at 60°C, indicating that H_2O_2 added early or not at all, results in optimal phosphate solubility. In continuous operation, CR1b proved best for phosphate, although with lower results than semi-continuous run results at 60°C. The addition of H_2O_2 in CR2 did not increase phosphate concentration, relative to heat alone.

Figure 21 summarizes the best SP and phosphate results achieved in both semi-continuous and continuous operation: respectively, SR1 and CR1b. Results for SR6 are also provided, given that it was the only treatment used that gave good settling and a clear supernatant, both important precursors for struvite recovery. Results are given for SR1 and SR6 at temperatures of 60 and 90°C + 5 min, while CR1b represents results in continuous operation, per HRT. Results for CR1b are somewhat similar to SR5 at 60°C, although they require higher specific energy. In terms of energy efficiency, continuous operation does not provide as clear an advantage for phosphorus as it does for SCOD and VFA release. In any case, SR6 may be the only effective treatment for immediate struvite recovery. However, if the objective is maximum phosphorus recovery, recovering the high concentration of SP made available by other treatments may be more desirable, with subsequent processing to separate phosphate.

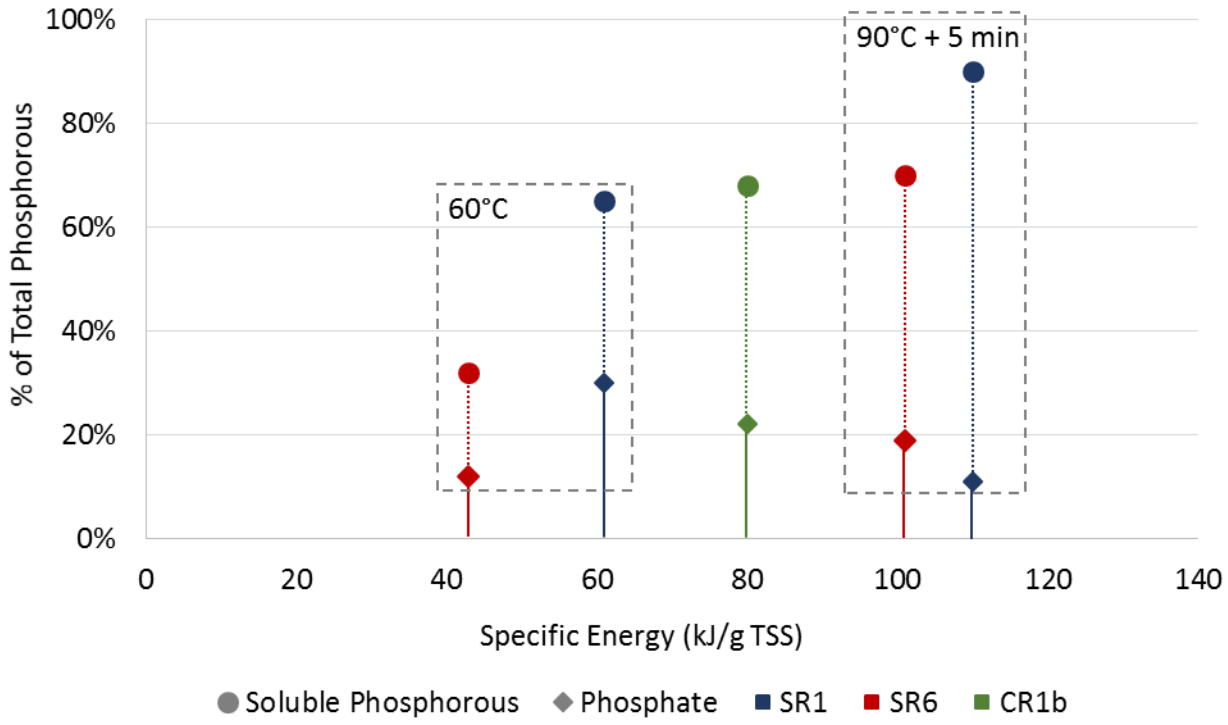

Figure 21: Soluble Phosphorus and Phosphate as a Percent of Total Phosphorus versus Specific Energy

As mentioned, H_2O_2 played a minor or inconsequent role in increasing SP and phosphate concentrations. However, it was pivotal for other precursors of struvite recovery. The late addition of H_2O_2 proved necessary to induce settling. It also severely disrupted nitrogen compounds,

achieving the highest concentration of SKN, and the release of ammonia in required proportions for potential struvite recovery. Semi-continuous and continuous treatments produced a similar outcome for ammonia, the highest average achieved being 3.1-3.2% of TKN by the end of the run in SR2, SR4, SR8 and CR2.

Metals results showed that the solubilisation of magnesium is primarily determined by temperature, and is minimally affected by the dose and timing of H_2O_2 additions. Soluble magnesium is sufficient for potential struvite recovery at a temperature of 60°C and above for every run, in both operating modes. Ultimately, empirical testing is needed to confirm the benefits of treatment for potential struvite recovery.

6.7.5 Energy Efficiency

This study helps to contrast and compare the impacts of operation mode on the efficiency of MW heating. A fundamental difference of semi-continuous and continuous processing is consistency. Semi-continuous operation introduced more variability to the system, including transient temperature, chemical and mechanical properties of the target fluid. Manual tuning was employed in an attempt to compensate for this variability, with minimal success at lower temperature. Automatic tuning is recommended for subsequent investigations into process scale-up and energy efficiency.

Power and energy results reflect the variability of semi-continuous operation. In semi-continuous runs, reflected power (RP) is initially high, declining as temperature increases. With decreasing RP, the efficiency of power delivered to the target fluid increased. In turn, the efficiency of power absorbed and converted to measurable temperature rise varied drastically, stabilizing in some runs, fluctuating in others. This reflects variations in temperature rise per pass and RP. Variability in RP was noticeably reduced in SR6, following acidification and the release of free ions, reported by high conductivity. In theory, and supported here by results, this greater availability of ions likely lends to stronger ionic conductance, increased MW energy absorption, and faster heating.

Alternatively, continuous operation is essentially steady-state, with constant temperature and consistent H_2O_2 addition, requiring only a slight change in forward power (FP) to maintain

stability. In continuous runs, following preheating to 90°C, the initiation of continuous fresh feed and H_2O_2 dosing, RP was consistently lower than 10% of FP. Power delivered remains steady at 54% of the total power drawn. Of the power delivered, consistently over 80%, and up to 87%, was absorbed.

Semi-continuous operation was able to treat 12 L of WAS to 90°C, plus various timing and dose of H_2O_2, as well as a holding time of 5 minutes, in 22.5 to 32.7 minutes. This does not include time to drain and refill. Continuous operation treated 20 L of WAS to 90°C every 31.5 minutes. Continuous operation treats more fluid in less time, and, given observations of more stable power delivery, it is also more energy efficient. However, treatment objectives must be weighed in reference to energy consumption, to conclusively determine an optimally efficient configuration.

In this study, improvements to TSS reduction, SCOD and VFA release, and dewatering seemed to pivot on H_2O_2 addition. Continuous results are comparable, although slightly lower than semi-continuous, using considerably less energy. For these objectives, it is clear that using a higher dose of H_2O_2 in continuous operation could give results comparable or better than semi-continuous runs, while capitalising on the lower energy requirement of the continuous configuration.

An optimal, energy-efficient configuration or operation mode for potential nutrient recovery as struvite is not as definitive. Out of necessity for a clear supernatant, SR6 emerges as an optimal treatment, even though it results in lower solubilised phosphate than a majority of the other runs. Further study is required to definitively describe the efficacy and energy efficiency of alternative treatments for any phosphate recovery, in an effort to recover more of this valuable nutrient.

7 Conclusions and Recommendations for Further Study

This chapter summarizes the entire research program reported in this document. It provides key conclusions from each chapter, as well as recommendations for further research.

7.1 Conclusions

This study explored the efficacy, in terms of predefined treatment objectives, and efficiency of a novel, pilot-scale, microwave (MW) thermal-oxidative treatment process. Where comparison was available, treatment results for both liquid dairy manure and waste activated sludge (WAS) showed marked similarity to previous studies, even where MW frequency and the specific configurations of processing differed.

Despite the vast difference between dairy manure and WAS, similar treatment trends were apparent in both trials. Heat alone had a substantial impact on solids dissolution, with an especially consistent and considerable release seen in many of the results of WAS treatment at 60°C. Around this temperature, sludge bound proteins are expected to denature. Due to their prevalence in WAS, their disruption would be very destructive to sludge floc integrity. For both dairy manure and WAS, heightened doses of H_2O_2 had mixed results, in some cases showing detriment to the solubility of inorganics, such as phosphorus. However, it proved essential to improve bulk properties, such as settling, and the release of certain beneficial organic constituents, such as nitrogen, soluble COD (SCOD) and volatile fatty acids (VFA). An increased dose of H_2O_2 – additionally beneficial when added late – and higher heat resulted in optimal settling, which is an important prerequisite for potential phosphorus recovery as struvite. For both wastes, it achieved the best release of ammonia, solubilising it in proportions necessary for struvite recovery. Heat and high dose of H_2O_2 also displayed optimal increases in SCOD and VFA concentrations, showing most acute impact on WAS. This could help to expedite and augment potential biogas production in any subsequent anaerobic digestion process. Again considering WAS, treatment with high heat and H_2O_2 resulted in the most substantial dissolution of total suspended solids.

Finally, acidification had a similar effect, although drastically different results for manure and WAS. In both materials, it caused the immediate dissociation of inorganics, as well as the conglomeration of humic organics. Acidification had the most immediate and impactful effect on

dairy manure, accounting for the majority of phosphorus solubilised in every run. Except for settling, the impact of heat and H_2O_2 treatment on dairy manure was slight, when compared to acid alone.

The impact of acid on WAS was more subtle. Compared to other semi-continuous WAS treatments, it solubilised less phosphorus, while seeming to fix carbon and nitrogen. However, it showed immediate benefit to settling, achieving the only clear supernatant and improved dewaterability. Although acidification resulted in less soluble phosphate than many of the other treatments employed, due to the clear supernatant, it is most attractive for the potential recovery of struvite from thermal-oxidative treated dairy manure and WAS.

As mentioned, the outcomes of treatment efficacy confirmed similarity between different MW frequencies and operating modes used in previous studies. However, this study also provided evidence that outcomes of energy efficiency vary substantially between different operating mode and process configuration. This research highlights the sensitivity of MW energy absorption to different target fluids and variations in their mechanical and chemical properties as treatments proceed. Especially notable is the ability of target fluids to absorb MW energy through ionic conductance, a mechanism which increases in strength as temperatures rise. Ionic conductance was controlled in water experiments with the addition of salt. Water with higher salt concentration displayed more consistent energy absorption throughout the run. This was indicated by low reflected power (RP), leading to reductions in heating time and energy consumption. In acidified dairy manure, reported metals data indicated a high concentration of free ions, resulting in very consistent energy absorption, and heating rates similar to water dosed with 5-10 g NaCl/L. Where ion concentration was high, the ability of target fluids to absorb MW energy was consistently high.

The comparison between semi-continuous and continuous operation in WAS experiments showed how process design can help to control variability in energy absorption, when variability in the target fluid is unavoidable. In semi-continuous WAS experiments, acidification also resulted in high free ion concentrations and consistent energy absorption patterns, similar to those observed in salt water and dairy manure runs. However, acidification of WAS proved detrimental to some treatment objectives, especially potential biogas production. Waste activated sludge is not

inherently high in free ions, so without acid, semi-continuous runs displayed high variability in energy absorption. Runs began with initially high inefficiency, improving as the run progressed, temperatures rose, and the relative strength of ionic MW conductance increased. This instability had an adverse effect on energy absorption and efficiency. Additional instability was contributed by late H_2O_2 addition.

Continuous operation resolved this instability and improved energy efficiency, although it achieved slightly lower results in efficacy, relative to semi-continuous runs (thought to result from different fluid retention patterns). Since continuous runs operated at steady temperatures, mechanisms of MW absorption, including ionic conductance, were relatively invariable. The generator and applicator can, therefore, be tuned to a single, effective setting to achieve an optimally low RP. Further, oxidant additions can be dosed continuously, thereby avoiding the instability introduced by plug or short term dosing.

It is inescapable that outcomes of treatment will be affected by the source and character of the target material. Despite this, following years of study, there is strong evidence to suggest that thermal-oxidative treatments can be performed with relatively reproducible outcomes. In advancing the treatment technology further, research might begin to move away from what it can do, to instead, focus on how it should be designed. Choosing appropriate designs will lead to reduced costs in energy, capital or operating requirements, and help to develop treatments for full-scale application.

7.2 Recommendations for Further Study

To evaluate the effects of treatment, this study relies in large part on trends identified in literature, drawing comparisons, where available, to add legitimacy to observed outcomes. However, an exhaustive evaluation of the equipment, and the process designs employed, requires empirical validation of the ‘potential’ benefits discussed throughout.

Select treatments should be repeated, in advance of experimental reactors, such as anaerobic digesters and struvite reactors, to validate potential benefits. Using the same (or similar) equipment and set-ups used in the present study, many of the same procedures could be repeated, including:

retaining a flow rate around 6.5 L/min; heating to an ultimate temperature of 90°C; for semi-continuous runs, sampling at 45, 60, 75 and 90°C; and for continuous runs, sampling up to 5 HRTs or longer. These procedures should be repeated using both semi-continuous and continuous systems, to evaluate whether savings in energy gained by these differences in process design, also translate to observable benefits in the subsequent, experimental reactors.

To summarize the above in point form, using WAS as a feedstock, select treatments from this study should be repeated, followed by:

- Anaerobic Digestion Experiment Reactors, to:
  - Determine an optimal dose of H_2O_2 in thermal-oxidative treatment that:
    - Maximizes biogas production volumes and/or reduces required digestion retention time
    - Maximizes the reduction of TSS volumes
- Nutrient Recovery Processes:
  - Evaluate whether acidified, as well as acidified and thermal-oxidative treated sludge is a suitable feedstock for struvite recovery reactors
  - Using thermal treatment alone:
    - Evaluate whether treating to a temperature below or above 90°C allows more phosphate to be recovered for struvite nutrient recovery
    - Investigate other techniques (aside from those gains attained by oxidation) for solids/liquids separation, to capitalize on the higher phosphate concentrations shown in this study in treating to 60°C
    - Investigate the feasibility of recovering the high concentrations of soluble phosphorus, shown in this study, from liquid streams with high suspended solids:
      - Evaluate the feasibility of using soluble phosphorus directly, or:
      - Providing further treatment to release reactive phosphate
  - Using thermal-oxidative treatment:
    - Perform a focused study on the effects of H_2O_2 on the partitioning of phosphorus as treatments proceed, including analysis for organic phosphorus, polyphosphate and phosphate in total and soluble portions

An overarching aim of the experiments listed above would be to evaluate whether gains in energy from biogas production, or gains in saleable product made available by nutrient recovery,

are enough to offset the costs of thermal-oxidative treatment. Ultimately, this information would allow for a more comprehensive comparison of thermal-oxidative, MW and H_2O_2 processes to the performance of existing, commercial technologies.

Further study might also be pursued for liquid dairy manure. From this study, and other comparative studies, it is apparent that acidification has the most acute and drastic effect on dairy manure, solubilizing the vast majority of phosphorus. Subsequent, thermal-oxidative treatment improved bulk settling, and made minor improvements to phosphorus solubility; however, gains were less dramatic than acid alone, and resulting supernatants were visibly high in suspended solids. This suggests that the additional costs of thermal-oxidative treatment may be unwarranted, if an effective means of separating the liquid phase of acid treated dairy manure, and the rich source of soluble phosphorus therein, can be identified. One vein of research in solids/liquids separation of dairy manure that may show promise is chitosan coagulation/precipitation (Garcia et al., 2009; Geetha Devi et al., 2013; Renault et al., 2009). There does not seem to be any precedent of this technique used in aid of nutrient recovery.

References

Abe, N., Tang, Y.-Q., Iwamura, M., Morimura, S., Kida, K., 2013. Pretreatment followed by anaerobic digestion of secondary sludge for reduction of sewage sludge volume. Water Sci. Technol. 67, 2527–33. doi:10.2166/wst.2013.154

Abramovitch, A., 1998. Decomposition of PCB's and other polychlorinated aromatics in soil using microwave energy. Chemosphere 37, 1427–1436.

Anantheswaran, R.C., Liu, L., 1994. Effect of viscosity and salt concentration on microwave heating of model non-Newtonian liquid foods in a cylindrical container. Int. Microw. Power Inst. 29, 119–126.

APHA, 2005. Standard Methods for the Examination of Water and Wastewater, 21st ed. American Public Health Association.

Appels, L., Houtmeyers, S., Degreve, J., Impe, J. Van, Dewil, R., 2013. Influence of microwave pre-treatment on sludge solubilization and pilot scale semi-continuous anaerobic digestion. Bioresour. Technol. 128, 598–603.

Asay, B., Tebaykina, Z., Vlasova, A., Wen, M., 2008. Membrane Composition as a Factor in Susceptibility of Escherichia coli C29 to Thermal and Non-thermal Microwave Radiation 12, 7–13.

Baier, U., Schmidheiny, P., 1997. Enhanced Anaerobic Degradation of Mechanically Disintegrated Sludge. Water Sci. Technol. 36, 137–143.

Baisier, W.M., Labuza, T.P., 1992. Maillard Browning Kinetics in a Liquid Model System. J. Agric. Food Chem. 40, 707–713.

Baldwin, R.R., Doran, P., Mayor, L., 1961. The dissociation of hydrogen peroxide and its role in the hydrogen-oxygen reaction. Symp. Combust. 8, 103–109.

Bhuiyan, M.I.H., Mavinic, D.S., Koch, F. a, 2008. Phosphorus recovery from wastewater through struvite formation in fluidized bed reactors: a sustainable approach. Water Sci. Technol. 57, 175–81. doi:10.2166/wst.2008.002

Bi, X., Wang, P., Jiao, C., Cao, H., 2009. Degradation of remazol golden yellow dye wastewater in microwave enhanced ClO2 catalytic oxidation process. J. Hazard. Mater. 168, 895–900. doi:10.1016/j.jhazmat.2009.02.108

Boehler, M., Siegrist, H., 2007. Potential of activated sludge ozonation. Water Sci. Technol. 55, 181. doi:10.2166/wst.2007.407

Bolton, J.R., Bircher, K.G., Tumas, W., Tolman, C.A., 2001. Figures-of-merit for the technical development and application of advanced oxidation technologies for both electric- and solar-driven systems (IUPAC Technical Report).

Bougrier, C., Albasi, C., Delgenès, J.P., Carrère, H., 2006. Effect of ultrasonic, thermal and ozone pre-treatments on waste activated sludge solubilisation and anaerobic biodegradability. Chem. Eng. Process. Process Intensif. 45, 711–718. doi:10.1016/j.cep.2006.02.005

Bougrier, C., Delgenès, J.P., Carrère, H., 2007. Impacts of thermal pre-treatments on the semi-continuous anaerobic digestion of waste activated sludge. Biochem. Eng. J. 34, 20–27. doi:10.1016/j.bej.2006.11.013

Bougrier, C., Delgenès, J.P., Carrère, H., 2008. Effects of thermal treatments on five different waste activated sludge samples solubilisation, physical properties and anaerobic digestion. Chem. Eng. J. 139, 236–244. doi:10.1016/j.cej.2007.07.099

Brisolara, K.F., Qi, Y., 2013. Biosolids and Sludge Management. Water Environ. Res. 85, 1283–1297. doi:10.2175/106143013X13698672322101

Britton, A., Koch, F.A., Mavinic, D.S., Adnan, A., Oldham, W.K., Udala, B., 2005. Pilot-scale struvite recovery from anaerobic digester supernatant at an enhanced biological phosphorus removal wastewater treatment plant. J. Environ. Eng. Sci. doi:10.1139/S04-059

Burger, G., Parker, W., 2013. Investigation of the impacts of thermal pretreatment on waste activated sludge and development of a pretreatment model. Water Res. 47, 5245–56. doi:10.1016/j.watres.2013.06.005

Camacho, P., Deleris, S., Geaugey, V., Ginestet, P., Paul, E., 2002. A comparative study between mechanical, thermal and oxidative disintegration techniques of waste activated sludge. Water Sci. Technol. 46, 79–87.

Canada Gazette, 2010. Archived - Wastewater Systems Effluent Regulations [WWW Document]. Gov. Canada. URL http://gazette.gc.ca/rp-pr/p1/2010/2010-03-20/html/reg1-eng.html (accessed 11.6.14).

Carrère, H., Bougrier, C., Castets, D., Delgenès, J.P., 2008. Impact of initial biodegradability on sludge anaerobic digestion enhancement by thermal pretreatment. J. Environ. Sci. Health. A. Tox. Hazard. Subst. Environ. Eng. 43, 1551–5. doi:10.1080/10934520802293735

Chan, I., Srinivasan, A., Liao, P.H., Lo, K. V., Mavinic, D.S., Atwater, J., Thompson, J.R., 2013. The Effects of Microwave Pretreatment of Dairy Manure on Methane Production. Nat. Resour. 04, 246–256. doi:10.4236/nr.2013.43031

Chang, C.-J., Tyagi, V.K., Lo, S.-L., 2011. Effects of microwave and alkali induced pretreatment on sludge solubilization and subsequent aerobic digestion. Bioresour. Technol. 102, 7633–40. doi:10.1016/j.biortech.2011.05.031

Chauzy, J., Cretenot, D., Bausseron, A., Deleris, S., 2008. Anaerobic digestion enhanced by thermal hydrolysis : Water Pract. Technol. 3, 2–9. doi:10.2166/WPT.2008004

Christensen, H., Sehested, K., Corfitzen, H., 1982. Reactions of Hydroxyl Radicals with Hydrogen Peroxide at Ambient and Elevated Temperatures. J. Phys. Chem. 92, 1588–1590.

Chu, L., Yan, S., Xing, X.-H., Sun, X., Jurcik, B., 2009. Progress and perspectives of sludge ozonation as a powerful pretreatment method for minimization of excess sludge production. Water Res. 43, 1811–22. doi:10.1016/j.watres.2009.02.012

Climent, M., Ferrer, I., Baeza, M.D.M., Artola, A., Vázquez, F., Font, X., 2007. Effects of thermal and mechanical pretreatments of secondary sludge on biogas production under thermophilic conditions. Chem. Eng. J. 133, 335–342. doi:10.1016/j.cej.2007.02.020

Coelho, N.M.G., Droste, R.L., Kennedy, K.J., 2011. Evaluation of continuous mesophilic, thermophilic and temperature phased anaerobic digestion of microwaved activated sludge. Water Res. 45, 2822–34. doi:10.1016/j.watres.2011.02.032

Comte, S., Guibaud, G., Baudu, M., 2008. Biosorption properties of extracellular polymeric substances (EPS) towards Cd, Cu and Pb for different pH values. J. Hazard. Mater. 151, 185–93. doi:10.1016/j.jhazmat.2007.05.070

Conte, P., Piccolo, A., 1999. Conformational Arrangement of Dissolved Humic Substances. Influence of Solution Composition on Association of Humic Molecules. Environ. Sci. Technol. 33, 1682–1690. doi:10.1021/es9808604

Crittenden, J.C., Trussel, R.R., Hand, D.W., Howe, K.J., Tchobanoglous, G., 2012. Water Treatment Principles and Design, 3rd ed. John Wiley & Sons, Hoboken, New Jersey.

Danesh, P., Hong, S.M., Moon, K.W., Park, J.K., 2008. Phosphorus and Heavy Metal Extraction from Wastewater Treatment Plant Sludges Using Microwaves for Generation of Exceptional Quality Biosolids. Water Environ. Res. 80, 784–795. doi:10.2175/106143008X276714

De, a K., Chaudhuri, B., Bhattacharjee, S., Dutta, B.K., 1999. Estimation of .OH radical reaction rate constants for phenol and chlorinated phenols using UV/H2O2 photo-oxidation. J. Hazard. Mater. 64, 91–104.

De la Hoz, A., Díaz-Ortiz, A., Moreno, A., 2005. Microwaves in organic synthesis. Thermal and non-thermal microwave effects. Chem. Soc. Rev. 34, 164–78. doi:10.1039/b411438h

Dewil, R., Appels, L., Baeyens, J., Degreve, J., 2007. Peroxidation enhances the biogas production in the anaerobic digestion of biosolids. J. Hazard. Mater. 146, 577–581. doi:http://dx.doi.org/10.1016/j.jhazmat.2007.04.059

Dhar, B.R., Elbeshbishy, E., Hafez, H., Nakhla, G., Ray, M.B., 2011. Thermo-oxidative pretreatment of municipal waste activated sludge for volatile sulfur compounds removal and enhanced anaerobic digestion. Chem. Eng. J. 174, 166–174. doi:10.1016/j.cej.2011.08.070

Dhar, B.R., Nakhla, G., Ray, M.B., 2012. Techno-economic evaluation of ultrasound and thermal pretreatments for enhanced anaerobic digestion of municipal waste activated sludge. Waste Manag. 32, 542–9. doi:10.1016/j.wasman.2011.10.007

Dohanyos, M., Zabranska, J., Jenicek, P., 1997. Enhancement of Sludge Anaerobic Digestion by Using a Special Thickening Centrifuge. Water Sci. Technol. 36, 145–153.

Dytczak, M. a, Londry, K.L., Siegrist, H., Oleszkiewicz, J. a, 2007. Ozonation reduces sludge production and improves denitrification. Water Res. 41, 543–50. doi:10.1016/j.watres.2006.11.009

Elovitz, M.S., von Gunten, U., 1999. Hydroxyl Radical/Ozone Ratios During Ozonation Processes. I. The R ct Concept. Ozone Sci. Eng. 21, 239–260. doi:10.1080/01919519908547239

Environment Canada, 2013. Municipal Wastewater Treatment Data [WWW Document]. Gov. Canada. URL https://www.ec.gc.ca/indicateurs-indicators/default.asp?lang=en&n=673220A5-1 (accessed 11.17.14).

EPA, 1984. Conductance [WWW Document]. EPA Approv. Gen. Purp. Methods. URL http://water.epa.gov/scitech/methods/cwa/bioindicators/upload/2007_07_10_methods_method_120_1.pdf (accessed 9.24.14).

Eskicioglu, C., Droste, R.L., Kennedy, K.J., 2007a. Performance of Anaerobic Waste Activated Sludge Digesters After Microwave Pretreatment. Water Environ. Res. 79, 2265–2273. doi:10.2175/106143007X176004

Eskicioglu, C., Kennedy, K.J., Droste, R.L., 2006. Characterization of soluble organic matter of waste activated sludge before and after thermal pretreatment. Water Res. 40, 3725–36. doi:10.1016/j.watres.2006.08.017

Eskicioglu, C., Kennedy, K.J., Droste, R.L., 2007b. Enhancement of Batch Waste Activated Sludge Digestion by Microwave Pretreatment. Water Environ. Res. 79, 2304–2317. doi:10.2175/106143007X184069

Eskicioglu, C., Kennedy, K.J., Droste, R.L., 2008. Initial examination of microwave pretreatment on primary, secondary and mixed sludges before and after anaerobic digestion. Water Sci. Technol. 57, 311–7. doi:10.2166/wst.2008.010

Eskicioglu, C., Prorot, A., Marin, J., Droste, R.L., Kennedy, K.J., 2008. Synergetic pretreatment of sewage sludge by microwave irradiation in presence of H2O2 for enhanced anaerobic digestion. Water Res. 42, 4674–82. doi:10.1016/j.watres.2008.08.010

Eskicioglu, C., Terzian, N., Kennedy, K.J., Droste, R.L., Hamoda, M., 2007c. Athermal microwave effects for enhancing digestibility of waste activated sludge. Water Res. 41, 2457–2466.

Esplugas, S., Giménez, J., Contreras, S., Pascual, E., Rodríguez, M., 2002. Comparison of different advanced oxidation processes for phenol degradation. Water Res. 36, 1034–42.

Frølund, B., Griebe, T., Nielsen, P.H., 1995. Enzymatic activity in the activated-sludge floc matrix. Appl. Microbiol. Biotechnol. 43, 755–761.

Garcia, M.C., Szogi, a a, Vanotti, M.B., Chastain, J.P., Millner, P.D., 2009. Enhanced solid-liquid separation of dairy manure with natural flocculants. Bioresour. Technol. 100, 5417–23. doi:10.1016/j.biortech.2008.11.012

Gavala, H.N., Yenal, U., Skiadas, I. V, Westermann, P., Ahring, B.K., 2003. Mesophilic and thermophilic anaerobic digestion of primary and secondary sludge. Effect of pre-treatment at elevated temperature. Water Res. 37, 4561–72. doi:10.1016/S0043-1354(03)00401-9

Geetha Devi, M., Dumaran, J.J., Feroz, S., 2013. Dairy Wastewater Treatment Using Low Molecular Weight Crab Shell Chitosan. J. Inst. Eng. Ser. E 93, 9–14. doi:10.1007/s40034-012-0005-2

George, D.F., Bilek, M.M., McKenzie, D.R., 2008. Non-thermal effects in the microwave induced unfolding of proteins observed by chaperone binding. Bioelectromagnetics 29, 324–30. doi:10.1002/bem.20382

Glaze, W.H., 1988. Drinking-water treatment with ozone. Environ. Sci. Technol. 21, 224–230.

Gogate, P.R., Pandit, A.B., 2004. A review of imperative technologies for wastewater treatment I: oxidation technologies at ambient conditions. Adv. Environ. Res. 8, 501–551. doi:10.1016/S1093-0191(03)00032-7

Guellil, A., Boualam, M., Quiquampoix, H., Ginestet, P., Audic, J.M., Block, J.C., 2001. Hydrolysis of wastewater colloidal organic matter by extra-cellular enzymes extracted from activated sludge flocs. Water Sci. Technol. 43, 33–40.

Guibaud, G., Bordas, F., Saaid, A., D'abzac, P., Van Hullebusch, E., 2008. Effect of pH on cadmium and lead binding by extracellular polymeric substances (EPS) extracted from environmental bacterial strains. Colloids Surf. B. Biointerfaces 63, 48–54. doi:10.1016/j.colsurfb.2007.11.002

Guibaud, G., Comte, S., Bordas, F., Dupuy, S., Baudu, M., 2005. Comparison of the complexation potential of extracellular polymeric substances (EPS), extracted from activated sludges and produced by pure bacteria strains, for cadmium, lead and nickel. Chemosphere 59, 629–38. doi:10.1016/j.chemosphere.2004.10.028

Haag, W.R., Yao, C.C.D., 1992. Rate constants for reaction of hydroxyl radicals with several drinking water contaminants. Environ. Sci. Technol. 26, 1005–1013. doi:10.1021/es00029a021

Han, D.-H., Cha, S.-Y., Yang, H.-Y., 2004. Improvement of oxidative decomposition of aqueous phenol by microwave irradiation in UV/H2O2 process and kinetic study. Water Res. 38, 2782–90. doi:10.1016/j.watres.2004.03.025

Haug, R.T., Stuckey, D.C., Gossett, J.M., Mccarty, P.L., 1978. Effect of thermal pretreatment on digestibility and dewaterability of organic sludges. Water Pollut. Control Fed. 50, 73–85.

He, Z., Griffin, T.S., Honeycutt, C.W., 2004. Phosphorus Distribution in Dairy Manures. J. Environ. Qual. 33, 1528–1534.

Herrero, M.A., Kremsner, J.M., Kappe, C.O., 2008. Nonthermal microwave effects revisited: on the importance of internal temperature monitoring and agitation in microwave chemistry. J. Org. Chem. 73, 36–47. doi:10.1021/jo7022697

Hoigne, J., Staehelin, J., 1982. Decomposition of Ozone in Water: Rate of Initiation by Hydroxide Ions and Hydrogen Peroxide 16, 676–681.

Hong, S.M., Park, J.K., Lee, Y.O., 2004. Mechanisms of microwave irradiation involved in the destruction of fecal coliforms from biosolids. Water Res. 38, 1615–25. doi:10.1016/j.watres.2003.12.011

Hospido, A., Carballa, M., Moreira, M., Omil, F., Lema, J.M., Feijoo, G., 2010. Environmental assessment of anaerobically digested sludge reuse in agriculture: potential impacts of emerging micropollutants. Water Res. 44, 3225–33. doi:10.1016/j.watres.2010.03.004

Jones, D. a., Lelyveld, T.P., Mavrofidis, S.D., Kingman, S.W., Miles, N.J., 2002. Microwave heating applications in environmental engineering—a review. Resour. Conserv. Recycl. 34, 75–90. doi:10.1016/S0921-3449(01)00088-X

Jou, C.G., Tai, H., 1998. APPLICATION OF GRANULATED ACTIVATED CARBON PACKED-BED REACTOR IN MICROWAVE RADIATION FIELD TO TREAT BTX. Chemosphere 37, 685–698.

Kang, Y.W., Cho, M.-J., Hwang, K.-Y., 1999. Correction of hydrogen peroxide interference on standard chemical oxygen demand test. Water Res. 33, 1247–1251. doi:10.1016/S0043-1354(98)00315-7

Kappe, C.O., 2004. Controlled microwave heating in modern organic synthesis. Angew. Chem. Int. Ed. Engl. 43, 6250–84. doi:10.1002/anie.200400655

Kappe, C.O., 2013. How to measure reaction temperature in microwave-heated transformations. Chem. Soc. Rev. 42, 4977–90. doi:10.1039/c3cs00010a

Kappe, C.O., Pieber, B., Dallinger, D., 2013. Microwave effects in organic synthesis: myth or reality? Angew. Chem. Int. Ed. Engl. 52, 1088–94. doi:10.1002/anie.201204103

Kappe, C.O., Stadler, A., Dallinger, D., 2012a. Microwave Theory, in: Microwaves in Organic and Medicinal Chemistry. Wiley-VCH, pp. 9–39.

Kappe, C.O., Stadler, A., Dallinger, D., 2012b. Equipment Review, in: Microwaves in Organic and Medicinal Chemistry. Wiley-VCH, pp. 41–82.

Katsoyiannis, I. a, Canonica, S., von Gunten, U., 2011. Efficiency and energy requirements for the transformation of organic micropollutants by ozone, O3/H2O2 and UV/H2O2. Water Res. 45, 3811–22. doi:10.1016/j.watres.2011.04.038

Kenge, A. a, Liao, P.H., Lo, K. V, 2009. Treating solid dairy manure using microwave-enhanced advanced oxidation process. J. Environ. Sci. Health. B. 44, 606–12. doi:10.1080/03601230903000693

Kenge, A.A., 2008. Enhancing nutrient solubilization from organic waste using the microwave technology. University of British Columbia.

Kepp, U., Machenbach, I., Weisz, N., Solheim, O.E., 1995. Enhanced stabilisation of sewage sludge through thermal hydrolysis – three years of experience with full scale plant. Water Sci. Technol. 42, 89–96.

Kim, J., Park, C., Kim, T.-H., Lee, M., Kim, S., Kim, S.-W., Lee, J., 2003. Effects of various pretreatments for enhanced anaerobic digestion with waste activated sludge. J. Biosci. Bioeng. 95, 271–5.

Klán, P., Vavrik, M., 2006. Non-catalytic remediation of aqueous solutions by microwave-assisted photolysis in the presence of H2O2. J. Photochem. Photobiol. A Chem. 177, 24–33. doi:10.1016/j.jphotochem.2005.05.008

Klučáková, M., Kargerová, A., Nováčková, K., 2012. Conformational changes in humic acids in aqueous solutions. Chem. Pap. 66, 875–880. doi:10.2478/s11696-012-0199-2

Koutchma, T., Ramaswamy, H.., 2000. Combined Effects of Microwave Heating and Hydrogen Peroxide on the Destruction of Escherichia Coli. LWT - Food Sci. Technol. 33, 30–36. doi:10.1006/fstl.1999.0607

Kubrakova, I. V, 2000. Effect of Microwave Radiation on Physicochemical Processes in Solutions and Heterogeneous Systems: Applications in Analytical Chemistry. Jounral Anal. Chem. 55, 1113–1122.

Kuglarz, M., Karakashev, D., Angelidaki, I., 2013. Microwave and thermal pretreatment as methods for increasing the biogas potential of secondary sludge from municipal wastewater treatment plants. Bioresour. Technol. 134, 290–297. doi:10.1016/j.biortech.2013.02.001

Kuroda, A., Takiguchi, N., Gotanda, T., Nomura, K., Kato, J., Ikeda, T., Ohtake, H., 2002. A Simple Method to Release Polyphosphate from Activated Sludge for Phosphorus Reuse and Recycling. Biotechnol. Bioeng. 78, 2–7. doi:10.1002/bit.10205

Langlais, B., Reckhow, D.A., Brink, D.R., 1991. Ozone in Water Treatment: Application and Engineering. Lewis Publishers, Chelsea, Michigan.

LeBlanc, R.J., Matthews, P., Richard, R.P., 2008. Global atlas of excreta, wastewater sludge, and biosolids management: United Nations Human Settlements Programme, Nairobi.

Liao, P., Wong, W., Lo, K., 2005. Advanced Oxidation Process Using Hydrogen Peroxide/ Microwave System for Solubilization of Phosphate. J. Environ. Sci. Heal. Part A Toxic/Hazardous Subst. Environ. Eng. 40, 1753–1761. doi:10.1081/ESE-200068038

Liao, P.H., Lo, K.V., Chan, W.I., Wong, W.T., 2007. Sludge reduction and volatile fatty acid recovery using microwave advanced oxidation process. J. Environ. Sci. Health. A. Tox. Hazard. Subst. Environ. Eng. 42, 633–9. doi:10.1080/10934520701244417

Liao, W., Liu, Y., Liu, C., Wen, Z., Chen, S., 2006. Acid hydrolysis of fibers from dairy manure. Bioresour. Technol. 97, 1687–95. doi:10.1016/j.biortech.2005.07.028

Liao, W., Liu, Y., Wen, Z., Frear, C., Chen, S., 2007. Studying the effects of reaction conditions on components of dairy manure and cellulose accumulation using dilute acid treatment. Bioresour. Technol. 98, 1992–9. doi:10.1016/j.biortech.2006.08.021

Lidström, P., Tierney, J., Wathey, B., Westman, J., 2001. Microwave assisted organic synthesis - a review. Tetrahedron 57.

Lin, L., Yuan, S., Chen, J., Xu, Z., Lu, X., 2009. Removal of ammonia nitrogen in wastewater by microwave radiation. J. Hazard. Mater. 161, 1063–8. doi:10.1016/j.jhazmat.2008.04.053

Liu, H., Fang, H.H.P., 2002. Extraction of extracellular polymeric substances (EPS) of sludges. J. Biotechnol. 95, 249–256. doi:10.1016/S0168-1656(02)00025-1

Mehdizadeh, M., 1994. Engineering and scale-up considerations for microwave induced reactions. Res. Chem. Intermed. 20, 79–84. doi:10.1163/156856794X00081

Mehdizadeh, S.N., Eskicioglu, C., Bobowski, J., Johnson, T., 2013. Conductive heating and microwave hydrolysis under identical heating profiles for advanced anaerobic digestion of municipal sludge. Water Res. 47, 5040–51. doi:10.1016/j.watres.2013.05.055

Menéndez, J. a, Inguanzo, M., Pis, J.J., 2002. Microwave-induced pyrolysis of sewage sludge. Water Res. 36, 3261–4.

Menéndez, J. a., Arenillas, a., Fidalgo, B., Fernández, Y., Zubizarreta, L., Calvo, E.G., Bermúdez, J.M., 2010. Microwave heating processes involving carbon materials. Fuel Process. Technol. 91, 1–8. doi:10.1016/j.fuproc.2009.08.021

Menéndez, J. a., Domínguez, a., Inguanzo, M., Pis, J.J., 2005. Microwave-induced drying, pyrolysis and gasification (MWDPG) of sewage sludge: Vitrification of the solid residue. J. Anal. Appl. Pyrolysis 74, 406–412. doi:10.1016/j.jaap.2004.10.013

Menéndez, J. a., Domínguez, a., Inguanzo, M., Pis, J.J., 2004. Microwave pyrolysis of sewage sludge: analysis of the gas fraction. J. Anal. Appl. Pyrolysis 71, 657–667. doi:10.1016/j.jaap.2003.09.003

Meredith, R.J., 1998. Engineers Handbook on Industrial Microwave Heating. Institution of Electrical Engineers, London, UK.

Metaxas, A.C., Meredith, R.J., 1983. Industrial Microwave Heating. P. Peregrinus on behalf of the Institution of Electrical Engineers, London, UK.

Mishra, S., Meda, V., Dalai, A.K., Headley, J. V, Peru, K.M., McMartin, D.W., 2010. Microwave treatment of naphthenic acids in water. J. Environ. Sci. Health. A. Tox. Hazard. Subst. Environ. Eng. 45, 1240–7. doi:10.1080/10934529.2010.493801

Monbet, P., Mckelvie, I.D., Saefumillah, A., Worsfold, P.J., 2007. A protocol to assess the enzymatic release of dissolved organic phosphorus species in waters under environmentally relevant conditions. Environ. Sci. Technol. 41, 7479–7485. doi:10.1021/es070573c

Moseley, J.D., Kappe, C.O., 2011. A critical assessment of the greenness and energy efficiency of microwave-assisted organic synthesis. Green Chem. 13, 794. doi:10.1039/c0gc00823k

Mudhoo, A., Sharma, S.K., 2011. Microwave Irradiation Technology In Waste Sludge And Wastewater Treatment Research. Crit. Rev. Environ. Sci. Technol. 41, 999–1066. doi:10.1080/10643380903392767

Mukherjee, S.R., Levine, A.D., 1992. Chemical Solubilization of Particulate Organics as a Pretreatment Approach. Water Sci. Technol. 26, 2289–2292.

Müller, J. a, 2001. Prospects and problems of sludge pre-treatment processes. Water Sci. Technol. 44, 121–8.

Novak, J.T., Sadler, M.E., Murthy, S.N., 2003. Mechanisms of floc destruction during anaerobic and aerobic digestion and the effect on conditioning and dewatering of biosolids. Water Res. 37, 3136–44. doi:10.1016/S0043-1354(03)00171-4

Nüchter, M., Müller, U., Ondruschka, B., Tied, a., Lautenschläger, W., 2003. Microwave-Assisted Chemical Reactions. Chem. Eng. Technol. 26, 1207–1216. doi:10.1002/ceat.200301836

Ødegaard, H., Paulsrud, B., Karlsson, I., 2000. Sludge Disposal Strategies and Corresponding Treatment Technologies Aimed at Sustainable Handling of Wastewater Sludge.

Oller, I., Malato, S., Sánchez-Pérez, J. a, 2011. Combination of Advanced Oxidation Processes and biological treatments for wastewater decontamination--a review. Sci. Total Environ. 409, 4141–66. doi:10.1016/j.scitotenv.2010.08.061

Ostara Nutrient Recovery Technologies Inc., 2014. Installations [WWW Document]. URL http://www.ostara.com/nutrient-management-solutions/installations (accessed 10.8.14).

Park, B., Ahn, J.H., Kim, J., Hwang, S., 2004. Use of microwave pretreatment for enhanced anaerobiosis of secondary sludge. Water Sci. Technol. 50, 17–23.

Park, C., Lee, C., Kim, S., Chen, Y., Chase, H. a, 2005. Upgrading of anaerobic digestion by incorporating two different hydrolysis processes. J. Biosci. Bioeng. 100, 164–7. doi:10.1263/jbb.100.164

Perreux, L., Loupy, A., 2001. A tentative rationalization of microwave effects in organic synthesis according to the reaction medium , and mechanistic considerations. Tetrahedron 57, 9199–9223.

Pino-Jelcic, S. a, Hong, S.M., Park, J.K., 2006. Enhanced anaerobic biodegradability and inactivation of fecal coliforms and Salmonella spp. in wastewater sludge by using microwaves. Water Environ. Res. 78, 209–16.

Procházka, J., Dolejš, P., Máca, J., Dohányos, M., 2012. Stability and inhibition of anaerobic processes caused by insufficiency or excess of ammonia nitrogen. Appl. Microbiol. Biotechnol. 93, 439–47. doi:10.1007/s00253-011-3625-4

Quan, X., Zhang, Y., Chen, S., Zhao, Y., Yang, F., 2007. Generation of hydroxyl radical in aqueous solution by microwave energy using activated carbon as catalyst and its potential in removal

of persistent organic substances. J. Mol. Catal. A Chem. 263, 216–222. doi:10.1016/j.molcata.2006.08.079

Remya, N., Lin, J.-G., 2011. Current status of microwave application in wastewater treatment—A review. Chem. Eng. J. 166, 797–813. doi:10.1016/j.cej.2010.11.100

Renault, F., Sancey, B., Badot, P.-M., Crini, G., 2009. Chitosan for coagulation/flocculation processes – An eco-friendly approach. Eur. Polym. J. 45, 1337–1348. doi:10.1016/j.eurpolymj.2008.12.027

Rivero, J.A.C., Madhavan, N., Suidan, M.T., Ginestet, P., Audic, J., 2006. Oxidative Co-Treatment Using Hydrogen Peroxide with Anaerobic Digestion of Excess Municipal Sludge. Water Environ. Res. 78, 691–700. doi:10.2175/106143006X101647

Saha, M., Eskicioglu, C., Marin, J., 2011. Microwave, ultrasonic and chemo-mechanical pretreatments for enhancing methane potential of pulp mill wastewater treatment sludge. Bioresour. Technol. 102, 7815–26. doi:10.1016/j.biortech.2011.06.053

Sairem, 2013. 915 MHz , 5 kW MICROWAVE GENERATOR Technical specification. Neyron, France.

Sakai, Y., Fukase, T., Yasui, H., Shibata, M., 1997. An activated sludge process without excess sludge production. Water Sci. Technol. 36, 163–170.

Saktaywin, W., Tsuno, H., Nagare, H., Soyama, T., Weerapakkaroon, J., 2005. Advanced sewage treatment process with excess sludge reduction and phosphorus recovery. Water Res. 39, 902–10. doi:10.1016/j.watres.2004.11.035

Schumb, W.C., Satterfield, C.N., Wentworth, R.L., 1955. Hyrdogen Peroxide. Reinhold Publishing Corporation, New York, NY.

Shanableh, A., Jomaa, S., 2001. Production and transformation of volatile fatty acids from sludge subjected to hydrothermal treatment. Water Sci. Technol. 44, 129–35.

Shazman, A., Mizrahi, S., Cogan, U., Shimoni, E., 2007. Examining for possible non-thermal effects during heating in a microwave oven. Food Chem. 103, 444–453. doi:10.1016/j.foodchem.2006.08.024

Skiadas, I. V, Gavala, H.N., Lu, J., Ahring, B.K., 2005. Thermal pre-treatment of primary and secondary sludge at 70 degrees C prior to anaerobic digestion. Water Sci. Technol. 52, 161–6.

Sommer, S.G., Christensen, M.L., Schmidt, T., 2013. Animal Manure Recycling: Treatment and Management. John Wiley & Sons.

Srinivasan, A., Nkansah-Boadu, F., Liao, P.H., Lo, K. V, 2014. Effects of acidifying reagents on microwave treatment of dairy manure. J. Environ. Sci. Health. B. 49, 532–9. doi:10.1080/03601234.2014.896681

Sui, P., Nishimura, F., Nagare, H., Hidaka, T., Nakagawa, Y., Tsuno, H., 2011. Behavior of inorganic elements during sludge ozonation and their effects on sludge solubilization. Water Res. 45, 2029–37. doi:10.1016/j.watres.2010.12.011

Tai, H., Jou, C.G., 1999. Application of GAC packed-bed reactor in microwave radiation field to treat phenol. Chemosphere 38, 2667–2680.

Taylor, M., Atri, B.S., Minhas, S., 2005. Developments in Microwave Chemistry.

Tchobanoglous, G., Burton, F.L., Stensel, D.H., 2003. Wastewater Engineering: Treatment and Reuse, 4th ed. McGraw-Hill Inc, New York, NY.

Tipping, E., 2002. Cation Binding by Humic Substances. Cambridge University Press, Cambridge, UK.

Toreci, I., Droste, R.L., Kennedy, K.J., 2010. Microwave Pretreatment for Soluble Phase Mesophilic Anaerobic Digestion. Environ. Prog. Sustain. Energy 29, 242–248. doi:10.1002/ep

Toreci, I., Droste, R.L., Kennedy, K.J., 2011. Mesophilic Anaerobic Digestion with High-Temperature Microwave Pretreatment and Importance of Inoculum Acclimation. Water Environ. Res. 83, 549–559. doi:10.2175/106143010X12780288628651

Toreci, I., Kennedy, K.J., Droste, R.L., 2009. Evaluation of continuous mesophilic anaerobic sludge digestion after high temperature microwave pretreatment. Water Res. 43, 1273–1284. doi:http://dx.doi.org/10.1016/j.watres.2008.12.022

Troe, J., 2011. The thermal dissociation/recombination reaction of hydrogen peroxide H2O2(+M)⇐⇒2OH(+M) III. Combust. Flame 158, 594–601. doi:10.1016/j.combustflame.2010.08.013

Tsang, K.R., Vesilind, P.A., 1990. Moisture Distribution in Sludges. Water Sci. Technol. 22, 135–142.

Tyagi, V.K., Lo, S.-L., 2012. Enhancement in mesophilic aerobic digestion of waste activated sludge by chemically assisted thermal pretreatment method. Bioresour. Technol. 119, 105–13. doi:10.1016/j.biortech.2012.05.134

US EPA, 1974. Total Phosphorous [WWW Document]. EPA Approv. Gen. Methods. URL http://water.epa.gov/scitech/methods/cwa/bioindicators/upload/2007_07_10_methods_method_365_4.pdf (accessed 8.13.14).

US EPA, 1993a. Standards for the Use or Disposal of Sewage Sludge [WWW Document]. Stand. Use or Dispos. Sew. Sludge. URL http://water.epa.gov/scitech/wastetech/biosolids/upload/fr2-19-93.pdf (accessed 10.11.14).

US EPA, 1993b. Determination of Total Kjeldahl Nitrogen by Semi-automated Colorimetry [WWW Document]. URL http://water.epa.gov/scitech/methods/cwa/bioindicators/upload/2007_07_10_methods_method_351_2.pdf (accessed 8.13.14).

US EPA, 1999. 3.1 Ozone Chemistry [WWW Document]. EPA Guid. Man. URL http://water.epa.gov/lawsregs/rulesregs/sdwa/mdbp/upload/2001_01_12_mdbp_alter_chapt_3.pdf (accessed 11.22.14).

US Peroxide, 2009. How much does H2O2 cost? [WWW Document]. US Peroxide, LLC. URL http://www.h2o2.com/faqs/FaqDetail.aspx?fId=25 (accessed 9.9.14).

US Peroxide, 2014. Idiometric Titration [WWW Document]. US Peroxide, LLC Tech. Libr. URL http://www.h2o2.com/technical-library/analytical-methods/default.aspx?pid=70&name=Iodometric-Titration (accessed 6.2.14).

Vesilind, P.A., 1994. The Role of Water in Sludge Dewatering. Water Environ. Res. 66, 4–11.

Von Gunten, U., 2003. Ozonation of drinking water: part I. Oxidation kinetics and product formation. Water Res. 37, 1443–67. doi:10.1016/S0043-1354(02)00457-8

Von Sonntag, C., 2006a. Formation of Reactive Free Radicals in an Aqueous Environment, in: Schreck, S. (Ed.), Free-Radical-Induced DNA Damage and Its Repair. Springer-Vertag, New York, pp. 9–46.

Von Sonntag, C., 2006b. The Hydroxyl Radical, in: Schreck, S. (Ed.), Free-Radical-Induced DNA Damage and Its Repair. Springer-Vertag, New York, pp. 49–75.

Wang, L.-F., Wang, L.-L., Ye, X.-D., Li, W.-W., Ren, X.-M., Sheng, G.-P., Yu, H.-Q., Wang, X.-K., 2013. Coagulation kinetics of humic aggregates in mono- and di-valent electrolyte solutions. Environ. Sci. Technol. 47, 5042–9. doi:10.1021/es304993j

Wang, Q., Noguchi, C., Hara, Y., Sharon, C., Kakimoto, K., Kato, Y., 1997. Studies on Anaerobic Digestion Mechanism: Influence of Pretreatment Temperature on Biodegradation of Waste Activated Sludge. Environ. Technol. 18, 999–1008. doi:10.1080/09593331808616619

Wang, Y., Wei, Y., Liu, J., 2009. Effect of H2O2 dosing strategy on sludge pretreatment by microwave-H2O2 advanced oxidation process. J. Hazard. Mater. 169, 680–4. doi:10.1016/j.jhazmat.2009.04.001

Wei, Y., Van Houten, R.T., Borger, A.R., Eikelboom, D.H., Fan, Y., 2003. Minimization of excess sludge production for biological wastewater treatment. Water Res. 37, 4453–67. doi:10.1016/S0043-1354(03)00441-X

Wong, W.T., Chan, W.I., Liao, P.H., Lo, K. V, 2006a. A hydrogen peroxide/ microwave advanced oxidation process for sewage sludge treatment. J. Environ. Sci. Health. A. Tox. Hazard. Subst. Environ. Eng. 41, 2623–33. doi:10.1080/10934520600928086

Wong, W.T., Chan, W.I., Liao, P.H., Lo, K. V, Mavinic, D.S., 2006b. Exploring the role of hydrogen peroxide in the microwave advanced oxidation process: solubilization of ammonia and phosphates. J. Environ. Eng. Sci. 5, 459–465.

Wong, W.T., Lo, K.V., Liao, P.H., 2007. Factors affecting nutrient solubilization from sewage sludge using microwave-enhanced advanced oxidation process. J. Environ. Sci. Health. A. Tox. Hazard. Subst. Environ. Eng. 42, 825–9. doi:10.1080/10934520701304914

Yang, S., Wang, P., Yang, X., Wei, G., Zhang, W., Shan, L., 2009. A novel advanced oxidation process to degrade organic pollutants in wastewater: Microwave-activated persulfate oxidation. J. Environ. Sci. 21, 1175–1180. doi:10.1016/S1001-0742(08)62399-2

Yang, Y., Wang, P., Shi, S., Liu, Y., 2009. Microwave enhanced Fenton-like process for the treatment of high concentration pharmaceutical wastewater. J. Hazard. Mater. 168, 238–45. doi:10.1016/j.jhazmat.2009.02.038

Yin, G., Liao, P.H., Lo, K.V., 2007. An ozone/hydrogen peroxide/microwave-enhanced advanced oxidation process for sewage sludge treatment. J. Environ. Sci. Health. A. Tox. Hazard. Subst. Environ. Eng. 42, 1177–81. doi:10.1080/10934520701418706

Yoshida, H., Christensen, T.H., Scheutz, C., 2013. Life cycle assessment of sewage sludge management: a review. Waste Manag. Res. 31, 1083–101. doi:10.1177/0734242X13504446

Yu, Q., Lei, H., Li, Z., Li, H., Chen, K., Zhang, X., Liang, R., 2010. Physical and chemical properties of waste-activated sludge after microwave treatment. Water Res. 44, 2841–9. doi:10.1016/j.watres.2009.11.057

Yu, Y., Chan, W.I., Lo, I.W., Liao, P.H., Lo, K.V., 2010. Sewage Sludge Treatment by a Continuous Microwave Enhanced Advanced Oxidation Process. Can. J. Civ. Eng. 37, 796–804.

Yu, Y., Lo, I.W., Liao, P.H., Lo, K. V, 2010. Treatment of dairy manure using the microwave enhanced advanced oxidation process under a continuous mode operation. J. Environ. Sci. Health. B. 45, 804–9. doi:10.1080/03601234.2010.515474

Zhang, G., Yang, J., Liu, H., Zhang, J., 2009. Sludge ozonation: disintegration, supernatant changes and mechanisms. Bioresour. Technol. 100, 1505–9. doi:10.1016/j.biortech.2008.08.041

Zhang, H., Lo, V.K., Thompson, J.R., Koch, F. a, Liao, P.H., Lobanov, S., Mavinic, D.S., Atwater, J.W., 2014. Recovery of phosphorus from dairy manure - a pilot-scale study. Environ. Technol. 1–15. doi:10.1080/09593330.2014.991354

Zhang, L., Guo, X., Yan, F., Su, M., Li, Y., 2007. Study of the degradation behaviour of dimethoate under microwave irradiation. J. Hazard. Mater. 149, 675–9. doi:10.1016/j.jhazmat.2007.04.039

Zhang, Y., Zhang, P., Guo, J., Ma, W., Fang, W., Ma, B., Xu, X., 2013. Sewage sludge solubilization by high-pressure homogenization. Water Sci. Technol. 67, 2399–405. doi:10.2166/wst.2013.141

Zheng, J., Kennedy, K.J., Eskicioglu, C., 2009. Effect of low temperature microwave pretreatment on characteristics and mesophilic digestion of primary sludge. Environ. Technol. 30, 319–27. doi:10.1080/09593330902732002

Zhu, J., Kuznetsov, a. V., Sandeep, K.P., 2007. Mathematical modeling of continuous flow microwave heating of liquids (effects of dielectric properties and design parameters). Int. J. Therm. Sci. 46, 328–341. doi:10.1016/j.ijthermalsci.2006.06.005

Zimmermann, S.G., Wittenwiler, M., Hollender, J., Krauss, M., Ort, C., Siegrist, H., von Gunten, U., 2011. Kinetic assessment and modeling of an ozonation step for full-scale municipal

wastewater treatment: micropollutant oxidation, by-product formation and disinfection. Water Res. 45, 605–17. doi:10.1016/j.watres.2010.07.080